Optimization of Detention Basin Operation at the Lower Rur River in Germany

H.P.D. Urbach

Delft University of Technology

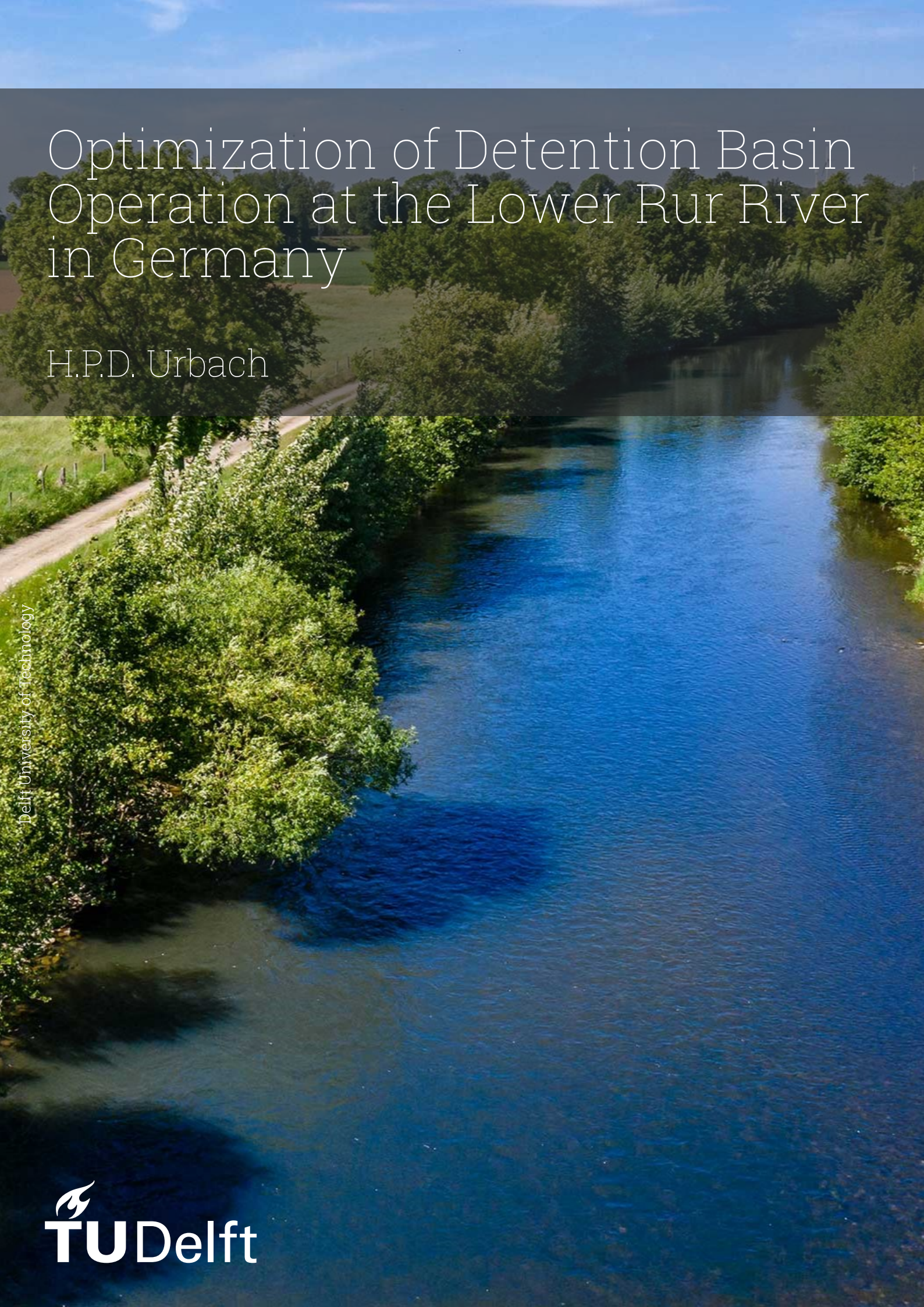

TU Delft

Optimization of Detention Basin Operation at the Lower Rur River in Germany

by

H.P.D. Urbach

Student Name	Student Number
Heleen Urbach	5418666

Thesis committee:	Dr. Davide Wüthrich
	Dr. Kieran Dunne
	Dr.-Ing Bernhard Becker
	Dr.-Ing Stefanie Wolf
	ir. Sebastian Hartgring
Date:	09-12-2024
Faculty:	Faculty of Civil Engineering and Geosciences, Delft

Cover: Photo from RurUfer Randweg ©2021 Grünmetropole e. V.
Style: TU Delft Report Style, with modifications by Daan Zwaneveld

TU Delft

Preface

This MSc thesis reports on the approach and outcome of the research project on investigating the potential of detention basins along the Rur river in Germany by optimizing their operational strategy. For a given hydrograph of a flood wave, the opening times and the crest heights of the weirs of four detention basins, at sites along the Rur river between Jülich and Ophoven as proposed in an earlier study, where optimized to minimize the peak downstream water height near Ophoven. The operation of the weirs is a flexible approach because it is adapted to the flood wave, but it is also prone to human or mechanical failure. Therefore, in addition a compound weir was studied of which the crest height are fixed.

The study was part of the Joint Cooperation programme on Applied scientific Research (JCAR) to improve the cooperation on flood and drought management and research to Accelerate Transboundary Regional Adaptation to Climate Extremes (ATRACE).

In Chapter 1 the research context, the research objectives and questions as well as the societal impact are discussed. In Chapter 2 a literature review is presented. In Chapter 3 information is given about the proposed detention basins and their inlets along the Rur river between Jülich and Ophoven. Also flood scenarios are described and the current gauging stations along the Rur river are considered for real-time operation of detention basins. In the first phase of the project a 1D kinematic model for a river with floodplains and an arbitrary number of detention basins was implemented. Because this model is computationally fast, it was used in optimizing the operation of the weirs. The 1D model was for a number of cases compared to simulations with HydroAS2D, which solves the 2D shallow water equations. Both models are described in Chapter 4. Also the optimization problems studied are described in that chapter. In Chapter 5 the results of the optimization problem for the operated weirs and for a compound weir are discussed. Also the results of the comparison between the 1D model and HydroAS2D are presented. Chapter 6 is a discussion of the results of the project, and provides recommendations. Chapter 7 contains the conclusions. There are five appendices. In the first appendix progress made with the optimization of detention basins with the software RCT-Tools which is being developed in Deltares is reported. The remaining appendices mostly provide background information.

In my search for an interesting master thesis project, I was introduced to the joint cooperation JCAR-ATRACE by Prof.dr.ir. Bas Jonkman, who was at the time head of the Hydraulic Structures and Flood Risk section within the Faculty of Civil Engineering of TU Delft. I was immediately enthusiastic because JCAR is a international collaboration of leading institutes in two countries on the very relevant topic of reducing cross-border flood risks.

I want to thank one of the main instigators of the JCAR-ATRACE collaboration, Dr. ir. Kymo Slager of Deltares for his support in hosting me at Deltares and for his interest in my project.

Since my project was part of an international collaboration, it may not be surprising that I received supervision form researchers from different institutes in two different countries, namely Deltares, TU Delft, RWTH Aachen and Wasserverband Eifel-Rur.

My daily supervisors at the host institute Deltares were Dr.-Ing Bernhard Becker and ir. Sebastian Hartgring. I thank Bernhard for the valuable feedback he has given and for providing his expertise and experience about the German Rur. Sebastian's recent MSc thesis on hindcasting the 2021 flood event in the Rur was relevant for this research. I am very grateful to him for the many occasions during which he gave support and advise.

Throughout the thesis work I was also supervised by Dr.-Ing Stefanie Wolf from RWTH Aachen. In the beginning of my research, I was invited by her to stay a week in Aachen, where I was kindly received and supported by Stefanie and colleagues. I thank her for her help and support through the past months.

I would also like to thank M.Eng. Vincent Hochfeldt from Wasserverband Eifel-Rur, with whom I had

intensive contacts at various stages of my research. Vincent provided the HydoAS2D model of the Rur river and the Digital Elevation Model which I have been using in the project. Vincent was always very helpful and always promptly answered my questions, whether via email or during online meetings.

I also thank Frau Deppe from Hydrotech Ingenieurgesellschaft für Wasser und Umwelt mbH for her support in using the HydroAs2D software.

Last but certainly not least, I thank the chair and first supervisor of my thesis comittee Dr. Davide Wüthrich and my second supervisor from TU Delft Dr. Kieran Dunne for very valuable advise and feedback throughout the project. They made me think more critically about my work, for which I am very grateful.

I am very happy to complete my Master's degree with this report. I really enjoyed working on the topic and had the chance to learn from and collaborate with many experienced and knowledgeable scientists and engineers in two countries.

H.P.D. Urbach
Delft, December 2024

Abstract

In mid-July 2021, record breaking precipitation fell in Western Europe, causing rivers to overflow their banks. This event has demonstrated that measures are necessary, leading to the JCAR-ATRACE collaboration which brings together multiple hydraulic engineering institutes across Europe to enhance resilience to extreme climate events and fosters long-term research partnerships. This MSc thesis is a contribution to this joint collaboration. The goal of this project was to investigate the potential of detention basins along the Rur river in Germany and optimize their operational strategy to mitigate flood risk near in particular the village of Ophoven, which had suffered from recent floods. A one-dimensional kinematic model was developed of the main river, the floodplains and basins between Jülich and Ophoven. Initially for four basins, the opening times and crest heights of the weirs were sequentially optimized to minimize the peak water height near Ophoven for the 1/100 years flood event. The predictions of the 1D model were verified against the HydroAS2D model which solves the 2D shallow water equations. The optimization revealed that the chosen volumes of the four basins were too small. A method to estimate the required storage volume for a desired downstream peak water height reduction was applied. Then a much larger basin, close to Jülich, was considered. It was found that apart from choosing the appropriate opening time and crest height, not only the storage volume but also the width of the inlet is important. In addition to optimizing the operation of the weirs, the potential of a basin with an un-operated compound weir with four fixed crests was studied. The crest heights were optimized for the 1/100 flood wave. The optimized compound weir, tested for the small detention basin 1 as an alternative to the operated weir, achieved similar level of peak reduction when optimized for the same flood event. However, when the compound weir is applied to another flood event, it can become ineffective. The operated weir is more flexible, but requires that the upstream hydrograph is measured at sufficiently large distance from the basin.

Samenvatting

In juli 2021 veroorzaakte recordhoeveelheid neerslag in West-Europa dat rivieren buiten hun oevers traden, hetgeen grote overstromingen tot gevolg had. Deze gebeurtenis toonde aan dat maatregelen nodig zijn. Dit leidde tot de oprichting van de JCAR-ATRACE-samenwerking. Hieraan nemen verschillende onderzoeksinstituten uit heel Europa deel met als doel de ernstige gevolgen van extreme klimaatgebeurtenissen te verminderen en onderzoekssamenwerkingen te bevorderen. Dit afstudeerwerk is een onderdeel van deze samenwerking en richtte zich op het onderzoeken van de effectiviteit van potentiële retentiebekkens langs de rivier de Rur in Duitsland en op het optimaliseren van operationele strategieën om overstromingsrisico's te verminderen. De nadruk lag met name op de gevolgen voor het dorp Ophoven, dat in 2021 en eerder zwaar getroffen werd. Een eendimensionaal kinematisch model werd ontwikkeld om de rivier, de uiterwaarden en de bekkens tussen Jülich en Ophoven te modelleren. In de eerste fase werden de openingstijden en kruinhoogten van de stuwen bij vier retentiebekkens geoptimaliseerd om de piekwaterhoogte bij Ophoven tijdens een 1/100-jarige overstroming te minimaliseren. De voorspellingen van het 1D-model werden gevalideerd met het HydroAS2D-model, dat gebruikmaakt van de tweedimensionale ondiepe watervergelijkingen. De resultaten van de optimalisatie toonden aan dat de opslagcapaciteit van de vier bekkens onvoldoende was om significante piekreductie te bereiken. Vervolgens is een methode toegepast om de benodigde opslagcapaciteit te schatten voor een gewenste reductie van de piekwaterhoogte bij Ophoven. Daarna werd een groot retentiebekken (Indesee) in de omgeving van Jülich onderzocht. Hierbij bleek dat naast de juiste openingstijd en kruinhoogte ook de breedte van de inlaat een cruciale rol speelt. Naast het optimaliseren van gestuurde stuwen werd ook het potentieel onderzocht van een retentiebekken met een niet-gestuurde stuw met vier vaste verschillende kruinhoogten. De kruinhoogten van deze stuw werden geoptimaliseerd voor de 1/100-jarige hoogwatergolf. De resultaten toonden aan dat de geoptimaliseerde vaste kruinhoogten vergelijkbare piekreducties geven als de geoptimaliseerde gestuurde stuw, indien geoptimaliseerd wordt voor dezelfde hoogwatergolf. Echter, de effectiviteit van de geoptimialiseerde vier kruinhoogten kan sterk verminderen bij een ander overstromingsscenario. Hoewel een gestuurde stuw meer flexibiliteit biedt, heeft deze het nadeel dat de hydrograaf stroomopwaarts tijdig en op voldoende afstand van het bekken moet worden gemeten.

Zusammenfassung

Mitte Juli 2021 führten außergewöhnlich starke Niederschläge in Westeuropa zu schweren Überschwemmungen. Dieses Ereignis verdeutlichte die Notwendigkeit besser vorbereitet zu sein auf solche Naturkatastrophen. Nach diesem Ereignis entstand die JCAR-ATRACE-Kooperation, die mehrere Institute in ganz Europa zusammenbringt um die Widerstandsfähigkeit gegen extreme Klimaereignisse zu verbessern und langfristige Forschungspartnerschaften zu fördern. Die vorliegende MSc-Arbeit ist Teil dieser Zusammenarbeit. Ziel dieser Masterarbeit war es, das Potenzial von Rückhaltebecken (Poldern) entlang der Rur in Deutschland zu untersuchen und ihre Betriebsstrategie zu optimieren. Der Schwerpunkt lag insbesondere auf dem Dorf Ophoven, dass von dem Juli-2021 Hochwasser betroffen war. Es wurde ein eindimensionales kinematisches Modell für den Hauptfluss, die Flussauen sowie die potenziellen Polder zwischen Jülich und Ophoven entwickelt. Zunächst wurden die Öffnungszeiten und Kronenhöhen der Wehre von vier Poldern sequentiell optimiert, um die Scheitelhöhe der Ganglinie bei Ophoven während eines 1/100-jährlichen Hochwasserereignisses zu minimieren. Die Vorhersagen des 1D-Modells wurden anhand des HydroAS2D-Modells validiert, das die 2D-Flachwassergleichungen löst. Die Optimierung ergab, dass die Volumina der vier Polder zu klein waren. Eine Methode zur Abschätzung des erforderlichen Speichervolumens für eine gewünschte flussabwärts gerichtete Reduzierung der Scheitelhöhe wurde angewandt. Anschließend wurde ein deutlich größeres Becken in der Nähe von Jülich untersucht. Dabei zeigte sich, dass neben der Wahl der optimalen Öffnungszeit und Kronenhöhe nicht nur das Speichervolumen, sondern auch die Breite des Einlaufs entscheidend ist. Neben der Optimierung des Betriebes der Wehre wurde zudem das Potenzial eines Beckens mit einem unbeweglichem Wehr mit vier festen aber verschiedenen Kronenhöhen untersucht. Die Kronenhöhen wurden für ein 1/100-jährliches Hochwasserereignis optimiert. Das optimierte ungesteuerte Wehr erreichte bei der Optimierung für dieses Hochwasserereignis eine vergleichbare Scheitelreduzierung. Allerdings kann das ungesteuerte Wehr bei einem anderen Hochwasserereignis an Wirksamkeit verlieren. Das betriebene Wehr ist flexibler, erfordert jedoch, dass die flussaufwärts gerichtete Ganglinie in ausreichendem Abstand vom Becken gemessen wird.

Contents

Nomenclature

Abbreviations

Abbreviation	Definition
1D	One-Dimensional
2D	Two-Dimensional
DEM	Digitial Elevation Model
NHN	Normalhöhennul (datum used in Germany)
OSM	Open Street Map
QGIS	Quantum Geographic Information System
RTC	Real Time Control
WVER	Wasserverband Eifel-Rur

Symbols

Symbol	Definition	Unit
A_c	Conveyance area	[m^2]
b	Width of weir	[m]
B	Width of river	[m]
B_j	Width of segment j	[m]
B_c	Conveyance width	[m]
$B_{c,j}$	Conveyance width of segment j of a cross-section	[m]
c_f	Bed resistance coefficient	[-]
c_{HW}	Propagation speed of flood wave	[m/s]
c_s	Reduction factor	[-]
d	Water depth	[m]
d_j	Water depth of segment j	[m]
g	gravitational acceleration	[m$/$s^2]
h	Water height	[m]
h_b	Water height in a basin	[m]
H_c	Crest height	[m]
$H_{c,j}$	Crest height of compound weir	[m]
$\vec{H_c}$	$(H_{c,1} \ldots, H_{c,N})$ vector of crest heights of compound weir	[m]
i_b	Bed slope	[-]
j	Index	[-]
μ	Discharge coefficient	[-]
n	Manning coefficient	[s$/$m$^{1/3}$]
n_j	Manning coefficient of segment j	[s$/$m$^{1/3}$]
R	Hydraulic radius	[m]
Q	Discharge	[m^3/s]
Q_j	Discharge of segment j	[m^3/s]
Q_0^{tot}	Total Discharge before a weir	[m^3/s]
Q^{tot}	Total discharge after a weir	[m^3/s]
Q_{weir}	Discharge of a weir	[m^3/s]
Q_u	Discharge in quasi-uniform flow	[m$^3/$s]
t	Time variable	[s]
t_1	Time of opening of a weir	[s]

Symbol	Definition	Unit
t_2	Time that a basin is full	[s]
t_c	Earliest time that the water height on the floodplain equals the crest height	[s]
U_u	Flow velocity in quasi-uniform flow	[m/s]
$V_{\text{max}}(H_c)$	Maximum volume of basin as function of crest height	[m^3]
$V_{\text{basin}}(h_b)$	Volume of basin as function of water height	[m^3]
x	Spatial variable in the direction of the floodwave	[m]
y	Spatial variable in cross-section	[m]
$Z_b(y)$	Bed level as function of cross-sectional coordinate y	[m]
$Z_{b,j}(y)$	Bed level of segment j as function of cross-sectional coordinate y	[m]
$\overline{Z}_b$	Averaged bed level	[m]
$\overline{Z}_{b,j}$	Averaged bed level of segment j	[m]

1

Introduction

The flood event of mid-July 2021 has been a wake-up call for the responsible authorities of Western Europe to take action to adapt to extreme climate events. Germany, the Netherlands, and Belgium were among the countries most severely affected, with record-breaking precipitation recorded in various regions. In parts of western Germany and eastern Belgium, the rainfall was associated with a return period of 1 in more than 100 years. In the Netherlands, rainfall amounts reached double the typical levels for the region (Junghänel et al., 2021).

Recognizing the importance of cross-border collaboration and the exchange of expertise among neighboring countries, the Joint Cooperation program on Applied scientific Research in order to Accelerate Transboundary Regional Adaptation to Climate Extremes (JCAR ATRACE) has been launched by several European research institutes (JCAR ATRACE, 2024). This master thesis project may be considered part of the joint cooperation program, focusing on the investigation of detention basins as a flood risk mitigation measure along the Lower Rur river in Germany. This MSc thesis was co-supervised by TU Delft, Deltares and RWTH Aachen.

This introductory chapter describes the research context, gives the problem statement and defines and examines the scope and societal implications of the project. The final section contains an outline of the thesis structure.

1.1. Research context and problem statement

The Rur river originates from the High Fens - Eifel National Park in eastern Belgium and flows through North Rhine-Westphalia in Germany before converging with the Meuse river at Roermond in the Netherlands (see Figure 1.1). The Rur river spans approximately 160 kilometers and, while moderately sized, plays an important role in various river functions (WVER, 2024a). It serves as a water source for industries, provides drinking water, and contributes to electricity generation through hydropower. In its upstream course, the Rur river has typical characteristics of a low mountain river flanked by gravel banks. As it progresses into the middle reach, the river slope becomes steep. Finally, in the lower reaches, starting a few kilometers donwstream of Jülich, the Rur river flows through flatland terrain, similar to the Dutch landscape further downstream. Multiple dams upstream regulate the flow of water to downstream (WVER, 2024a).

In July 2021, various regions in Europe were affected by heavy rainfall caused by a quasi-stationary low-pressure system called ”Bernd”. In Germany the flooding resulted in 189 fatalities and caused the most significant damages related to floodings in recent history of up to 33 billion euros. While the Ahr Valley experienced the most severe consequences of the flood event, the region upstream of the Rurtalsperre dam in the Rur river also was significantly impacted, with 15 casualties reported. Although the dam successfully prevented the lower Rur river from surpassing its historical discharge record, it was unable to prevent flooding in downstream villages, such as the village Ophoven, resulting in considerable material damage (DKKV, 2022; Mertins, 2021).

The village Ophoven in Germany is located along the Lower Rur river, near the Dutch border (Figure 1.1) and is one of the villages that has been inundated during the 2021 flood event. Roadways and underground areas within residences were flooded, leading to material damages to buildings, personal property, gardens, and infrastructure. Ophoven has suffered from an earlier flood event in 2013 which also has resulted in substantial damage (Mertins, 2021).

Additional protective measures are necessary to reduce the risk of future flooding in and around Ophoven. The responsible water management authority for the Rur river basin, Wasserverband Eifel-Rur (WVER), has initiated a study of measures to reduce flood risk in Ophoven. Improving the resilience against flooding is of great importance for this area because a higher frequency of torrential rains is anticipated (WVER, 2024c). According to V. Hochfeldt (personal communication, April, 2024), preliminary study into potential measures was conducted by WVER, that indicated that widening floodplains may not sufficiently reduce flood peaks due to inadequate retention time and volume.

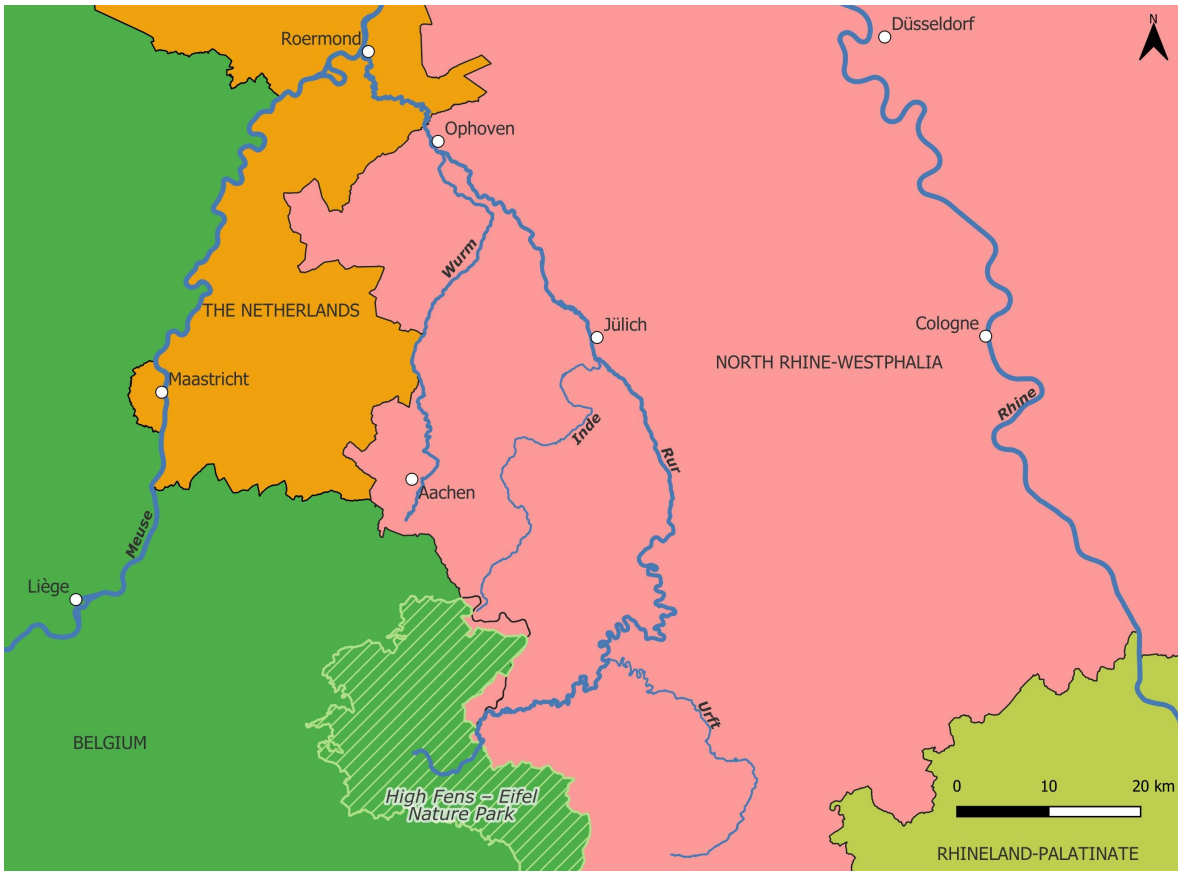

Figure 1.1: The Rur Basin. Image generated in QGIS using OSM Place Search.

This raised the question of whether a detention basin could effectively attenuate flood peaks. Detention basins, also commonly referred to as dry detention ponds or storm water basins, are areas that are designed to temporarily store water during a flood event, thereby attenuating and delaying flood peaks (Dickson, 2018). After the flood event has passed, the basins are gradually emptied. This means that the basins are dry during most of the time.

Detention basins are typically located next to rivers and surrounded by dikes to contain the floodwaters. Inside the dike, there is an inlet structure (a weir) that allows water to flow into the basin. The weir can either be unregulated, with a fixed crest height, or actively controlled, where it is opened and closed at appropriate times. Figure 1.2 provides an aerial view of a detention basin located next to a river, showing the typical layout of such a system.

Recent Bachelor thesis research from Schweim (2024) has explored potential sites for detention basins

along the Lower Rur river. Four possible sites were identified, with one basin near the village of Ophoven which was further investigated by Schweim (2024). The detention basin sites are described in Chapter 3. Schweim (2024) focused on a passive control approach, where the crest of the inlet structure remains fixed throughout. Initial findings indicated a minimal reduction of only 1 cm in water level at the Stah gauge, with negligible downstream impact at the border to the Netherlands. However, through optimization of the terrain of the basin, local water level reductions of up to 7 cm at the Stah gauge and approximately 3 cm at the Dutch border were achieved.(Schweim, 2024).

These findings raised the question of whether strategic active control of the inlets of multiple detention basins, adaptable to the flood wave, could provide more effective flood peak attenuation. Active control involves selecting the opening times and fixing the crest heights of the inlet weirs to specific levels, which requires an optimization procedure to determine the most effective configuration. Additionally also the use of a multi-compound weir was proposed.

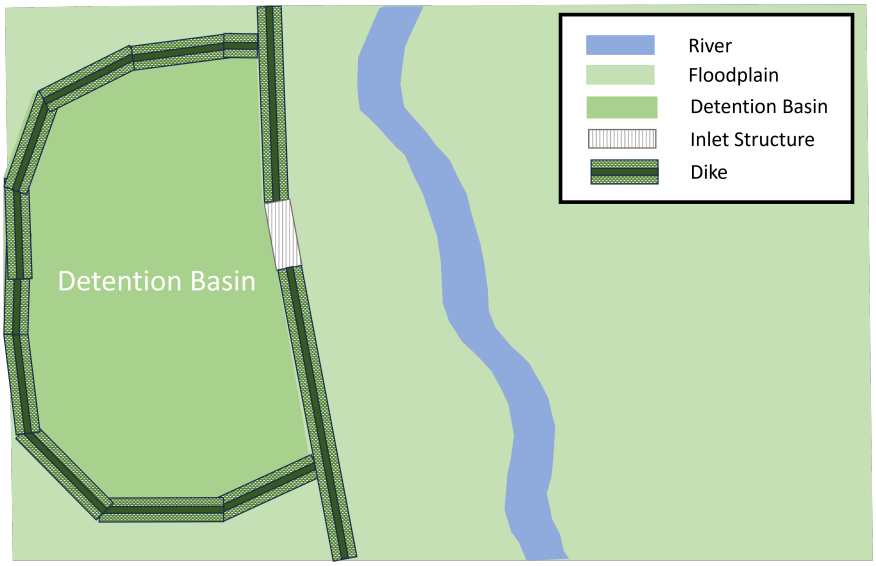

Figure 1.2: Areal view of a detention basin adjacent to a river.

1.2. Research problem

To optimize detention basin operation for peak reduction, a model is required to evaluate operating strategies and identify the most effective approach. Ideally, a model with a short simulation time would be used to test possible operational strategies. However, to the best of the author's knowledge, the only available model for the Lower Rur river is a highly detailed 2D-hydrodynamic model (HydroAS2D), which requires multiple days to simulate a single operational strategy. Therefore, a more time efficient model is required to be able to optimize the operation of detention basins. Furthermore, a faster model could have the potential to be used for real-time control of basins during flood events.

1.3. Research objectives

Operated detention basins have proven their effectiveness in the past, for instance along the Rhine river Homagk and Bremicker, 2006). However, identifying appropriate locations and sizes and optimizing the management strategy remains challenging. The long simulation times of HydroAS2D make this model unfeasible for optimizing the operational strategy.

This master thesis study has the following aims:

1. Develop a rather simple and fast model that allows efficient optimization of management strategies.
2. Optimize operational strategies for detention basins and estimate their expected peak reduction and quantify whether these reductions are sufficient to mitigate flood risk at Ophoven.

3. Validate the new modeling method by comparing its results with those obtained from HydroAS2D.
4. For the case of one basin, investigate the potential of a compound weir with several optimized fixed crest heights and compare its effectiveness with the optimized operated weir. The compound weir has the advantage of being not prone to risks associated with operated structures, such as human errors, but the disadvantage that it can not be adapted to a flood wave.

1.4. Research scope

This study first focuses on four detention basin locations along a 30-kilometer stretch of the Rur river, between Jülich and Ophoven (see Figure 1.1). These locations were proposed by Schweim (2024) and will be adopted in the first part of the current research. While the location of the fourth detention basin has been clearly defined in the prior study, the other three locations have only been roughly indicated and thus require further investigation in this study.

As mentioned above, the research will involve the development and application of a 1D model that is much simpler and faster than 2D hydrodynamic models such as HydroAS2D. The aim is to use the 1D model to optimize the operation of detention basins for a flood event with a 1/100-year return period, which is in line with German flood safety standards. More specifically, the time of opening of the inlets and the crest heights of the weirs are optimized to achieve the largest reduction of water height downstream of the last basin. This method of flood reduction will be referred to as **operated detention basins**.

The predictions of the 1D model will be verified by comparison with HydroAS2D, which solves the 2D shallow water equations.

Apart from the four basin locations as proposed by Schweim (2024) the area currently occupied by the Inden Lignite mine, which is to be repurposed into a more natural environment in the future featuring a lake called Indesee, will be investigated as a potential site for a detention basin. Furthermore, the problem of determining an appropriate volume for an operated basin to achieve a desired reduction of water height downstream at Ophoven is included. Alongside the primary focus on optimizing detention basin management strategies by optimizing opening times of inlets and crest heights of weirs, the study will also explore the potential of using a compound weir with several fixed crest heights. The crest heights of the compound weir are optimized using the 1D model for the 1/100-year flood event and its effectiveness is compared with the optimized operation strategy for the case of one basin, for both the 1/100 and 1/1000 flood events.

In addition to analyzing predefined flood events, practical issues that occur when applying a real-time operated weir for a detention basis in the reach of the Rur river between the surroundings of Jülich and the village of Ophoven are also discussed.

The scope of the study excludes:

- The management strategy for emptying the detention basins. It is assumed that the basins will be emptied after the flood wave has passed.
- The optimization of dike heights surrounding the detention basins.
- Terrain modifications within the four detention basins to increase their storage capacity. In fact, the basins are intended for multi functional use and flood only during extreme high-water events.
- The schematization of the Rur river and Indesee at its actual location.

1.5. Research questions

The primary research question is:

How can operational strategies for potential detention basins along the Lower Rur river in Germany be optimized, to achieve maximum peak reduction at Ophoven?

The following sub-questions have been defined:

1. What model can be developed as alternative to the 2D-hydrodynamic model, which is sufficiently fast and accurate to optimize operational strategies for detention basins?

2. What are the optimum operational strategies for the detention basins, and how much do they attenuate the flood peak?
3. How do the prediction of the new 1D model compare to the results obtained with HydroAS2D?
4. Can a compound weir with fixed crests be an alternative to operated weirs?

1.6. Societal impact

Flood events often have significant societal impact, ranging from loss of life and property damage to destruction of community services such as infrastructure. Detention basins, as a flood mitigation measure, can help attenuate flood peaks. However, their implementation may have implications for areas downstream. Moreover, the construction and operation of detention basins will affect land use, thereby changing social-economic structures.

In this section the thesis topic will be considered from an ethical perspective. Important stakeholders affected by the research are identified and analyzed based on how they are affected by the MSc work. Additionally, the section will discuss the values held by the stakeholders and legal regulations that must be considered for this research.

The stakeholders of the research project and their interest in the research are described below:

Residents and property owners living in flood-prone areas near/in Ophoven are directly impacted by flood events and would benefit from improved flood protection measures. Their involvement is important for understanding concerns, and preferences regarding flood risk management strategies. Residents and property owners in the area directly benefit from this research as it provides insight into the effectiveness of mitigating flood risk by implementing detention basins. However, they can on the contrary also be negatively impacted by the proposed measures, because the basins presently are used for agriculture. It is the task of responsible authorities to weigh the different interests involved and base on this their decisions and policies.

Residents and property owners value safety and economic prosperity. This MSc research aligns with these values by recommending flood risk management strategies which are effective yet have limited negative side-effects.

The Ministry for Environment, Conservation of Nature, and Traffic of North Rhine-Westphalia (Ministerium für Umwelt, Naturschutz und Verkehr) supports the work of municipalities and water-boards to realize sustainable and proactive flood protection and participates in financing these objectives (Ministerium für Umwelt, Naturschutz und Verkehr, 2024). Since this MSc research concerns the effectiveness and potential consequences of the implementation of detention basins, the results of the study may provide insight for policymakers and regulators concerning appropriate measures to improve flood protection and therefore may influence future decision-making processes regarding the Lower Rur river. The ministry values sustainability and public safety align with the objectives of this research. The German law and specific regulations for the state of North Rhine-Westphalia (NRW) will have to be considered, in particular nature conservation laws, and land use regulations.

Wasserverband Eifel-Rur is responsible for water management, flood protection and for water safety in their designated area. As detention basins are a mitigation measure of interest which was proposed by WVER, the research and outcomes reported in this MSc thesis are relevant for WVER. They could use the findings as a starting point for a more elaborate investigation. WVER values effective water management and flood protection. These values align with the objectives of the research conducted in this MSc project. As a regional water management authority, WVER operates within the federal and state laws.

Province of Limburg has a similar role in the Netherlands as the Ministry for Environment, Conservation of Nature, and Traffic of North Rhine-Westphalia has in Germany regarding flood protection along the rivers in the province. The results of the study will be of interest for the Province of Limburg as any measures proposed for the German upstream part of the Rur can have impact on the downstream part flowing in the Netherlands.

Waterschap Limburg and Rijkswaterstaat (RWS) are responsible for water management and flood protection in the downstream areas of the German Rur river. They are impacted by this research as

they may use the findings to assess potential changes of flood risk for their area of responsibility. This research aligns with values such as enhancing flood resilience and protecting downstream areas by providing insight into the potential impacts of detention basins. Waterschap Limburg and RWS operate within the Dutch water management laws. The research needs to comply with ethical guidelines and research standards from The Netherlands, which includes reporting the effects of upstream measures for downstream areas transparently.

Environmental Non-Governmental Organizations advocate environmental conservation and biodiversity protection. Investigating the effect of detention basins is of interest for these organizations as they want to stimulate environmentally friendly flood management solutions. Moreover, the basins could be used as water reservoir in the case of drought.

1.7. Outline

In Chapter 2 the existing literature is discussed regarding modeling detention basins, how to optimize the basin management strategy and relevant literature on flood routing and peak attenuation. In Chapter 3 the proposed detention basin locations and dimensions are presented and the considered flood scenario's are discussed. In Chapter 4 the methodology is explained, in particular the 1D model is elaborated including the optimization methods for operated weirs and for fixed compound weirs. Chapter 5 the results of this thesis are presented, summarizing the findings regarding the 1D model outcomes for the case with and without basins. Furthermore, the solutions of the optimization problems are presented. The results are further discussed and interpreted in Chapter 6. Also suggestions for further research are made. Finally, the conclusion are given in Chapter 7.

2

Literature review

With the anticipation of more torrential rains and increasing occurrences of floods, policymakers have to make important decisions regarding measures to mitigate floods. Detention basins, as a measure to mitigate flood risk, have been widely studied in the past. However, it remains challenging to manage detention basins effectively for a certain site. In this thesis two optimization problems are studied to achieve this goal. The aim of this chapter is to explore the existing knowledge on modeling and optimizing detention basins. This includes examining case studies from Germany and other countries. Additionally literature regarding in particular the 2021 flood event has been examined, to derive lessons that can be drawn for future improvements.

2.1. 2021 Flood Event in the German and Dutch part of the Rur River

In July 2021, the Rur river basin experienced one of the most severe flood events in recent history. This section provides context for the necessity of this research by outlining the progression of the 2021 flood, its impacts on the German and Dutch part of the river, and the lessons learned for improving flood risk management.

The 2021 flood event in western Germany was caused by the low-pressure system Bernd. During this event, the German Weather Service (Deutscher Wetterdienst) recorded locally more than 150 mm of rain within 72 hours, and the flood was attributed a return period of 1 in 500 years (Manandhar et al., 2023). The study by Manandhar et al. (2023) also investigated the resilience against the 2021 flood, stressing the need for better land-use planning, especially in anticipation of more frequent flooding due to climate change.

During the 2021 flood event, the Inde river, a tributary of the Rur river located upstream of Jülich, experienced record-breaking discharges, which resulted in severe erosion near the Inden lignite mine. According to Keßels et al. (2024), this led to the formation of a 700-meter-long channel cut caused by the reactivation of a historical river channel that had been abandoned when the Inde was relocated decades earlier for mining purposes. Their study highlights how extreme hydrological conditions combined with heavily modified landscapes triggered this significant geomorphological change. As Keßels et al. (2024) emphasize, this demonstrates the critical need to consider the impact of historical land-use modifications on the effects of extreme flood events.

Despite severe erosion, a large volume of floodwater was captured in the Inden lignite mine during the 2021 event. This raises an important question about the potential of this site in the long term. Plans are already in place to cease mining operations in 2029 and repurpose the site into a lake known as the Indesee (StadtJülich, 2012). No investigation has yet been conducted into the potential of this site to serve as a detention basin.

The 2021 flood event has demonstrated the efficacy of peak attenuation in the Meuse in the Netherlands due to measures such as “Room for the river” and the “Maaswerken”. Downstream river reaches benefit from upstream peak discharge attenuation. The amount of peak attenuation depends on various factors,

including the shape of the flood wave, river geometry and the availability of storage areas (Asselman, De Jong, et al., 2022).

Between July 13th and 15th, 2021, the province of Limburg experienced record-breaking water levels in its rivers and streams due to extreme rainfall. In some areas, up to 160 millimeters of precipitation fell within just 48 hours (Asselman, van Heeringen, et al., 2022).

Following this event, Waterschap Limburg and the province of Limburg evaluated the water system. An already existing D-HYDRO 1D2D model has been improved to analyze the high water event of 2021 (Horn and Hurkmans, 2022). At the Gauging Station Stah in Germany, close to the Dutch border near Ophoven, manual discharge measurements recorded a peak of 267 m^3/s. German model calculations, however, indicated a peak discharge of 354 m^3/s. This difference shows that there are significant inaccuracies in the modeling of the peak discharge. Horn and Hurkmans (2022) validated the D-HYDRO model using measured data downstream and found that the high peak discharge of 354 m^3/s would result in unreasonably high water levels at Roermond. They also noted that the shape of the flood wave significantly affects downstream water levels. Furthermore, the roughness parameters used in the model were too low because they were for winter conditions whereas the 2021 event took place in the summer (Horn and Hurkmans, 2022).

2.2. Climate Projections and Simulations for the Rur Basin

With the anticipation of climate change, there is a growing expectation that flood events will become both more frequent and more extreme. However, most analyses of historical flood data currently assume stationarity, i.e. that statistical properties of hydrological processes remain constant over time. This assumption is increasingly contested (Milly et al., 2008). This section discusses the Rur basin in the context of climate projections and simulations, highlighting potential changes in rainfall patterns and their implications for flood risk.

Eingrüber and Korres (2022) explored trends in the frequencies of extreme precipitation and floods within the Rur catchment until 2099, under two emission scenarios obtained from HadCM3. The non-parametric Mann-Kendall tendency test was used to analyze whether there are statistically significant trends in the frequency of extreme precipitation or flood events between 1961 and 2099. It was found that, on average, the frequency of extreme precipitation is expected to increase throughout the entire Rur catchment. Moreover, analysis of water depth gauge data at Stah, located close to Ophoven, showed an increase of 31 to 36% in the magnitudes of flood return periods by 2099 compared to the base period. These findings suggest that the assumption of stationarity will underestimate future flood intensity in the Rur river basin.

The Rur river basin is significantly influenced by anthropogenic measures through its network of six dams with a combined storage volume of 300 million m^3 (WVER, 2024d). Accurate forecasting of flood events in such a regulated catchment necessitates considering both the catchment area and the dam control dynamics. Demny and Lohr (2014) provides a methodology for quantifying the impact of climate change through high-water simulations in the Rur catchment, Germany. The TalsimNG software has been extended to simulate the current state and to forecast high- and low-water flows, including the effects of climate change. Multiple climate scenarios have been explored by simulating discharges using a rainfall-runoff model (NASIM), which were subsequently used for the high-water simulations (known as ”Hochwassermerkmalsimulation” in German), which are flood simulation representing scenario’s such as the HQ100 or HQ1000 flood event (Demny and Lohr, 2014).

2.3. Detention Basins as a Measure to Mitigate Flood Risk

Detention basins have been widely implemented to mitigate flood risk by temporarily storing excess water during heavy rainfall or floods. In the United States for instance, nearly 2 million artificial water bodies existed when Avakyan and Polyuskin conducted their study in 1988, with 99% of these being ponds or basins (Avakyan and Polyushkin, 1989). By 1970, 2500 reservoirs had been constructed to protect approximately 5.2 million hectares of land from flooding. The average effectiveness of the reservoirs is estimated to be 150-200 million dollars per year (Avakyan et al., 1986) This shows the importance that detention basins and reservoirs have in managing flood risks.

Recent studies have shown the effectiveness of detention basins in other regions. Pirone et al. (2024) derived simplified relationships which fit detailed simulations of flood-routings for river catchment which are representative for the Mediterranean region. Nakamura (2022), investigated basins in Japan and found that they can store large amounts of storm water during extreme rainfall events. For instance, four basins near the Tone and Watarase rivers were estimated to have stored 250 million m^3 of water during Typhoon Hagibis in 2019. It was noted that, besides their flood-control capabilities, these basins can also have ecological benefits depending on their multi-function use. However, expanding the use of detention basins requires considerable land, sometimes in rural areas, which in practice often leads to resistance from landowners (Nakamura, 2022).

2.4. Case Studies of Operated Detention Basins

Detention basins have been used all over the world for decades to mitigate flood peaks. In Germany a case study by Asenkerschbaumer et al. (2012) from the Technical University of Munich has investigated using operated basins for the Danube. They categorized potential basin locations based on elevation data and studied each basin individually. Historical flood hydrographs, corresponding to a return period of approximately 1 in 100 years, were used to estimate the required basin volume by integrating the area under the hydrograph between the peak and the desired reduced peak. It was proposed to monitor the water height in the Danube continuously and when it is above a certain value, to open the weir of the basin. Once the water level is sufficiently below the threshold, the basin is closed again. In the study the 2D hydrodynamic HydroAS2D model was used in this research. To represent the dikes, Asenkerschbaumer et al. (2012) deactivated the meshes surrounding the basins. The moment of opening of detention basins was modeled using a water level threshold.

It was found that the flood peaks could be reduced by about 2 to 10%, depending on the location of the basin. It was concluded that the magnitude of peak flow reduction depends on various factors, including usable retention volume, site location, interactions between river and floodplain areas, and the specific hydrological scenario (Asenkerschbaumer et al., 2012).

Giehl (2019) examined the Inn and Salzach rivers in the Alps, using a 2D hydrodynamic model to assess the impact of multiple operated detention basins. Similar to Asenkerschbaumer et al. (2012), Giehl evaluated the efficacy of each basin individually. The optimization of management strategies was based on the same method as applied by Asenkerschbaumer et al. (2012) to the Danube. A risk assessment was conducted using the results of HydroAS2D simulations for inundation depths, flow velocities, and retention times. These findings were then compared to current risk assessment, and the optimization was aimed at minimizing risk.

The effectiveness of operated detention basins with a total capacity of 260 million m^3 for the upper Rhine, between Basel (Switzerland) and Worms (Germany), was studied by Homagk and Bremicker (2006). The chosen basin locations were historically important natural inundation areas. Sixteen historical winter flood events were extrapolated to assess 200-year and 220-year peak flows at the Maxau and Worms gauges. The situation along the Rhine is particularly complex due to its long reach and the involvement of various cross-boundary stakeholders. The positive effect of existing detention basins along the Upper Rhine has been proven during flood events in the late 1980s and 1990s. These basins at that time reduced peak water levels by 33 cm, equivalent to a reduction of 7% (Homagk and Bremicker, 2006).

The method of operating a basin as proposed by Asenkerschbaumer et al. (2012) differs from the method studied in the current thesis research. In this MSc thesis, for a given flood wave, both the opening time of the weir and its crest height are optimized to achieve minimum water level downstream near Ophoven. Using both the opening time and the water height as optimization parameters enables to more efficiently use the available storage volume of the basin.

2.5. Modeling Flood Waves and Optimizing Detention Basins

Hydrodynamic models are widely used to predict flood routing in rivers. This section reviews different hydrodynamic modeling techniques. Furthermore, flood routing approaches, detention basin modeling techniques, and optimization methods for detention basin operation, as found in literature are discussed.

2.5.1. Models for Flood Wave Propagation

One-dimensional models based on the De Saint Venant equations (Battjes & Labeur, 2017; Chow et al., 1988; Subramanya, 2009) have been popular due to their short computation times. The De Saint Venant equations consist of two coupled partial differential equations for the water height and the discharge, one expressing the conservation of mass and the other the conservation of momentum. One key assumption is hydrostatic pressure, which requires that the river slope be roughly less than 6 degrees (Zidan, 2015) and that the flood wave should be long and not rapidly changing. A wave is considered long if the ratio between water depth and wavelength is less than or equal to 0.055. Zidan (2015) state that this criterion is in general met by flood waves in rivers.

For flood waves the inertia terms in the momentum equation can in general be neglected. However, the time dependent term in the mass conservation is retained. This is called the quasi-static assumption Battjes and Labeur (2017). In uniform flow, the water depth gradient is zero and the momentum equation then implies the following instantaneous relation between the discharge Q_u and the water depth d

$$Q_u = B_c \cdot d^{3/2} \cdot \sqrt{\frac{g \cdot i_b}{c_f}},$$

where B_c is the conveyance width, g is the gravitational acceleration, i_b is the river bed slope and c_f is the roughness coefficient. As explained in Battjes and Labeur (2017), in the quasi-uniform assumption, this relationship is also used for flood waves when the gradient of the water depth is nonzero. Substitution into the equation which expresses the conservation of mass yields the kinematic wave equation with the high water speed as wave velocity. Additionally, the Chezy or Manning formulas are used for the friction coefficients, which were originally developed for steady flow (Zidan, 2015). It has nevertheless been demonstrated that these approximations are sufficiently accurate for modeling flood waves in rivers because these waves are assumed to be quasi-steady, i.e. slowly varying (Zidan, 2015).

The kinematic model has been widely used for flood routing through rivers. The report by Miller (1984) outlines both the applicability and limitations of the kinematic wave model.

When the nonzero gradient of the water depth is taken into account, the discharge does not merely depend on the water depth itself but also on its gradient. By substituting this relation into the equation which expresses the conservation of mass, the so-called diffusion model for flood waves is obtained Battjes and Labeur (2017). In contrast to the kinematic model, with the diffusion model the broadening of the flood wave and the lowering of its peak due to resistance can be simulated. Diffusion effects are important when the propagation of flood waves over long distances is considered (Battjes & Labeur, 2017; Chow et al., 1988; Subramanya, 2009). Solutions of certain intitial and boundary value problems of the 1D diffusion model are derived in (Glinowiecka-Cox, 2022; Perez-Guerrero et al., 2016).

Floodplains adjacent to the Rur river are locally very wide (sometimes more than 300 meters), making it important to account for their effects on the water level. With the Divided Channel Methods (DCM) floodplains can be incorporated into the kinematic model. An overview of the main methods and their refinements is given in (Cao, 2006; Sturm, 2001; Subramanya, 2009). The model described in Chapter 4 employs the Vertical Interface Procedure (see § 3.16 of Subramanya, 2009).

Accurate modeling of flow resistance in channels and in particular on floodplains requires detailed information about roughness. In practice, friction coefficients are often calibrated using empirical data. Sun et al. (2010) investigated two methods to assess flow resistance due to vegetation on the floodplain of the Blackwater river in Hampshire, UK, namely the uniform Manning coefficient method and an emergent vegetal drag force method. In the second method, the resistance is determined such that the predicted velocity profiles derived from the emergent vegetational drag force closely matches empirical data. Notably, it was found that approximately 20% of the total floodplain flow resistance can be attributed to emergent vegetation. Hence vegetation is quite important in the calibration process (Sun et al., 2010).

In contrast to one-dimensional models described so far, with a two-dimensional hydrodynamic model it is possible to simulate lateral flow effects and processes induced by floodplain topography and meandering channels (Horritt and Bates, 2001). HydroAS2D, which is used in the present study to verify the prediction by the 1D kinematic model, is based on the 2D shallow water equations, which are also called

the 2D St. Venant equations. In contrast to the 1D model, the 2D model requires long computation times which makes it not possible to use it in optimizing designs.

2.5.2. Modeling and Optimization of Detention Basins

RTC (Real-Time Control)-Tools is an open source and general purpose tool developed by Deltares (Deltares, 2024) to support decision-making processes for the control and optimization of hydraulic assets and water systems. One of its novel features is the use of control theory and feedback mechanisms which enables to drive hydraulic systems in a time dependent manner to achieve a higher degree of optimality (Becker et al., 2024). RTC tools comes in the shape of a Python package, making it compatible with other software such as Modelica, which is used for modeling water systems with an user-interface (Deltares, 2024). RTC-Tools contains (multi-)objective optimization algorithms, which makes it a promising model to optimize detention basin operation.

A coupled 1D-2D hydrodynamic model for flood simulations with detention basins was proposed by Liu et al. (2015). The 1D De Saint Venant equations were applied to model channel flow, while the flow dynamics in the detention basins were represented using the 2D shallow water equations. The topic of how to couple 1D and 2D models in a numerically consistent manner is discussed in Morales-Hernandez et al. (2009). In their study, Liu et al. (2015) incorporated a weir-type source term to model flow into the detention basin which effectively couples the 1D river system with the 2D domain. The 1D-2D coupled model was validated through a test case, with dikes surrounding the basin represented by wall conditions. Liu et al. (2015) applied their approach to the Jiakouwa flood detention basins, with the aim to reduce peak discharge during flood events with 50- and 100-year return periods. They calibrated the Manning coefficients of the cross sections in the 1D river model using observed flood data and visualized inundation depths through GIS software. The results demonstrated that both flooding and recession processes in the Jiakouwa basin were accurately simulated using the coupled 1D2D approach. This study provides insight into modeling river-detention basin interactions. However, potential optimizations of detention basin dimensions or operational strategies were not studied.

The study of Jaffe and Sanders (2001) discusses a more dynamic approach to flood mitigation. The authors hypothesize that rapid filling of the floodplain creates a dynamic wave and modeled the weir structure as a dike breach. In their study the river is modeled as one single channel and flow is directed through a dike breach to a floodplain area surrounded by dikes. This approach differs from the expected conditions along the Rur, where detention basins would be located adjacent to, rather than within, the floodplain area (in the hinterland). Jaffe and Sanders (2001) defined as objective function the peak water depth. The object function is minimized as a function of the floodplain area, breach size and breach timing. The authors concluded that the floodplain area and breaching timing are most important to reduce the flood peak.

Sanders et al. (2006) investigated passive and active gate control strategies for directing flow to an off-line reservoir to mitigate flood peaks. The authors examined three idealized diversion control methods for a coastal watershed in northern California. Similar to their previous work, water was diverted from a channel directly into an initially empty off-line reservoir, with no intermediate floodplain interaction considered. Their findings indicate that, for effective flood peak reduction, gate operations need to be optimized depending on the flood hydrograph. The study demonstrates that actively controlled gates can achieve 2–3 times larger flood depth reduction than passive controls, stressing the critical role of optimized operational strategies.

In 2011, China constructed 94 detention basins along major rivers, covering a total area of approximately 35,000 square kilometers. In 2012, new policies were introduced for the operational strategy of these basins, taking into account factors such as topography, water flow, basin size, and the number of citizens affected by the basin (Wang et al., 2021). The study by Wang et al. (2021) proposes a framework for optimizing flood diversion sites and operational strategies applied to the Huayanghe detention basin. This framework consists of three modules: first, flood simulation using a 1D hydrodynamic model (MIKE11 or MIKE22); second, a cost-benefit analysis; and third, the optimization process. The optimization was conducted to maximize the total benefits of the river-detention basin-protection and minimize the costs. The benefits have been quantified by the reduction of inundated areas for the 1-100 flood event.

Similar to the studies of Jaffe and Sanders (2001) the method of a controlled breach was adopted, meaning that when the water level in the river exceeds a defined warning stage, the dike will be breached artificially at the designated location and repaired after the flood receded.

Gourbesville and Caignaert (2022a) investigated an approach using the 1D hydrodynamic model MIKE11. They used the global optimization tool AutoCal, using the Shuffled Complex Evolution (SCE) algorithm to identify the optimal flood control operating strategy. To achieve multiple objectives, their optimization model was coupled with the hydrodynamic model used for flow routing, incorporating physical constraints and operational policies. The optimization algorithm was designed to determine the best values for a combination of decision variables. The maximum water levels at downstream control points were used as the objective function for minimizing flood risk further downstream. If the objectives were not met in the first optimization, the model would repeat its optimization process using the SCE algorithm, meaning a new set of control variables was generated for the simulation model.

Shishegar et al. (2021) used a global predictive real-time control (RTC) approach, in which several control rules are integrated into an optimization model with the aim to minimize peak flows and maximizing the detention time, given several constraints. A simulation model was used to examine the performance of the system. An 1 hour design storm with a return period of 100 years was used for the sizing of the basins. The open-source Storm Water Management Model (SWMM) was used to simulate runoff volume.

2.6. Research Approach and Techniques

This section outlines the research approach and techniques that will be adopted in this study, while referring to relevant literature.

RTC-Tools was introduced as a potential software for detention basin optimization. In the initial stage of the project, RTC-Tools has been used to derive optimum time dependent in- and outflow of basins. Results of this preliminary study are described in Appendix A. It was however not straightforward to incorporate floodplains in the model. The Rur consists locally of wide floodplains, making it important to incorporate their effect on water level reduction. Therefore, and also to gain more flexibility by using a self made model and code, it was decided to make a 1D model based on De Saint-Venant equations which incorporates floodplains.

The modeling approach of Battjes and Labeur (2017) was adopted for developing a kinematic wave model, combined with the vertical interface method by Subramanya (2009) to include the effect of floodplains. This approach is computationally efficient, making it suitable for quickly estimating the impact of different operational strategies. Whether the kinematic wave model suffices for the Rur river is discussed in Appendix C. Friction coefficients will be expressed using Manning's formula, similar to Zidan (2015) and Sun et al. (2010).

Unlike the studies by Gourbesville and Caignaert (2022b) and Shishegar et al. (2021), this research does not apply an optimization algorithm. Instead, the minimum is determined of the peak discharges of all considered operational strategies. Although this approach may lead to slightly longer computational times, it is straightforward and always gives the global optimum. Furthermore, it allows the evaluation of sub-optimal strategies, which can improve insight into the effectiveness of different operations.

Because a one-dimensional model is less accurate than the available HydroAS2D model, the optimal strategies derived using the 1D model will be validated with HydroAS2D. The modeling approach in HydroAS2D for detention basins follows Asenkerschbaumer et al. (2012), where the dikes surrounding the basins are represented by deactivating specific meshes, and the weir is operated based on water level thresholds. Inflow into the basins is modeled similarly to dike breaches, as described by Jaffe and Sanders (2001) and Wang et al. (2021).

Finally, the method for estimating the storage volume needed to achieve a desired peak reduction is based on the approach described in Asenkerschbaumer et al. (2012).

3

Detention Basins and Flood Dynamics for the Rur River

This chapter provides an overview of the studied Lower Rur river reach and introduces the locations and characteristics of the proposed and studied detention basins. Four detention basins were selected based on current land-use considerations, while the Indesee basin, a future project that will repurpose the Inden lignite mine into a lake, is considered as a potential long-term flood mitigation measure. The chapter also outlines the flood scenarios relevant to this research, which are used to investigate the potential effects of these basins. Finally, the existing gauging stations and dams along the lower Rur river are listed for their potential application in real-time operation.

3.1. Locations and Characteristics of the Detention Basins

As mentioned in the introduction, four detention basin sites have been proposed in the study Schweim (2024). Potential locations were identified by removing existing dikes and analyzing the resulting flow patterns to the hinterland, as well as the achieved retention volume using HydroAS2D. In this thesis project, these four locations are initially adopted. Furthermore, the Indesee is considered as a potential future detention basin. This section provides information about the four detention basin areas and the Indesee basin.

3.1.1. Four Basins

The region of each detention basin was selected based on land-use considerations, aiming at on-urbanized areas to avoid residential zones. Currently, the land within these basins is used for agriculture. Each detention basin is situated behind existing dikes along the Rur river. As stated in the research scope, determining the required dike height around these detention basins is outside the scope of this study. Furthermore, the terrain within the basins was not modified and has been evaluated in its current state.

Figure 3.1 shows the reach of the Rur river which was studied in the project and the locations of the four detention basins. The reach spans approximately 30 km from Jülich to Ophoven. In the two figures shown in Figure 3.1, the flow direction of the Rur river is from the bottom to the top, with the left figure representing the upstream reach and the right figure the downstream reach. There is a small common region in the upper left of the right figure and the lower right of the left figure.

The width of the floodplains varies significantly over the reach. Depending on the urbanization, the floodplain can be very narrow (e.g. at Linnich). In other more rural regions the floodplains can be very wide (several hundred meters).

The first detention basin, located furthest upstream, is situated near Jülich. The second basin lies downstream of Linnich, while the third is positioned near Wassenberg. The fourth and final detention basin is adjacent to the Wurm tributary, close to Ophoven.

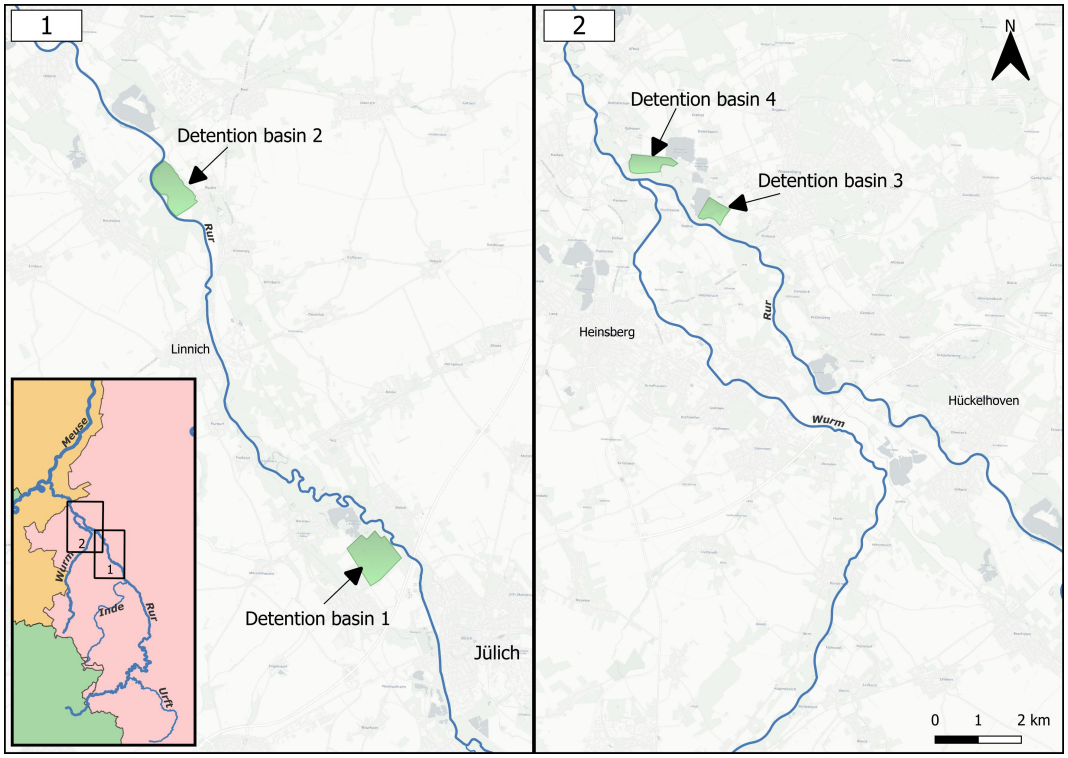

Figure 3.1: Potential detention basins along the Lower Rur river. Illustration made within QGIS with OpenStreetMap (OSM) background.

Figure 3.2 provides a close-up of the detention basins. It can be observed that the floodplain next to the first detention basin is quite narrow compared to the floodplain on the opposite side of the river. The second detention basin has a similar pattern as the first basin. The third detention basin has more symmetrical floodplains, while the width of the floodplain varies along the existing dike of the fourth detention basin.

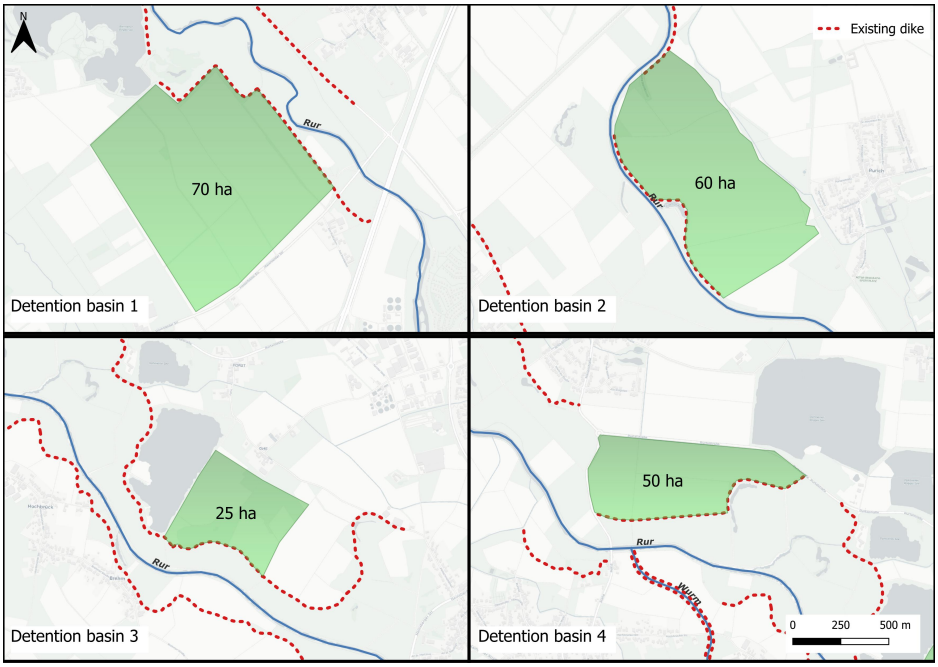

Figure 3.2: Potential detention basins along the Lower Rur river. Illustration made within QGIS with OpenStreetMap (OSM) background. Data from existing dike locations from WVER

The areas of the four basins are also shown in Figure 3.2. Detention basin 1 has the largest area, followed by detention basin 2 and 4 and lastly detention basin 3. The area of detention basin 3 was chosen such that the basin does not intervene with an existing road and a High voltage power grid which crosses the area east of the defined basin area (flosm, 2024).

3.1.2. Indesee: Former Lignite Mine Site as Detention Basin Location

The "Indesee" is a proposed project for a lignite mine site near Jülich, which will continue operations until 2029 (see Figure 3.3). After that the excavated area will be repurposed into a more natural environment by filling parts of the site with water. One plan for this site involves filling an area of 11.6 hectares with water (StadtJülich, 2012). Due to the considerable depth of the mine, which reaches several hundred meters, the filling process is expected to take until 2060 (LandesverbandNRW, 2023). Given that the Indesee is close to the Rur river, there may be potential for the lake as a reservoir in the case of severe flood events. This could perhaps lead to significant peak reductions downstream.

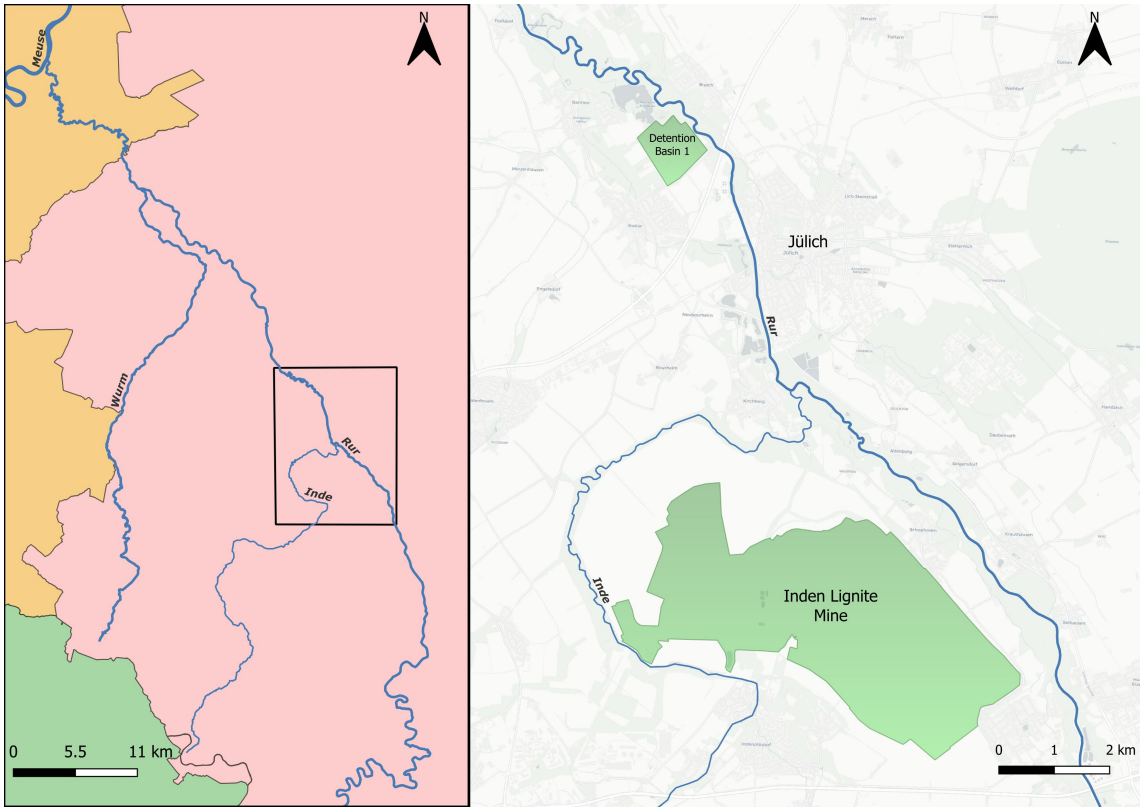

Figure 3.3: Map showing both the Inden Lignite Mine site, located upstream of Jülich, and the first detention basin. Generated in QGIS using OpenStreetMap (OSM) data.

If a flood water buffer of 1 meter water depth would be assumed, the storage volume of the Indesee equals approximately 11.6 million m^3. The area of the Indesee is significantly larger than that of the four detention basins discussed in Section 3.1, and it is therefore expected to have a greater effect.

The flooding of the Inden lignite mine during the 2021 flood event was briefly discussed in the literature review. Keßels et al. (2024) examined the impact of severe erosion caused by the Inde river breaching into the Inden lignite mine, forming a substantial channel. This event demonstrated that flooding the site could potentially have positive implications downstream.

In the current project, the focus is not on the actual location of the proposed Indesee but rather on a conceptual analysis. Specifically, an investigation into how a detention basin with a storage capacity equivalent to the proposed Indesee might influence peak flow reduction downstream. By scaling up the volume of Detention Basin 1 to match the proposed storage of the Indesee, the potential peak reduction that could be achieved under such conditions is examined. Consequently, the Indesee's impact was

assessed as if it were positioned downstream of the confluence of the Rur and Inde rivers.

3.2. Inlets of the Detention Basins

The inlet locations for the detention basins were chosen based on terrain data from the digital elevation model (DEM), selecting regions where water is likely to flow towards and thereby making it possible for the detention basins to capture water during a flood event. The DEM of the Rur river were obtained from the HydroAS2D models, which were provided by WVER.

The inlet locations are marked with arrows on the DEM of each detention basin in Figure 3.4. For the first detention basin, the inlet was selected such that the elevation in the basin behind the inlet was lower than the floodplain. Furthermore, the floodplain is narrow at this point, hence water will reach the inlet quickly. The same criteria were applied to select the inlet of the second detention basin. At the third detention basin, the inlet is located near an old branch of the Rur river. This location is beneficial because the height difference between the floodplain and the river branch makes it more probable that water will flow into the basin. For the fourth detention basin, the chosen inlet is not the first point where water would naturally flow towards. In fact, the water will flow to the lower situated green area on the floodplain in Figure 3.4. However, there the bed of the basin is relatively high. This is the reason for choosing the inlet as indicated by the arrow in Figure 3.4.

The width of the inlet structure and the crest height of the weir are critical parameters, as they determine the rate at which water flows into the detention basin. For the four detention basins an inlet width of 60 m as proposed by Schweim (2024) is chosen. For the Indesee also wider inlets are considered.

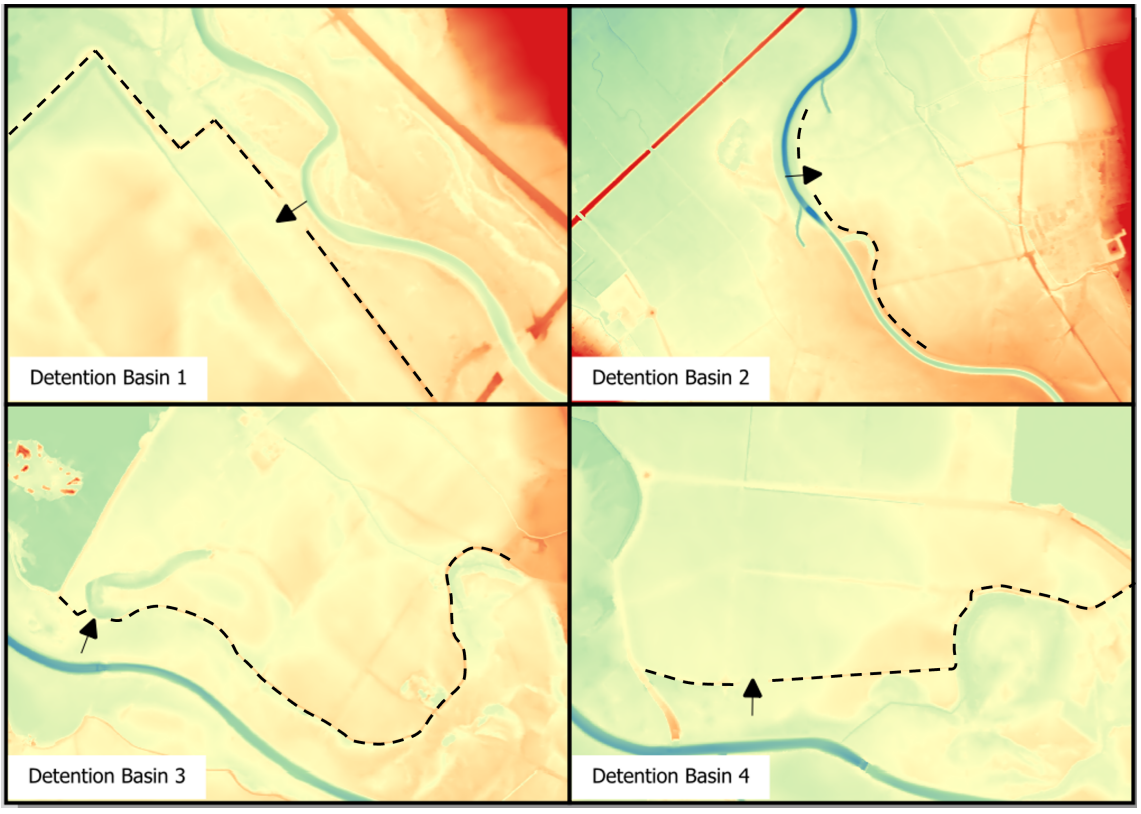

Figure 3.4: Inlet locations of the detention basins based on DEM data. Illustration is not to scale and is intended solely to show inlet locations relative to terrain elevation.

The Indesee is located slightly upstream of Jülich and hence is a bit outside the primary study area. The river geometry adjacent to the Indesee was not determined. Instead, the geometry of detention basin 1 was used as a reference, as determining an appropriate inlet location and corresponding river geometry would require a more dedicated study. The aim of the investigation is to provide an order-of-

magnitude estimate of the potential effect rather than a precise representation of real-world conditions. The geographical conditions of detention basin 1 were applied to the Indesee because it is located only a few kilometers downstream.

3.3. Flood Scenarios

The local government of Cologne (Bezirksregierung Köln) who is responsible for the German segment of the Rur river basin, follows the EU-guidelines for assessing and managing flood risk. These guidelines have led to the creation of high-water danger and risk maps (Hochwasser- und Risikokarten), which are the foundation for evaluating current flood susceptibility. The maps show the impact from flood events categorized by their probability of occurrence: low-probability events (once every 1000 years), moderately probable events (statistical occurrences expected once every 100 years), and high-probability scenarios (Köln, 2024).

WVER is legally responsible to ensure that the river system can withstand a flood event with a 1-in-100-year return period (HQ100). This means that the system must be resilient to an HQ100 flood without causing any damage. The WVER suggested to primarily use the HQ100 flood wave in the present study. Currently, not all areas meet the safety standard. The first objective of this study was therefore to optimize the detention basins as proposed in this chapter to ensure that the river system can, at a minimum, manage an HQ100 event.

Besides the HQ100 event, the HQ1000 and the 2021 flood event have also been investigated. Figure 3.5 shows the flood hydrographs of the HQ100, HQ1000, and 2021 flood events at the gauging station "Stah," located just downstream of the confluence with the Wurm. The data for the HQ100 and HQ1000 flood events were provided by WVER at 15-minute timesteps, while the hydrograph data for the 2021 flood event was estimated through hindcasting in the study by Hartgring (2023) and was initially modeled at a 30-second timestep, but was resampled to 15-minute intervals to improve computational efficiency during optimization The hydrograph for the HQ100 event, as shown in Figure 3.5, contains more detailed data during baseflow conditions compared to the HQ1000 and 2021 flood events. This was the format in which the data were provided.

The peak discharge of the HQ100 event is at 218 m^3/s and has duration of roughly 3.4 days. The peak discharges of the HQ1000 and the 2021 flood wave both are around 270 m^3/s. Although the tail of the 2021 flood wave is missing, both this flood wave and the HQ1000 wave have estimated duration of roughly 5 days.

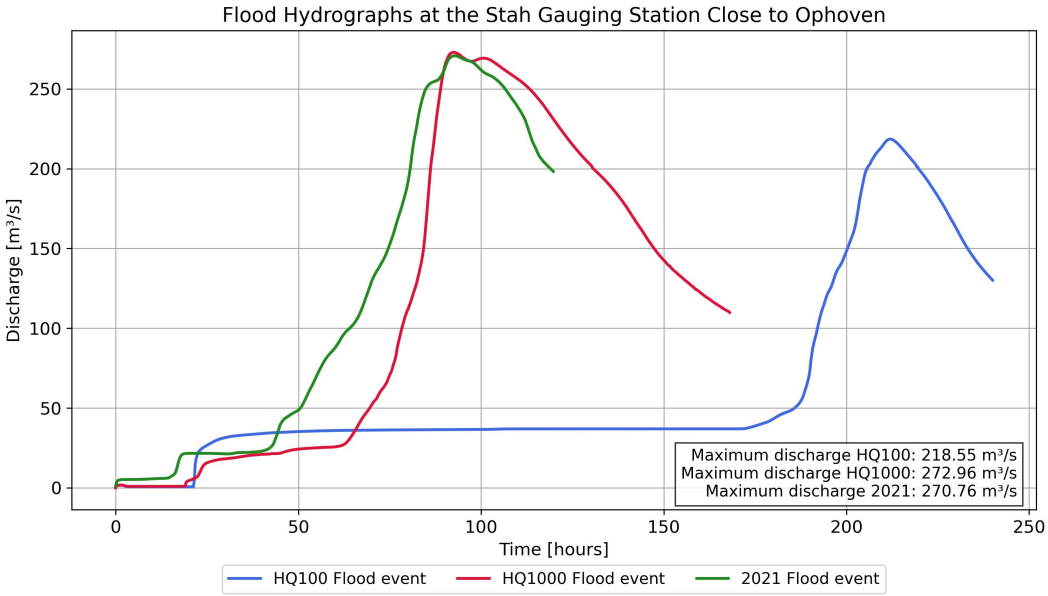

Figure 3.5: Flood hydrographs for the HQ100, HQ1000 and 2021 flood events at the Stah gauging station close to Ophoven

3.4. Flood Vulnerability of Ophoven under the HQ100 Event

In Chapter 1 the context of the 2021 flood event and its impact on the village of Ophoven was described. Although the 2021 flood has been classified as more severe than the statistically estimated 1/100 flood scenario (WVER, 2024b), in this study first detention basin operation for a HQ100 event is optimized.

The HydroAS2D results for the HQ100 scenario in the current state (i.e. without basins) are shown in Figure 3.6) and serve as reference to quantify the mitigation due to detention basins. It can be seen that for the HQ100 flood wave, the inundation of Ophoven is limited primarily to the outskirts and agricultural land (indicated by the red dashed circle). In these areas, the maximum observed inundation depth was approximately 35 cm.

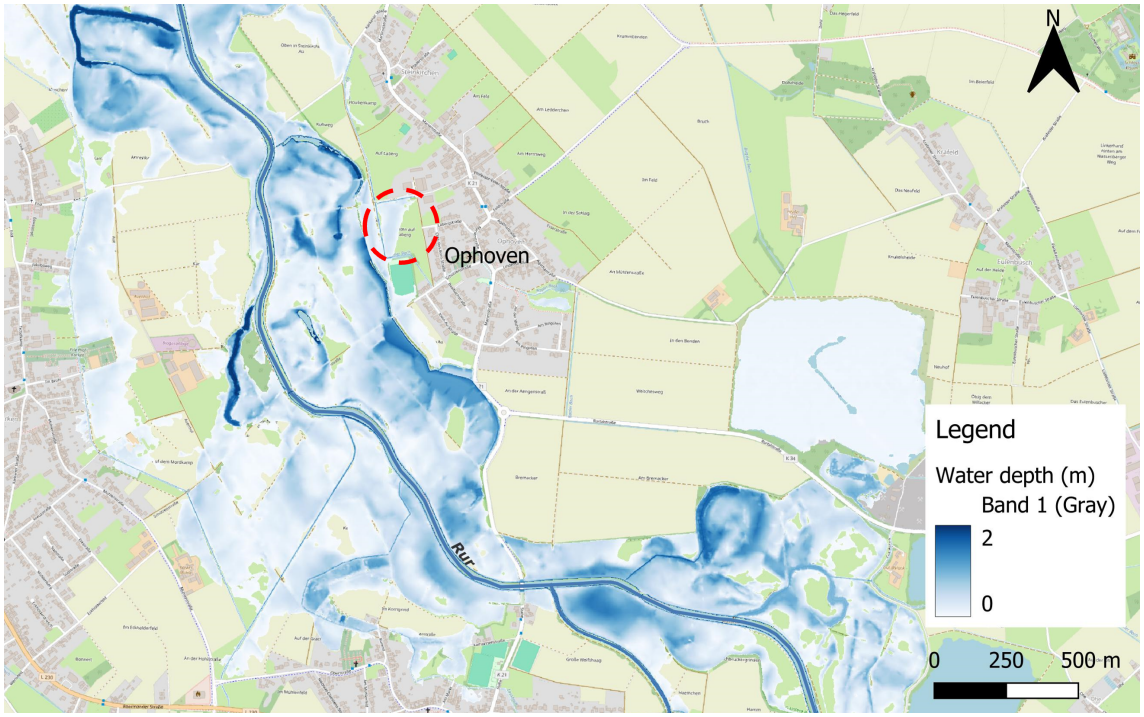

Figure 3.6: Results for the maximum inundation depths at Ophoven from HydroAS2D for the HQ100 flood event.

Ideally, the goal of the detention basins is to reduce the local water depth near Ophoven by 35 cm during the HQ100 flood event. Initially, the four proposed detention basins, as introduced in this chapter, will be assessed to determine the maximum peak reduction they can achieve. A similar approach will then be applied to the Indesee basin, where the potential peak reduction is investigated. After this, the minimum required storage volume to achieve the 35 cm reduction goal will be estimated, determining the necessary storage to meet this target.

3.5. Real-Time Operation of Detention Basins

In this study, a theoretical approach is applied, where it is assumed that the flood hydrograph can be determined in advance. In a real-world flood scenario, the flood hydrograph must be forecasted using hydrological models, measurements from gauging stations and dam operation protocols. To enable determining the optimum operational strategy of the basins depending on the flood wave, the gauging stations and dam should be situated far enough upstream of the first basin such that (at least) the main peak of the flood wave is known before it arrives at the first basin to determine the optimum operation of the basin(s). The propagation time from the gauging station or dam to the basin depends on the high wave speed. The propagation time must therefore be forecasted, to estimate the arrival of the peak. One potential approach would be through velocity measuring stations, like an ultrasonic Doppler.

Figure 3.7 shows the locations of the available gauging stations, represented by green triangles, and the existing dams, indicated by red squares. The objective is to investigate the current dams and sta-

tions to assess how real-time data could perhaps be used for forecasting and subsequently optimizing operations during actual flood events.

The studied reach begins at the Jülich-Stadion gauging station. Approximately 30 kilometers upstream, the Obermaubach dam is located, and its operation significantly influences the downstream discharge. Thus, the management of this dam is crucial for the real-time control of the detention basins, investigated in this study.

An approach for real-time operation, using the data from the gauging stations and dams, is proposed in Section 5.7.

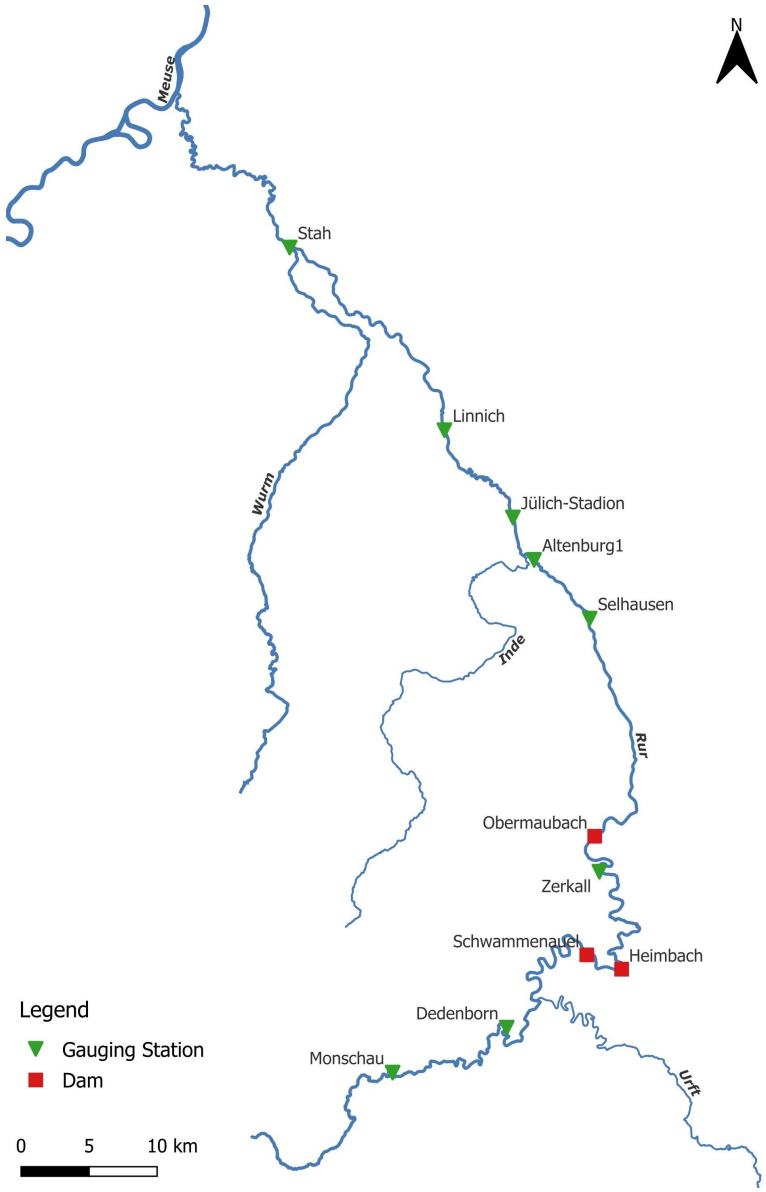

Figure 3.7: Gauging stations and dams along the Rur river. Data source: LANUV (2024). Map made within QGIS with OSM.

4

Methodology

In this chapter the methodology to investigate the optimal operating strategy for potential detention basins at the Lower Rur in Germany is described. The research structure is outlined, explaining how the applied methods align with the research objectives and research questions. A major part of the chapter is dedicated to describing the 1D kinematic flow model and the optimization problems.

4.1. Structure of the project

In the first stage of the project a 1D analytical model capable of simulating flow into detention basins was made. Methods for determining the parameters of the model will be described. The 1D model provides a first estimate of the most effective operational strategies, which are then compared to the results of the German 2D hydrodynamic model HydroAS2D. The 1D model requires computation times of minutes compared to days for the two-dimensional model. Therefore, finding an optimal operational strategy for opening the weirs, is only feasible with the 1D model. It is expected that the optimizations using the 1D model will help to understand phenomena at least qualitatively and will give insight in tendencies and dependencies.

The structure of the research is shown schematically in Figure 4.1. In the following subsections, each component of the methodology is explained in further detail, with the exception of the detention basin site investigation and flood scenario analysis, which are discussed in Chapter 3.

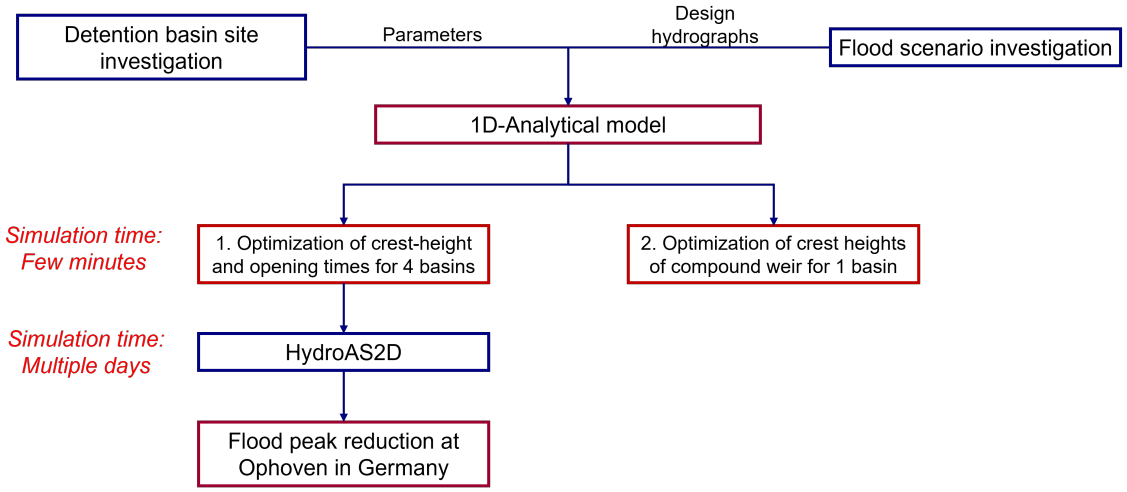

Figure 4.1: Flowchart of the project with all main activities.

4.2. 1D Analytical Model

The 1D model is based on the classical De Saint-Venant equations, which express the conservation of mass in Eq. (4.1) and the conservation of momentum in Eq. (4.2):

$$B\frac{\partial h}{\partial t} + \frac{\partial Q}{\partial x} = 0, \tag{4.1}$$

$$\frac{\partial Q}{\partial t} + \frac{\partial}{\partial x}\left(\frac{Q^2}{A_c}\right) + gA_c\frac{\partial h}{\partial x} + c_f\frac{|Q|Q}{A_c R} = 0, \tag{4.2}$$

where x is the coordinate along the main river, t is time and

$Q(x,t)$ = total discharge through a cross-sectional plain at x at time t in [m^3/s]
$h(x,t)$ = water height at x with respect to a fixed level and at time t in [m]
B = channel width in [m]
A_c = conveyance area in [m^2]
c_f = bed resistance coefficient [$-$]
R = hydraulic radius in [m]
g = gravitational acceleration in [m/s^2]

4.2.1. Derivation of the Kinematic Wave Equation

For convenience a brief summary is given of the derivation of the kinematic wave equation following the treatment in Battjes and Labeur (2017). For flood waves, the quasi-static-approach is often used, where the acceleration terms in the momentum equation are neglected. This is justified for flood waves in the Rur in Appendix C and leads to

$$gA_c\frac{\partial h}{\partial x} + c_f\frac{Q^2}{A_c R} = 0, \tag{4.3}$$

where $|Q|Q = Q^2$ was used since the flow is unidirectional (neglecting any backwater effects). For uniform flow, the gradient of the water depth $d = h - Z_b$, where Z_b is the bed, vanishes. Hence $\partial h/\partial x = \partial Z_b/\partial x = -i_b$, where i_b is the bed slope. Substituting $A_c = B_c d$, where B_c is the conveyance width and applying the shallow water assumption: $R = d$, it follows from (4.3)

$$Q = B_c d^{3/2}\sqrt{\frac{g i_b}{c_f}}. \quad (\text{ uniform flow}). \tag{4.4}$$

It is important to note that the (dimensionless) friction coefficient c_f depends on the water depth d. However, according to Eq. (4.5) in Battjes and Labeur (2017), c_f can be expressed in Manning's coefficient n [s/m$^{1/3}$] which is independent of water depth:

$$\frac{1}{\sqrt{c_f}} = \frac{1}{n}\frac{d^{1/6}}{\sqrt{g}}. \tag{4.5}$$

Substitution of () into (4.4) gives:

$$Q = \frac{B_c}{n}d^{5/3}\sqrt{i_b}. \tag{4.6}$$

Using Manning's coefficient is useful for calibration because HydroAS2D provides values for n for the floodplains and the main river along the Rur. It follows from (4.6) that the uniform flow discharge Q is a function of water depth d only: $Q = Q(d)$. In the quasi-uniform approach, this relation is assumed to be valid also for flood waves. Substitution into Eqn. (4.1) and applying the chain rule then leads to the kinematic wave equation for the water depth

$$\frac{\partial d}{\partial t} + c_{HW}\frac{\partial d}{\partial x} = 0, \tag{4.7}$$

where the speed of the flood wave ("the high wave speed") is given by

$$c_{HW} = \frac{1}{B}\frac{dQ_u}{dd} = \frac{5}{3}\frac{B_c}{B}d^{2/3}\frac{\sqrt{i_b}}{n} = \frac{5}{3}\frac{B_c}{B}U, \tag{4.8}$$

where $U = Q/A_c = Q/(B_c d)$ is the flow velocity. The high wave speed is of the order of magnitude of the flow velocity. In subcritical flow regimes, the flow velocity is smaller than the classical long wave speed and, if $B_c/B < 3/5$, also c_{HW} is smaller than the long wave speed. The value of c_{HW} is important to achieve an accurate prediction of the arrival time of the flood wave. The formula (4.8) which has been derived for uniform flow may not be accurate enough for flood waves. Therefore c_{HW} is determined by an alternative method explained in Section 4.3.

According to the kinematic model the wave height and length do not change while the flood wave propagates downstream. This is referred to as kinematic wave behavior. Solutions $d(x,t)$ and $Q(x,t)$ that satisfy $d(x=0,t) = d_0(t)$ and $Q(x=0,t) = Q_0(t)$ are:

$$d\,(x,t) = d_0\left(t - \frac{x}{c_{HW}}\right), \tag{4.9}$$

$$Q\,(x,t) = Q_0\left(t - \frac{x}{c_{HW}}\right). \tag{4.10}$$

A more accurate model is the diffusion model where it is not assumed that the gradient of the water depth vanishes. The discharge Q is then expressed in terms of both the water depth d and its derivative $\partial d/\partial x$. In this model the broadening and lowering of the flood wave during propagation due to friction is taken into account.

4.2.2. Modeling Floodplains

Incorporating floodplains in the model is important because of their significant size along the Lower Rur river and their impact on reducing local water depths. Since the proposed detention basins are situated behind the existing dikes, water must first flow across the floodplains before reaching the inlet structure of the detention basins. The water height on the floodplain, determines the flow rate into the detention basins. This will be further elaborated on in Section 4.2.3.

The floodplains near the inlets of the basins are modeled by dividing cross-sections into segments, and defining for every segment a mean bed elevation. To improve the accuracy, several cross-sections can be chosen. The interfaces between the segments is vertical and it is assumed that the interfaces are plains of zero shear where no transfer of momentum takes place. This "Divided Channel Method" is called the Vertical Interface Method (Subramanya, 2009). Other (more empirical or more numerical) methods to solve the compound channel distribution problem exist. For a review see (Cao, 2006; Sturm, 2001).

The minimum number of segments in a cross-section is three: the main channel and a floodplain on each side of the main channel. However, if needed a segment can be subdivided further. Each segment has its own bed roughness. Because the water height h is with respect to the standard level "Normalhöhennull" NHN, the water height in the 1D model is the same in all regions of a given cross-section. The average water depth d_j in every segment j can be determined if the water height is known:

$$h = d_j + \overline{Z}_{bj}. \tag{4.11}$$

where $\overline{Z}_{bj}$, is the bed level averaged over segment j with respect to NHN. Note that this convention implies that if there is no water on a particular segment j, i.e. if $d_j = 0$, then the water height in the segment is equal to the bed level $\overline{Z}_b^{(j)}$ averaged over that segment.

Here and in the rest of this section three segments are used. This is illustrated in Figure 4.2 for the case that the segments have rectangular shape and hence the bed levels Z_{bj} are equal to their averages

$\overline{Z}_{bj}$. Figure 4.5 shows are more general case, where the horizontal red dashed lines are the averaged bed levels of the three segments. The generalization to more segments is straightforward.

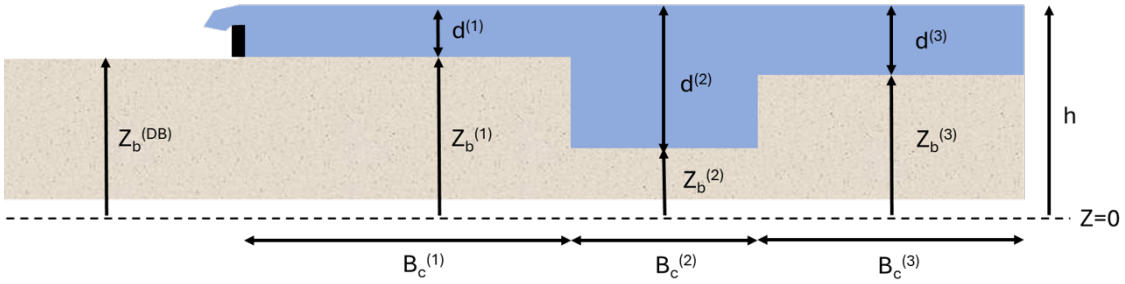

Figure 4.2: Cross-section of the main channel and floodplains, assuming a rectangular shape. In this case the bed levels are the same as their averages. The crest of the weir is also indicated in the left floodplain.

The momentum equation is applied to each segment separately, resulting in the division of the total discharge among the three segments:

$$Q^{\text{tot}} = Q_1 + Q_2 + Q_3, \tag{4.12}$$

where

$$Q_j = \frac{B_{c,j}}{n_j} d_j^{5/3} \sqrt{i_b}, \tag{4.13}$$

and $B_{c,j}$ and n_j are the conveyance width and the Manning coefficient for segment j, respectively. The bed slope i_b in Eqn. (4.13) is assumed to be the same for all three segments in contrast to the bed roughness which can differ for each segment. In particular on the floodplains vegetation can change the roughness characteristics depending on the season. The mass balance becomes:

$$(B_{c1} + B_{c2} + B_{c3}) \frac{\partial h}{\partial t} + \frac{\partial Q^{\text{tot}}}{\partial x} = 0, \tag{4.14}$$

where the first term represents the net increase of volume of mass and the second term describes the net outflow of mass. It follows by substituting Eqn. (4.13) into Eqn. (4.12):

$$Q^{\text{tot}} = \sum_{j=1}^{3} \frac{B_{c,j}}{n_j} d_j^{5/3} \sqrt{i_b}. \tag{4.15}$$

By using Eqn. (4.11), d_1, d_2 and d_3 can be eliminated and Q^{tot} can be expressed in the water height h:

$$Q^{\text{tot}} = \left[\frac{B_{c1}}{n_1} [h - Z_{b1}]_+^{5/3} + \frac{B_{c2}}{n_2} [h - Z_{b2}]_+^{5/3} + \frac{B_{c3}}{n_3} [h - Z_{b3}]_+^{5/3} \right] \sqrt{i_b}. \tag{4.16}$$

where the following notation is used:

$$[x]_+ = \begin{cases} 0 & \text{if } x \leq 0, \\ x & \text{if } x > 0 \end{cases} \tag{4.17}$$

This guarantees that if $(d_1 = h - Z_{b1})$ is zero or negative, the discharge on floodplain 1 is zero. Similar remarks apply to the other two terms in Eqn. (4.16)

For given total discharge $Q^{\text{tot}}(t)$ somewhere upstream (e.g. the hydrograph), the water height $h(t)$ at the same position and time can be determined by solving Eqn. (4.16) numerically using the Newton-Raphson scheme for every time step. Eqn. (4.18) shows the classical Newton-Raphson iteration

equation for solving an equation of the type $y = f(x)$ for x and Eqn. (4.19) gives the Newton-Raphson Equation combined with the finite difference method for the derivative.

$$x_{n+1} = x_n - \frac{f(x_n)}{f'(x_n)} \tag{4.18}$$

$$x_{n+1} = x_n - \frac{f(x_n)}{\frac{f(x_n+\delta)-f(x_n)}{\delta}} \tag{4.19}$$

Once $h(t)$ has been determined, the water depths $d_1(t)$ and $d_3(t)$ at the floodplains and the water depth $d_2(t)$ in the main river follow from Eqn. (4.11).

4.2.3. Modeling Flow into Detention Basins

The detention basins are positioned adjacent to floodplains, as illustrated in Figure 4.3. At each time step, the water depth on the adjacent floodplain determines the volume of water flowing into the detention basin. In case the adjacent floodplain is dry or the water height is below the crest height of the weir of the basin, there is no inflow into the detention basin.

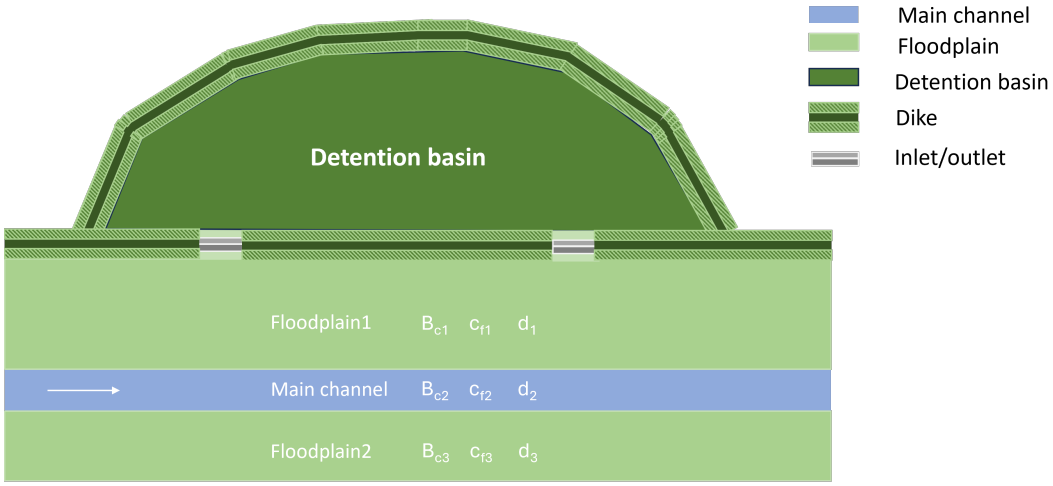

Figure 4.3: Aerial view of a detention basin, floodplains and main channel.

The weir equation, provided in the HydroAS2D user manual (Hydrotec Ingenieurgesellschaft für Wasser und Umwelt mbH, 2023), was used to model the discharge into the detention basins when the water level on the floodplain is higher than the crest of the weir. This equation by Poleni (1717) contains an empirical coefficient μ, which is selected based on the shape of the inlet structure. μ was chosen to be 0.5, which corresponds to a weir that is wide, with rounded edges, and horizontal, according to Poleni (Gerner and Blaurock, 2018). There is of course only flow into the basin when the water height on the floodplain adjacent to the basin is higher than the crest and higher than the water in the basin. In that case the discharge into the basin is:

$$Q_{\text{weir}}(t) = \tfrac{2}{3} \cdot \mu \cdot b \cdot \sqrt{2g} \cdot c_s \cdot [h(t) - H_c]_+^{3/2}, \quad \text{if } h(t) > H_c \text{ and } h(t) > h_b(t), \tag{4.20}$$

where the reduction factor c_s is given by:

$$c_s = \sqrt{1 - \left(\frac{[h_b(t) - H_c]_+}{[h(t) - H_c]_+}\right)^{16}} \tag{4.21}$$

and

$Q_{weir}(t)$ = discharge in $[m^3/s]$ at time t
μ = discharge coefficient [-]
b = weir width in $[m]$
$h(t)$ = water height on the floodplains and in
= the main channel in $[m]$ at time t.
$h_b(t)$ = water height in $[m]$ in the basin at time t
H_c = crest height of the weir $[m]$
g = gravitational acceleration in $[m/s^2]$

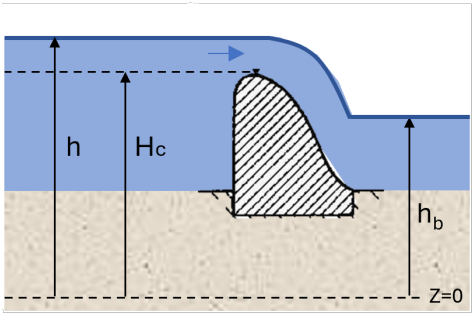

Figure 4.4: Side-view weir over flow with parameters

The velocity head $v^2/(2g)$, where v is the flow velocity perpendicular to the weir, has been neglected in (4.20). Hence instead of the energy, the height of the upstream water level above the crest: $h - H_c$ is used. A justification is given in e.g. (Hager, 1987), stating that this term may be neglected for lateral weirs.

Note that $h(t)$, $h_b(t)$ and H_c are all with respect to the NHN level. Because of the function $[.]_+$ (defined in Eqn.4.17), the weir inflow is zero until the water height $h(t)$ on the floodplain exceeds the crest height H_c. Furthermore, the function $[.]_+$ ensures that the correction factor c_s is equal to one at the times that the water height in the basin $h_b(t)$ is lower than the crest height H_c. The factor c_s becomes less than 1 only when the water heights on the floodplain and the basin are nearly equal and the weir is submerged, i.e. $h_b(t) > H_c$.

4.3. Estimation of the Parameters of the 1D Model

It is important to obtain an accurate value for the water height h on the floodplain adjacent to the inlet because this water height determines the inflow in the basin. The water height can be obtained from the total discharge $Q^{\text{tot}}(t)$ using Eqn. (4.16). But this equation depends on the way the cross-section at the inlet is modeled and on values for the bed elevation, friction coefficients and bed slope.

4.3.1. Approximations of Cross-Sections at Inlets of Detention Basins

For each detention basin, the inlet locations were chosen based on the Digital Elevation Model (DEM) as provided by WVER to determine sites where water is most likely to flow to the detention basin (Figure 3.4). For every inlet, four cross-sections were drawn from terrain data every 15 meter, based on the DEM. The cross-sections were divided into at least three segments along the Y-direction (see Fig. 4.5). The bed elevations are referenced to the local datum NHN. The average bed elevation value for each segment was computed by averaging $Z_b(y)$ over the segment (Eqns. 4.22 to 4.24). In the example shown in Figure 4.5, the cross-section is divided into three segments along the Y-direction (two floodplains and the main channel) and the averages are:

$$\overline{Z}_{b1} = \frac{1}{B_{c1}} \int_{y_1}^{y_A} Z_{b1}(y)\, dy \tag{4.22}$$

$$\overline{Z}_{b2} = \frac{1}{B_{c2}} \int_{y_A}^{y_B} Z_{b2}(y)\, dy \tag{4.23}$$

$$\overline{Z}_{b3} = \frac{1}{B_{c3}} \int_{y_B}^{y_2} Z_{b3}(y)\, dy \tag{4.24}$$

where: $B_{c1} = y_A - y_1$, $B_{c2} = y_B - y_A$ and $B_{c3} = y_2 - y_B$. If h is a water height which is higher than $\overline{Z}_{b2}$, we have

$$\int_{y_A}^{y_B} [h - Z_{b2}]\, dy = B_{c2}(h - \overline{Z}_{b2}). \tag{4.25}$$

This shows that, provided the water height is above the averaged bed level $\overline{Z}_{b1}$, the conveyance area above the actual bed $Z_{b1}(y)$ of segment 1 is identical to the area of water in the region $y_1 < y < y_A$ above the averaged bed level $\overline{Z}_{b1}$. The same remark applies to the conveyance areas of the other segments.

The four values for the water height h obtained from Eqn. (4.16) for each of the four cross-sections at a given inlet are averaged and this average value is then used in the weir equation to determine the flow into the basin.

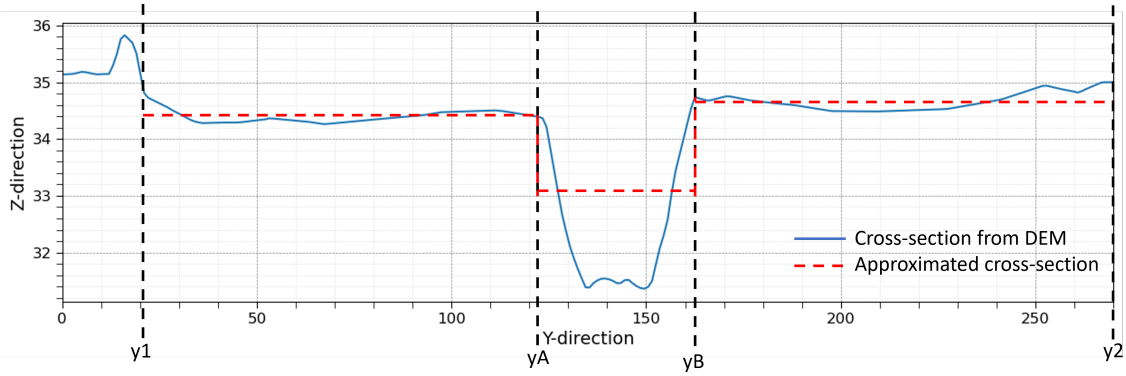

Figure 4.5: Example where the cross-section along the y-direction is divided in three segments.

Since the river cross-sections vary along the length of the inlet, four cross-sections were chosen at every inlet. Depending on the complexity of a cross-section, it was divided into a number of segments, in each of which the actual bed was replaced by an averaged bed value. The four values for the water height h obtained from Eqn. (4.16) for each of the four cross-sections at a given inlet were averaged and this average value was then used in the weir equation to determine the flow into the basin. The chosen cross-sections and their approximations for each of the inlets of the basins as proposed by Schweim (2024) are shown in Appendix D.

4.3.2. Friction Coefficients

In the previous section, the dimensionless friction coefficient c_f was converted into a Manning friction coefficient n. This conversion was done because, in HydroAS2D, each mesh is assigned a Strickler friction coefficient. This coefficient has been extracted at each inlet location in the main channel and on the floodplains. The Strickler friction coefficient is inversely proportional to the Manning coefficient ($K = 1/n$), making it possible to use the friction coefficients from HydroAS2D in the 1D model. In contrast to the c_f coefficient, the Manning coefficient is independent of water depth. Therefore, Eqn. (4.16) should be used instead of Eq, (4.15) to determine the water depths from the total discharge.

The Manning friction coefficients of the different sections which are used to calculate the water height in the cross-sections of the river and the floodplains at the four detention basin inlet locations are listed in Table 4.1. For the fourth detention basin two friction coefficients are given for the main channel: the transition to the floodplain has a Manning friction coefficient of 0.020 $[m^{-1/3}s]$, while the remainder of the main channel has a friction coefficient of 0.03030 $[m^{-1/3}s]$.

Table 4.1: Manning's friction coefficients $[m^{-1/3}s]$ for each river section at the detention basin inlet locations.

	Left Floodplain	Main Channel	Right Floodplain	Right Upland
Detention Basin 1	0.050	0.0303	0.040	0.055
Detention Basin 2	0.050	0.0303	0.040	0.055
Detention Basin 3	0.040	0.0303	0.040	-
Detention Basin 4	0.050	0.020/0.0303	0.050	-

4.3.3. Bed Slopes

The bed slope i_b has been determined using the DEM by drawing a longitudinal cross-section of the Rur river and estimating $\Delta z/\Delta x$. The bed slope has been estimated for each detention basin inlet location and is approximately 0.001 for the entire region studied in this research. The slope on the floodplains and the main river are the same. The results for the bed slopes are listed in Table 4.2.The estimates agrees with the findings of Woolderink et al. (2021), who studied patterns in river channel sinuosity for the Rur River.

Table 4.2: River bed slope at the detention basins.

	Detention Basin 1	Detention Basin 2	Detention Basin 3	Detention Basin 4
River Bed Slope [-]	0.0016	0.0016	0.0010	0.00085

4.3.4. Storage Capacity of the Detention Basins

Detention basins are normally dry and are only filled during flood events when storm water needs to be captured. The term 'basin' in this context does not refer to an excavated pond, but to a natural or agricultural area that can be intentionally flooded. The retention volume of basins therefore depends on characteristics of the local site such as the terrain and dike heights.

Potential detention basin site locations along the Rur river have been previously investigated by Schweim (2024). Four locations were identified by removing existing dikes in the 2D hydrodynamic model HydroAs2D and simulating the flow. The results were then compared to the reference case without dike removal to assess the areas with the most retained volume. This MSc project builds upon and extends the study in Schweim (2024), by initially using the identified sites, determining efficient inlets and by optimizing the times of opening of the basins and the crest heights. It is assumed that the chosen crest heights are lower than the dikes surrounding the basin.

Hence the basin is considered full when the water height reaches the crest height. Within QGIS it is possible to estimate the volume of water in the basin for a given crest height. Figure 4.6 shows the DEM for one of the detention basin locations, where the colors represent elevation heights with respect to the local datum NHN. Due to the strongly varying topography of the terrain (which contains a lot of areas of varying heights), the volume of water that can be stored strongly varies with the crest height. The relation between storage volume and crest height for the four basins is shown in Figure 4.7.

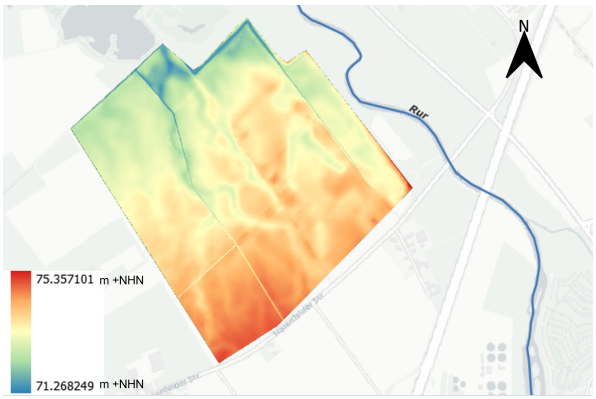

Figure 4.6: DEM of the first detention basin close to Jülich.

It can be seen that for example for detention basin 1 the volume of water in the basin increases by a factor of 3 when the crest height increases from 73.4 cm to 74.0 cm.

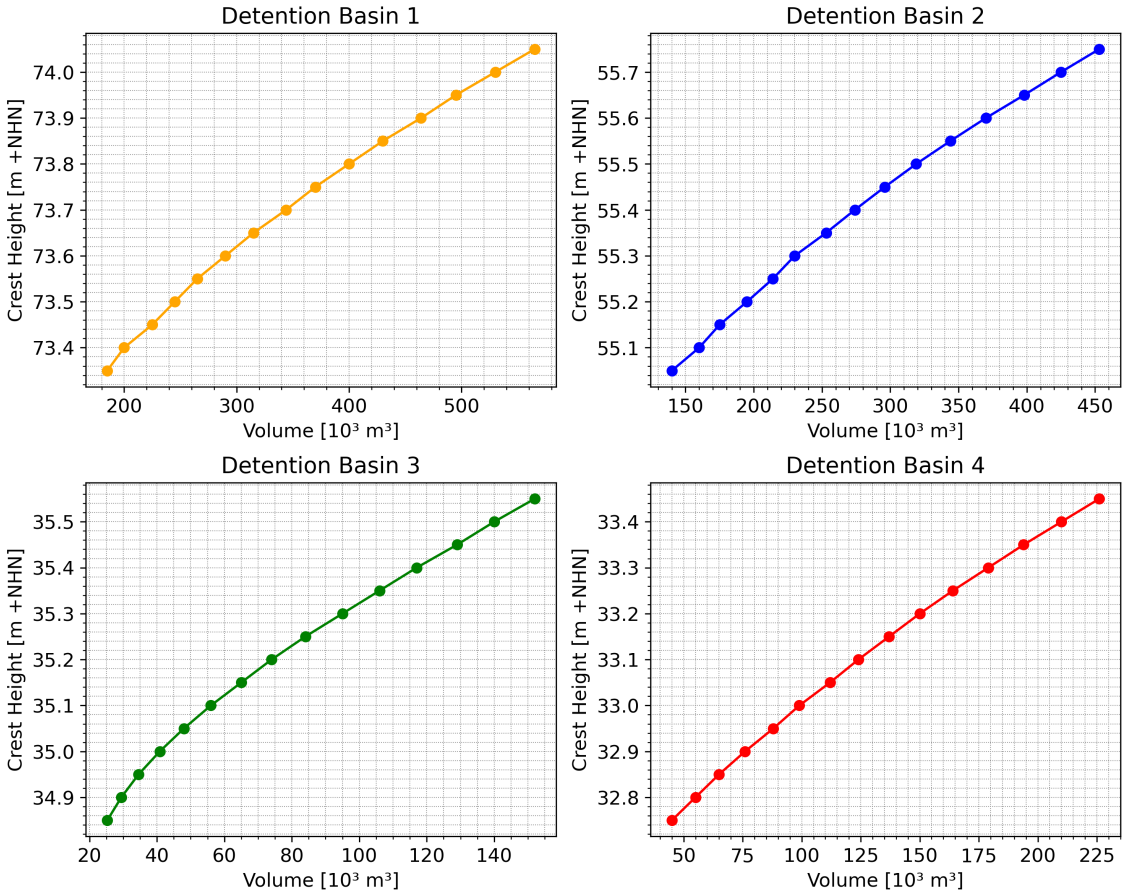

Figure 4.7: Volume of the detention basin for different crest heights.

4.3.5. Hydraulics of the Detention Basins

Detention basins consist of inlet and outlet structures that control water flow into and out of the basin. For this study, only the inlet structure is considered. In the first optimization problem that is studied it is assumed that as soon as the basin is full, i.e. when the water height in the basin equals the crest height of the weir, the inlet will be closed. The basin will be emptied only sufficiently long after the flood wave has passed, making the outlet structure less relevant.

The width of the inlet structure and the crest height of the weir are critical parameters, as they determine the capacity for water to flow into the detention basin. A width of 60 m has been used in most of the simulations, similar to Schweim (2024).

4.4. Optimization of Detention Basin Operation

The introduction and literature review have provided background information on the potential benefits of actively controlling detention basins to reduce flood peaks. The optimal timing for opening the inlet of a detention basin depends on factors such as the peak and duration of the flood wave, the volume of the basin and the dimensions of its inlet structure. To determine the optimal opening time and the optimal crest height, a mathematical optimization model has been developed that uses the one-dimensional analytical model in the simulations to estimate the effects of different opening times and crest heights of the weirs of the basins.

The optimization routine is performed separately for each detention basin. For a given incoming total discharge Q_0^{tot} as function of time at a particular basin, the aim is to determine the opening time and the crest height for which the flood peak (maximum discharge) just downstream of the weir of the detention basin is minimum. The downstream total discharge Q^{tot} is the input discharge Q_0^{tot} minus the discharge Q_{weir} into the basin.

The procedure is repeated four each of the four basins. It is therefore sufficient to consider here the optimization of the opening time and the crest height for one basin.

In the operated weir scenario, it is assumed that initially the crest height is so high that no water can enter the basin. Then at a certain time t_1 ("the opening time of the weir") the crest is lowered to some suitable value H_c. Both the opening time of the weir and the crest height are optimized, with the crest heights varying in steps of 5 cm between 5 and 75 centimeters above the inlet bed level and referenced to NHN. The time t_2 is the time that the water height in the basin equals the crest height. This is the time at which the basin is filled for this crest height and it is assumed that at t_2 the weir is closed. It is possible for certain opening time and crest height that the basin is never completely filled. In that case t_2 is defined as: $t_2 = \infty$

The optimization problem for one basin is formulated as follows:

*For a given maximum storage capacity $V_{max}(H_c)$ of the basin as function of crest height H_c (which for the four basins along the Rur was determined in Section 4.3.4), determine the weir opening time t_1 and crest height H_c such that the **peak discharge** ($\max_t Q^{\text{tot}}(t; t_1, H_c)$) just downstream of the detention basin is **minimum***:

$$\min_{t_1,\, H_c} F(t_1, H_c) \tag{4.26}$$

where:

$$F(t_1, H_c) = \max_t Q^{\text{tot}}(t; t_1, H_c) \tag{4.27}$$

$$Q^{\text{tot}}(t; t_1, H_c) = Q_0^{\text{tot}}(t) - Q_{\text{weir}}(t; t_1, H_c) \tag{4.28}$$

$Q_0^{\text{tot}}(t)$ is the discharge just before the weir (for the first basin this is the given hydrograph)

$$Q_{\text{weir}}(t; t_1, H_c) = \begin{cases} \frac{2}{3} \cdot \mu \cdot b \cdot \sqrt{2g} \cdot [h(t) - H_c]_+^{3/2} & \text{if } t_1 \le t \le t_2 \text{ and } h(t) - H_c > 0, \\ 0, & \text{otherwise} \end{cases} \tag{4.29}$$

where the time t_2 at which the basin is full depends on t_1 and $V_{\text{max}}(H_c)$ and is determined from:

$$\int_{t_1}^{t_2} Q_{\text{weir}}(t; t_1, H_c)\, dt = V_{\text{max}}(H_c). \tag{4.30}$$

Solving this equation for t_2 gives the time when the basin has been filled to volume $V_{\text{max}}(H_c)$, for given opening time t_1, crest height H_c and the other weir parameters. As mentioned above, for cases that the basin is not filled completely, t_2 becomes infinite.

A larger crest height implies a larger maximum storage volume, i.e.V_{max} is an increasing function of H_c. An exception is the case that the basin is so deep that $V_{\{}$max can be considered to be independent of crest height. This happens for the Indesee basin.

Note that the factor c_s given by Eqn. (4.21) has been omitted in equation (4.37). This is because the factor is always equal to 1 since the weir will never be submerged, as it remains closed whenever V_{max} is exceeded.

4.4.1. Optimization Procedure for One Detention Basin

Under normal conditions, the floodplains remain dry. However, when a flood wave occurs, the water depth on the floodplain rises to a peak and then decreases again to zero. The water height on the floodplain adjacent to the detention basin as estimated using the one-dimensional model were used in the optimization procedure to determine the inflow through the weir.

The opening time t_1 marks the moment when water is allowed to enter the detention basin. At this time, the crest height H_c of the inlet weir is decreased to a certain level H_c. The time t_c is the first time that the water height h is equal to H_c, i.e.

$$h(t_c) = H_c. \tag{4.31}$$

If the optimum opening time t_1 is before t_c, i.e. $t_1 < t_c$, water will only flow into the basin after time t_c. Hence, if the optimum opening time were t_c, then any opening time before t_c is also optimum and hence the opening time is not critical. The crest height is important because it determines both the rate at which water flows into the basin and the total volume of water which the basin can store. A higher crest height results in less water entering the basin, as the water height on the floodplain then exceeds the crest height for a shorter period (if at all), and the water level above the crest will be lower. For a higher crest, the volume of water that can be stored in the basin is larger, but the flow rate into the basin is less. Conversely, with a lower crest height, more water will flow into the basin, but the volume of water that can be stored in the basin is less.

Opening the weir too early results in the detention basin becoming full before the peak has arrived, making the basin ineffective. Opening the weir after passage of the peak of the flood wave is too late because the basin will capture water only after the peak has already passed, resulting in no peak reduction. Therefore, both the opening time t_1 and the time t_2 when the basin is full are critical. Figure 4.8 illustrates the two mentioned ineffective opening scenarios and one effective opening scenario.

The following routine has been implemented in Python:

- Define a range of possible opening times t_1 and crest heights H_c.
- For all opening times t_1 and crest heights H_c compute t_2 at which the basin is full from Eqn.4.30 (t_2 = ∞ if the detention basin is not completely filled).
- For all opening times t_1 and crest heights H_c, compute the maximum discharge as a function of time just downstream of the inlet ($F(t_1, H_c)$).
- Compute the minimum of the calculated downstream discharges $F(t_1, H_c)$ as a function of t_1 and H_c and verify the results in a contour plot.

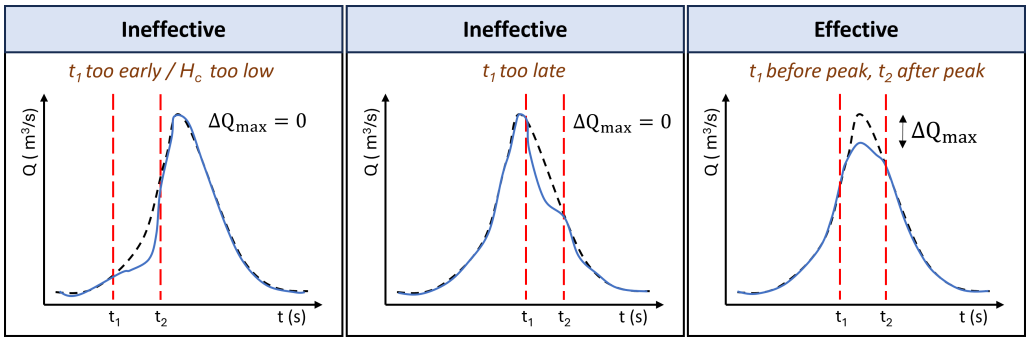

Figure 4.8: Examples of ineffective and effective opening times for an arbitrary flood wave

4.4.2. Optimization Procedure for Multiple Detention Basins

As remarked above, in the case of several basins, every detention basin is treated subsequently in the same way. The opening time and the crest height of the first weir are optimized with as input total discharge Q_0^{tot} just before the weir the given hydrograph. The reduced discharge of the flood wave due to the first detention basin, is then propagated downstream to the inlet of detention basin 2. The time of arrival of the flood wave at the inlet of basin 2 is derived from the reference run with HydroAS2D with all basins closed. The discharges of all tributaries between the two basins are also obtained from the HydroAS2D and are added to the input discharge for basin 2. After optimizing the opening time and crest height of the weir of basin 2, the reduced discharge is propagated to basin 3 and so on. The procedure for multiple detention basins is illustrated in Figure 4.9. The optimized flood wave after detention basin 4 is finally propagated downstream to Ophoven and was then converted into a water level by using Eqn. 4.16.

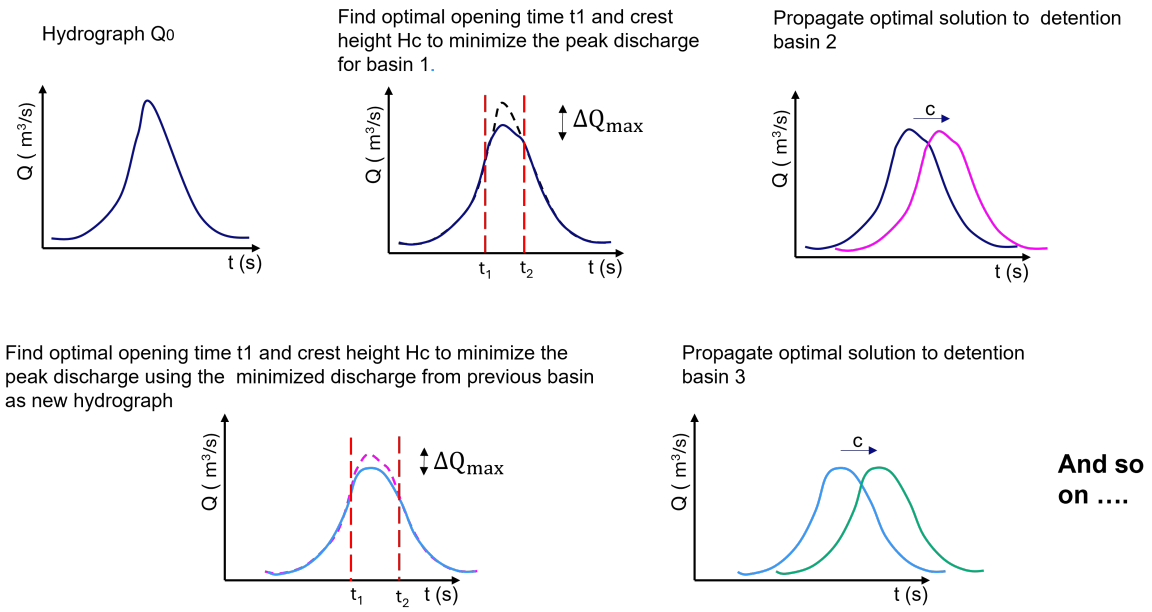

Figure 4.9: Optimization procedure for multiple basins.

4.5. Compound Weir

So far, an operable weir with a single crest has been optimized. This system has the advantage that the opening time and the crest height of the weir can be adjusted to the flood wave, allowing the flow of water into a detention basin to depend on the severity of the flood event. However, its effectiveness is significantly influenced by human operation. Additionally, there is a risk that the inlet structure may not move as intended at the critical moment due to some failure mechanism. In contrast, a compound weir with different but fixed crest heights does not depend on an operator. Therefore also the potential of a compound weir is studied by comparing its optimized crest heights to the performance of the optimized operated weir for the same flood wave. This comparison is done for only basin 1.

It is assumed that the compound weir consists of a number of crest with equal width. Initially, when the water level exceeds only the smallest crest, only small amounts of water will enter the basin. As the water level rises and exceeds the crest heights of additional segments of the weir, more water will flow into the basin. A potential disadvantage is that the basin could fill before the flood peak is reached, which could even potentially worsen the situation slightly because then water can flow back to the floodplain increasing the total discharge. A schematic representation of a compound weir with four crest heights is shown in Fig. 4.10. The crest heights of the compound weir are optimized for a given flood wave.

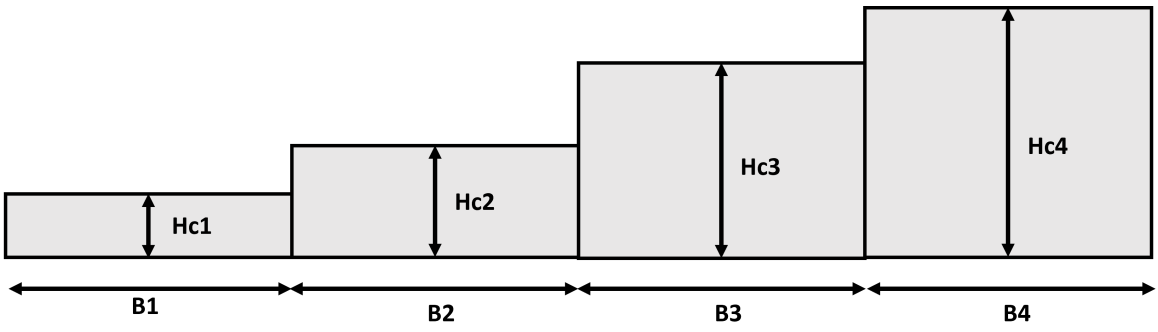

Figure 4.10: Example of a compound weir consisting of four segments (front view)

4.5.1. Modeling the Compound Weir

The compound weir is modeled in a similar manner as the operated weir. The key difference is that the inlet is now divided into a number of sections with equal widths but (in general) different crest heights. The number of sections is N.

The weir equation (4.20) is applied to each segment i of the compound weir with its own crest height $H_{c,i}$. At each time step t, the discharge $Q_{\text{weir},i}(t)$ is calculated for every segment that satisfies the conditions $h(t) > H_{c,i}$ and $h(t) > h_b(t)$, where $h(t)$ is the water height on the floodplain and $h_b(t)$ is the water height in the basin (both with respect to NHN).

The total discharge over the weir at each time step is then obtained by summing the contributions of all N sections:

$$Q_{\text{weir}}(t) = \sum_{i=1}^{N} Q_{\text{weir},i}(t)$$

In contrast to the operated weir discussed above, the static compound weir can become submerged, meaning that the water height in the detention basin exceeds at least one of the crest heights of the weir.

This situation may arise when the water level in the basin catches up with the water level on the floodplain. From this point onward, the inflow into the basin is no longer given by the weir equation (4.20). Instead, the discharge into the basin is then calculated at each time as the rate of increase of the water volume in the basin (see Figure 4.11), i.e. the volume increase ΔV_{basin} of the water in the basin during one time step ΔV_{basin}, divided by this time step:

$$\Delta V_{basin}/\Delta t. \tag{4.32}$$

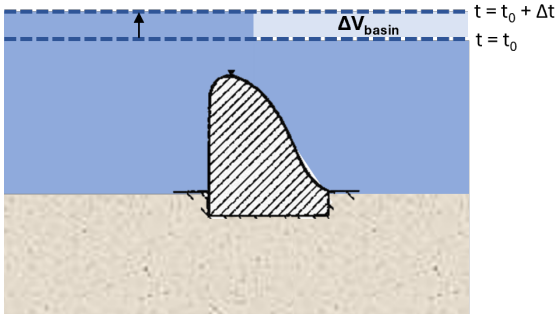

Figure 4.11: Side-view of submerged weir.

If the water level on the floodplain starts to decrease after reaching its peak, and the water levels on the floodplain and in the basin are the same, there is flow from the detention basin back to the floodplain with rate again given by Eqn. 4.32. In this case this quantity is negative.

4.5.2. Optimization of the Crest Heights

Suppose that there are N segments. The segments are indicated by the index i and the crest height of segment i is $H_{c,i}$. Without restricting the generality it may be assumed that the crest height are ordered as follows:

$$H_{c,1} \leq H_{c,2} \leq \ldots \leq H_{c,N}. \tag{4.33}$$

Furthermore the following vector notation is used:

$$\vec{H}_c = (H_{c,1}, ..., H_{c,N})$$

$h(t)$ and $h_b(t)$ are the water heights on the flood plain and in the basin, respectively. Then the optimization problem is:

$$\min_{\vec{H}_c} F(\vec{H}_c) \tag{4.34}$$

where

$$F(\vec{H}_c) = \max_t Q^{\text{tot}}(t; \vec{H}_c) \tag{4.35}$$

$$Q^{\text{tot}}(t; \vec{H}_c) = Q_0^{\text{tot}}(t) - Q_{\text{weir}}(t; \vec{H}_c) \tag{4.36}$$

$Q_0^{\text{tot}}(t)$is the given hydrograph just before the weir,

$$Q_{\text{weir}}(t,\vec{H_c}) = \begin{cases} \sum_{i=1}^{N} \frac{2}{3} \cdot \mu \cdot \frac{b}{N} \cdot \sqrt{2g} \cdot \sqrt{1 - \left(\frac{[h_b(t)-H_{c,i}]_+}{[h(t)-H_{c,i}]_+}\right)^{16}} [h(t) - H_{c,i}]_+^{3/2} & \text{if } h(t) > h_b(t), \\ \frac{dV_{\text{basin}(t)}}{dt} & \text{if } h(t) = h_b(t) \text{ and } h(t) > H_{c,1}, \\ 0 & \text{otherwise}, \end{cases} \tag{4.37}$$

where it is assumed that all the parts of the weir have the same width b/N and where V_{basin} is a function of the water height h_b determined e.g. by using the DEM. It follows

$$V_{\text{basin}}(h_b(t)) = \int_{-\infty}^{t} Q_{\text{weir}}^{\text{tot}}(t';\vec{H}_c)\, dt'. \tag{4.38}$$

and

$$\frac{dV_{\text{basin}}(t)}{dt} = \frac{dV_{\text{basin}}(h_b(t))}{dh_b} \frac{dh_b(t)}{dt} \tag{4.39}$$

If $h_b(t) < h(t)$, (4.38) can be used and a look-up table of the function $h_b \mapsto V_{\text{basin}}(h_b)$ to determine $h_b(t)$. If $h_b(t) = h(t)$, then (4.39) can be rewritten as

$$\frac{dV_{\text{basin}}(t)}{dt} = \frac{dV_{\text{basin}}(h(t))}{dh} \frac{dh(t)}{dt} \tag{4.40}$$

and use the right-hand side of (4.40) to compute $dV_{\text{basin}}(t)/dt$ and then use the result in the second line of (4.37).

Since the optimization is conducted for one particular flood wave, the question arises whether the optimized compound weir will also be effective for other flood waves. This issue will be considered in Subsection 5.6.1.

4.6. HydroAS2D

The 1D model has been used to optimize detention basin operational strategies. Its recommendations for the optimal crest height of the weir and opening time have been compared to the 2D hydrodynamic model HydroAS2D. The objective is to verify whether the simplified 1D model gives results similar to those of the more complex 2D hydrodynamic model. This section will explain the modeling approach in HydroAS2D in more detail.

4.6.1. Theoretical Background

In this section the theoretical background of HydroAS2D is explained, based on the HydroAS2D user manual (Hydrotec Ingenieurgesellschaft für Wasser und Umwelt mbH, 2023).

HydroAS2D solves the two-dimensional, depth-averaged shallow water equations, which are derived by integrating the three-dimensional continuity equation and the Reynolds-averaged Navier-Stokes equations over the water depth for incompressible fluids, under the assumption of a hydrostatic pressure distribution. Solving these shallow water equations requires the specification of initial and boundary conditions. An excess of boundary conditions or those lacking sufficient precision may lead to numerical instability, producing erroneous results. For this reason, inflow and outflow boundaries are generally recommended to be positioned at a distance from areas of primary interest.

The friction slope within the model is approximated using the Darcy-Weisbach equation, assuming that the hydraulic radius is equivalent to the water depth. HydroAS2D uses a combination of empirical and constant viscosity, a method that has been shown to be accurate when appropriately calibrated. Additionally, the 1-dimensional weir equation, as explained in Section 4.2.3, is implemented to simulate flow over hydraulic structures.

Numerical solutions to the 2D depth-averaged flow equations are obtained via the finite volume method. A model in HydroAS2D can be composed of both triangular and rectangular elements, with the choice

of element type depending on topographic and hydrodynamic conditions. The selection of time steps is constrained by the Courant-Friedrichs-Lewy (CFL) stability criterion, which must be satisfied for each pair of mesh nodes to ensure numerical stability.

4.6.2. The Use of HydroAS2D in This Project

To model a detention basin in HydroAS2D the same method was applied as in the study of Schweim (2024). To simulate no-flow conditions where the dikes are located, QGIS was used to define a boundary around the detention basins. This boundary layer was used to select and deactivate the meshes in areas where flow should be restricted.

In contrast to the 1D modeling approach, where inflow into the detention basin is represented by a weir equation, in HydroAS2D the inlet of the basin is defined by activating boundary meshes to allow inflow. The specific crest height of the weir is obtained by setting the bed level at the inlet equal to the crest height. The opening of the weir is thus simulated similar to a dike breach and the closing of the weir corresponds to repairing the dike. Such an approach has been applied in previous studies, including (Homagk & Bremicker, 2006; Jaffe & Sanders, 2001).

It is not possible in HydroAS2D to set the bed level at the inlet to the desired crest height at a specific time (t_1). Instead, the water height is monitored as function of time at a gauging station in front of the inlet and the crest is lowered (i.e. the inlet is opened) when the water height corresponds to the opening time t_1. To implement this a script was written in the Lua language. The Lua-script is shown in Appendix E. The closing of the inlet at the desired time (t_2) also had to be done by monitoring a water height, now at a gauging station inside the basin.

The HydroAS2D model setup for detention basin 1 is shown in Figure 4.12, which illustrates the weir and includes the two gauging stations to monitor water heights: station 1 positioned on the floodplain just before the weir inlet, and station 2 within the detention basin. The main river in Figure 4.6 is represented by the area where the meshes are colored blue/turquoise.

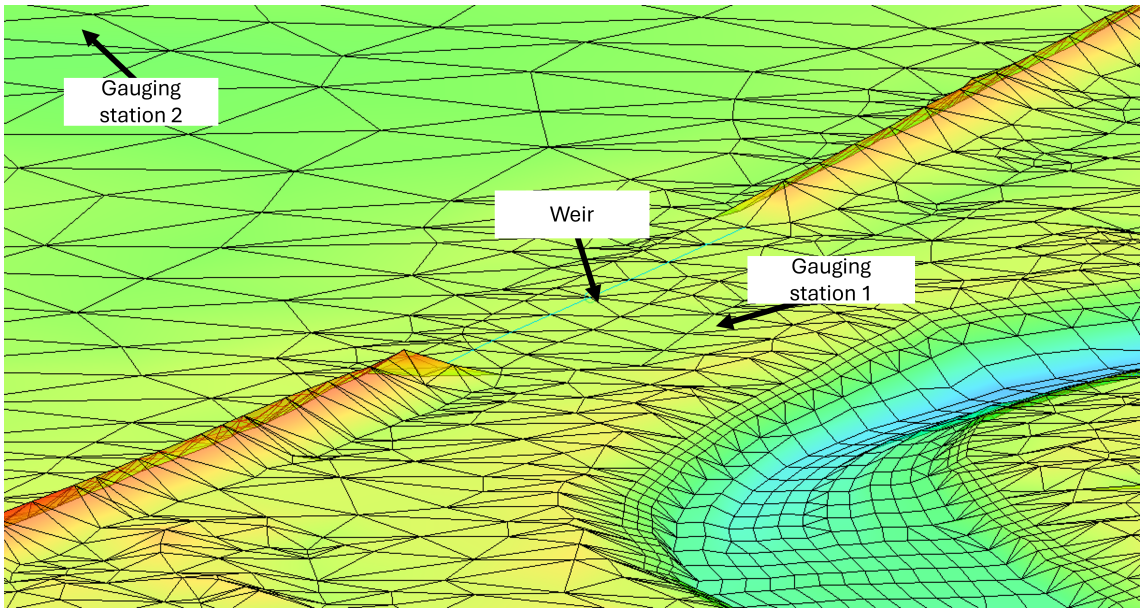

Figure 4.12: HydroAS2D model at detention basin 1 (screen-print from the model).

The Indesee, which was introduced in Chapter 3, was also modeled using HydroAS2D. As mentioned earlier in this chapter, the Indesee was modeled at the location of Detention Basin 1, since modeling it at its actual location would be highly complex due to the presence of the current mine site.

The volume of 11.6 million m^3 was simulated by deepening the 70-hectare detention basin by approximately 17 meters within HydroAS2D, which corresponds to the volume of the 1160-hectare Indesee,

assuming a water depth (buffer) of 1 meter. The operational procedure, involving the opening and closing of the basin and adjusting the crest height to the desired level, was executed in the same manner as previously described, using the Lua script.

4.6.3. Available Resources During This Project

The simulation time in HydroAS2D depends on factors such as the license configuration, with certain licenses providing more computational resources, and the PC setup, including the number of processing cores. For the specific license and PC setup available in this study, simulating one operation strategy for half of the Rur river reach takes approximately 2.5 days, while simulating the entire reach requires around 5 days.

At the start of this thesis, the most recent HydroAS2D software release was version 6.1.1. However, it was determined that the Rur river model was incompatible with this version, as the model had been developed in an earlier version that used a different modeling approach for 1D elements. Consequently, version 5.2.5 was used for this study. Unfortunately, this version lacked the capability to define initial conditions, meaning each simulation had to be run from the first timestep.

4.7. Error Analysis

The 1D model is expected not yield the same water height values as HydroAS2D. Assuming that HydroAS2D is more accurate and, therefore, more reliable, this section introduces a method to quantify the error between the two models.

Suppose that the water height h_2 just before the inlet of a basin has been obtained as function of time either by measurements or by computations using a model such as HydroAS2D which is expected to be more accurate than the 1D model. Let $h_1(t)$ be the water height at the same position as used in the 1D analytical model. The difference $\Delta h(t) = h_2(t) - h_1(t)$ is for convenience referred to as the "upstream error". It is of interest to quantify how this error is propagated downstream of a weir, i.e. what the downstream error is induced by this upstream error. The downstream error is evaluated using the 1D model and it is computed relatively close downstream of the weir.

To determine the downstream error, we need derivatives with respect to water height h of the discharge over the weir and of the total discharge of the river and the floodplains. The case of an operated weir is considered, for which the discharge over the weir is given by (4.37). Its derivative is:

$$\frac{dQ_{\text{weir}}(t)(h)}{dh} = \mu\, b\, \sqrt{2g}\, [h(t) - H_c]_+^{1/2}. \tag{4.41}$$

The derivative of the discharge in river and floodplains follows from (4.12):

$$\frac{dQ^{\text{tot}}(t)(h)}{dh} = \frac{5}{3}\sqrt{i_b} \sum_j \frac{B_{cj}}{n_j} [h(t) - Z_{bj}]_+^{2/3}. \tag{4.42}$$

where the summation is over the segments that have been chosen in the cross-section. According to the 1D model, the downstream discharges corresponding to the downstream water heights $\tilde{h}_1$ and $\tilde{h}_2$ are given by

$$Q^{\text{tot}}(\tilde{h}_1) = Q^{\text{tot}}(h_1) - Q_{\text{weir}}(h_1), \tag{4.43}$$

$$Q^{\text{tot}}(\tilde{h}_2) = Q^{\text{tot}}(h_2) - Q_{\text{weir}}(h_2). \tag{4.44}$$

By inverting these equations the downstream water heights $\tilde{h}_1$ and $\tilde{h}_2$ can be determined from their upstream counterparts. Subtract (4.43) from (4.44):

$$Q^{\text{tot}}(\tilde{h}_2) - Q^{\text{tot}}(\tilde{h}_1) = Q^{\text{tot}}(h_2) - Q^{\text{tot}}(h_1) - [Q_{\text{weir}}(h_2) - Q_{\text{weir}}(h_1)]\,, \tag{4.45}$$

and use the approximations valid for small $\widetilde{\Delta h} = \tilde{h}_2 - \tilde{h}_1$ and small $\Delta h = h_2 - h_1$:

$$\begin{aligned} Q^{\text{tot}}(\tilde{h}_2) - Q^{\text{tot}}(\tilde{h}_1) &\approx \frac{dQ^{\text{tot}}(\tilde{h}_1)}{dh}\widetilde{\Delta h}, \\ Q^{\text{tot}}(h_2) - Q^{\text{tot}}(h_1) &\approx \frac{dQ^{\text{tot}}(h_1)}{dh}\Delta h, \\ Q_{\text{weir}}(h_2) - Q_{\text{weir}}(h_1) &\approx \frac{dQ_{\text{weir}}(h_1)}{dh}\Delta h. \end{aligned}$$

Substitution in (4.45) gives:

$$\frac{dQ^{\text{tot}}(\tilde{h}_1)}{dh}\widetilde{\Delta h} = \left[\frac{dQ^{\text{tot}}(h_1)}{dh} - \frac{dQ_{\text{weir}}(h_1)}{dh}\right]\Delta h, \tag{4.46}$$

and hence

$$\widetilde{\Delta h} = \frac{\frac{dQ^{\text{tot}}(h_1)}{dh} - \frac{dQ_{\text{weir}}(h_1)}{dh}}{\frac{dQ^{\text{tot}}(\tilde{h}_1)}{dh}}\,\Delta h. \tag{4.47}$$

Apart from the delay due to propagation, this is an instantaneous relation between the downstream and upstream errors. Note that both derivatives (4.41) and (4.42) are positive.

If the water height $h_1(t)$ is smaller than the crest height H_c, then $\tilde{h}_1 = h_1$ and furthermore (4.41) implies that $dQ_{\text{weir}}(t)(h_1)/dh = 0$. Then (4.47) implies

$$\widetilde{\Delta h}(t) = \Delta h(t), \quad (\text{ if } h_1(t) \leq H_c), \tag{4.48}$$

as should be expected.

The following metrics will be used to quantify the difference of two functions of time $f(t)$ and $g(t)$:

$$L1 = \frac{1}{N}\sum_i^N |f(t_i) - g(t_i)|, \tag{4.49}$$

for the mean absolute difference and

$$RL1 = \frac{\frac{1}{N}\sum_i^N |f(t_i) - g(t_i)|}{\frac{1}{N}\sum_i^N |g(t_i)|}, \tag{4.50}$$

for the relative difference, where the t_i are the times used and the error is computed with respect to the average value of g.

5 Results

The main results of the project are discussed in this chapter. In the first section, the accuracy of the 1D analytical model is verified by comparing its results to those from the 2D hydrodynamic model, HydroAS2D, specifically for the case of closed basins, i.e. no effects from the detention basins.

In subsequent sections the results are described of the optimization of the detention basin. First, the opening times of the weirs and the crest heights are optimized for the hydrograph of the HQ100 flood wave and for the four detention basins as proposed in Chapter 3. In this section it is assumed that the hydrograph of the discharge which arrives at the first basin is known as function of time. The optimal operation strategy obtained with the 1D model is applied in the 2D model to validate the effectiveness. Then the weir operation is optimized for a single, large detention basin (Indesee). The optimal operational strategies derived from the 1D model is again applied in the 2D model for validation.

In HydroAS2D, the inlet of a basin is modeled by a dike breach. The predictions of this model are in Section 5.5 compared to those of the weir equation as used in the 1D model.

Next a method is proposed and investigated to estimate the storage volume required to reduce the flood peak downstream at Ophoven to a desired level. This method is applied to The HQ100, HQ1000 and 2021 flood event.

For the first basin, the efficacy of crest height optimization for a compound weir during the HQ100 flood event is evaluated and compared to the operated weir configuration. In contrast to the operated weir, the compound weir has fixed crests and does not need to be operated.

Practical aspects of applying the operated and compound weir, specifically for real-time operations, are discussed. This contrasts with the previous sections, which were focused on optimizing for pre-known flood hydrographs. The discussion includes the case of the Rur River in particular.

The chapter finalizes with a summary of the main results of the optimizations.

5.1. Verification of the 1D Model Against HydroAS2D Without Detention Basins

The accuracy of the 1D model has been verified by comparing its predicted water heights adjacent to the detention basin inlet locations with the results from HydroAS2D simulations for the HQ100 flood wave. This comparison was performed for the case that the detention basins are closed (i.e. no inflow into the basins).

5.1.1. Verification at the Site of Detention Basin 1

Figure 5.1 shows the water height in the center of the main channel near the (closed) inlet of the first basin as obtained with the 1D analytical model (blue solid curve) and with HydroAS2D (red solid curve), for the case that all basins are closed. Furthermore, the water heights at the floodplain close to the inlet of detention basin 1 are shown (dashed curves). Due to the higher elevation of the floodplain

bed, there is no water present for some time and in that case the water height is set equal to the bed level. When the floodplain is dry, the 1D model and HydroAS2D results do not align exactly, which can be attributed to a slight discrepancy between the averaged bed level in the 1D model and the actual bed level at the location where water height is measured. The mean absolute error in water heights in the main river, as predicted by the 1D model and HydroAS2D, is calculated from $t = 160$ hours (see equation 4.49). For the main river, the error is $L1 = 0.04$, m, while for the floodplains, it is $L1 = 0.12$, m.

Overall, the water heights in the main river as predicted by the two models agree well, but just after the peak the water height drops more slowly in HydroAS2D than in the 1D model. This could be due to lateral flows, a larger effect of the frictional forces or inertia effects in the 2D model. The water height in HydroAS2D is higher on the floodplain than in the 1D model. In the 1D-model the water height is uniform in each cross-section of the river. In HydroAS2D however, river bends can cause that water heights in the outer bend are elevated. Uneven terrain or 2D effects that the 1D-model cannot capture may also contribute to the discrepancy.

The low water heights near $t = 0$ differ also. This is due to the approximations used for the cross-sectional profiles. The averaged bed level of the main channel as used in the 1D model is higher and the channel is wider than in reality resulting in less accurate water heights for low discharges. Since this study focuses on modeling flood waves, the discrepancies at low discharges are not important.

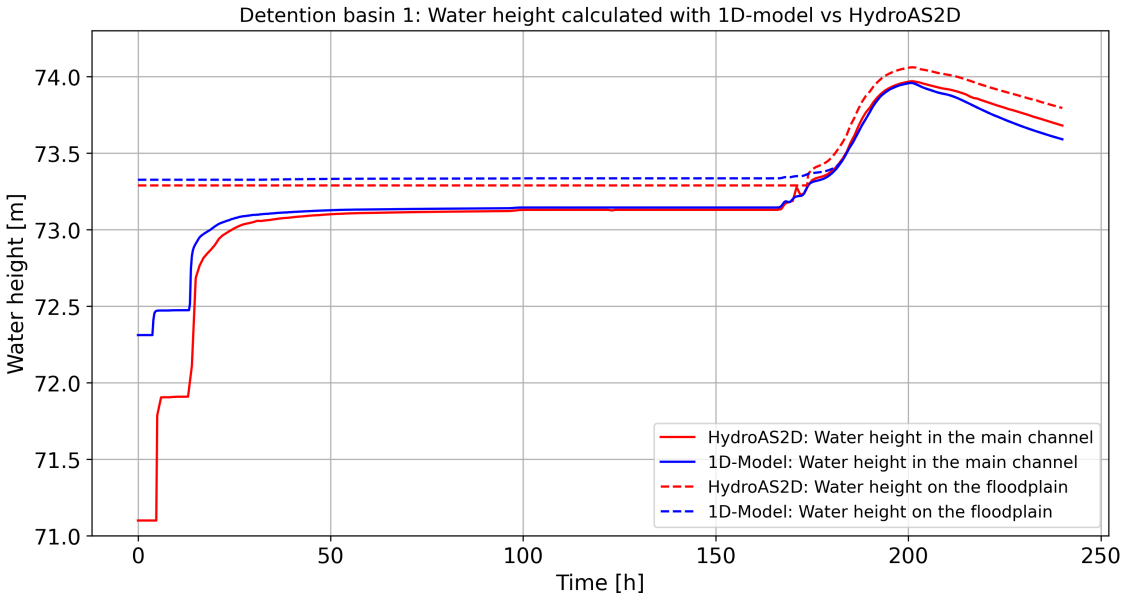

Figure 5.1: Water height comparison between HydroAS2D and the 1D-analytical model at the position of the inlet of basin 1 in the main channel and on the floodplain adjacent to the detention basin inlet. In these simulations all basins are closed.

5.1.2. Verification at the Site of Detention Basin 2 and 3

From the output of HydroAS2D and the one-dimensional analytical model at detention basins 2 and 3, it is evident that the water heights on the floodplain adjacent to the inlets of detention basins 2 and 3 are very low and therefore opening of these basins can have no significant effect on reducing the flood peak. Reason for this is the fact that the bed level of the floodplains adjacent to the basins and close to the inlets is too high, resulting in minimal inundation during the HQ100 flood event. It is therefore unclear why these locations were previously selected as potential detention basin sites. In the study by Schweim (2024), the dikes were completely removed and it is possible that this changed the flow pattern such that more water ended up on the floodplains compared to when the dikes are present.

Due to the negligible water heights at the inlets of detention basins 2 and 3, further optimization of their operation for flood wave HQ100 was deemed unnecessary. These basins were however still modeled in HydroAS2D to be able to confirm that they indeed have an insignificant impact on peak reduction.

5.1.3. Verification at the Site of Detention Basin 4

Figure 5.2 shows the water height in the main channel as estimated by the 1D model (blue solid curve) and HydroAS2D (red solid curve) close to the inlet of detention basin 4. The mean absolute error (4.49) in water height in the main river, taken from time t= 190 hours is $L1 = 0.15$ m whereas for the flood plain it is $L1 = 0.12$ m

The 1D model underestimates the peak water height compared to HydroAS2D, though it aligns well under base flow conditions. One possible explanation is that the 1D model is less precise in capturing floodplain dynamics, particularly given the uneven terrain. Additionally, the proximity of the Wurm confluence to the detention basin inlet may contribute to increased peak discharges, even though the Wurm lies slightly downstream of the inlet. Furthermore, a bridge downstream of the inlet may create backwater effects which are not accounted for in the 1D model.

On the floodplain, a similar pattern is observed, with the 1D model underestimating water height relative to HydroAS2D. In Figure 5.2, the blue dashed curve and orange dashed curve represent the results of the 1D model and of HydroAS2D, respectively. In this case, the water height in HydroAS2D appears relatively uniform across the main channel and floodplain.

As for detention basin 1, exact alignment between the 1D model and HydroAS2D is not to be expected for detention basin 4, but what is important is that both models show similar behavior.

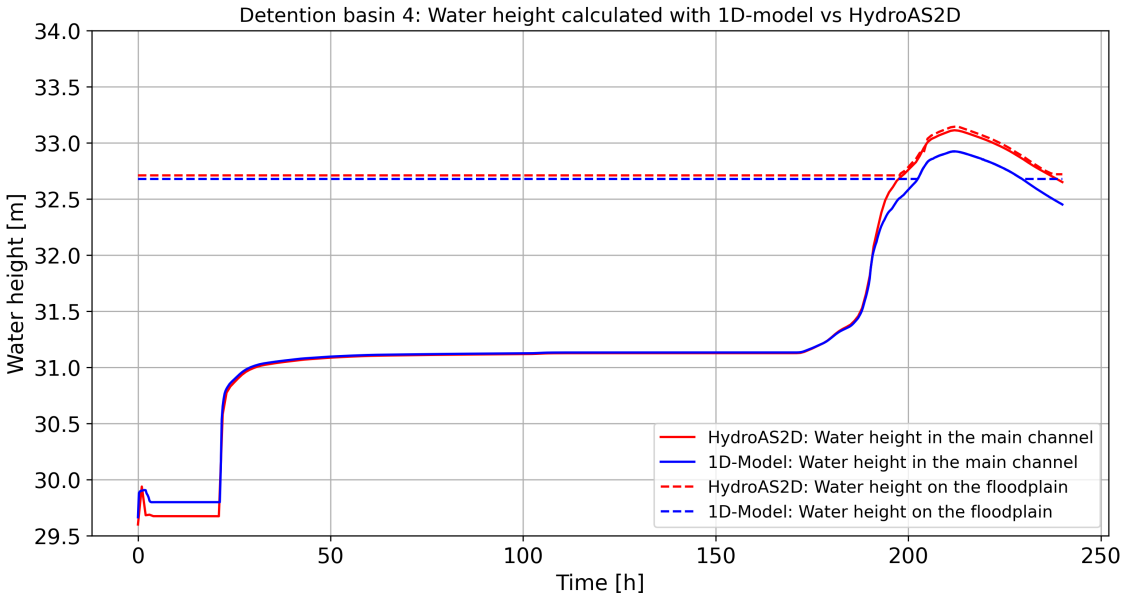

Figure 5.2: Water height comparison between HydroAS2D and the 1D-analytical model at the position of the inlet of basin 4 in the main channel and on the floodplain adjacent to the detention basin inlet. (Note that the basins are all closed).

A comparison of the red continuous curves in Figures 5.1 and 5.2 suggests that diffusion induced by friction does not play an important role in flow propagation over the 30-kilometer distance between detention basins 1 and 4 since the shapes of the flood hydrograph are quite similar.

5.2. Optimization of the Operation of the Four Proposed Detention Basins

First some general comments are made which apply to the optimization of any basin and any flood wave. As explained in Section 4.4, the crest height H_c of the inlet structure was varied in steps of 5 cm between 5 and 75 cm above the inlet bed elevation (the latter is at 73.30 m +NHN). Hence in total 15 crest heights are considered. Initially the crest height is so high that no water can flow into the basin. At opening time t_1, the crest height is lowered to one of the mentioned values. In Section 4.4.1, the

time t_c was defined as the first time at which the water height h on the floodplain is equal to H_c:

$$h(t_c) = H_c. \tag{5.1}$$

Only at times t such that both $t > t_1$ and $t > t_c$, water will flow into the basin. If at the time of opening, the water height already exceeded the lowered crest height, i.e. if $t_1 \geq t_c$), the total discharge in the river and floodplains decreases suddenly (i.e. discontinuously) at the time of opening.

At time $t_2 > t_1$ the basin is full, i.e. the water height in the detention basin has risen to the crest height H_c. This time marks the moment of closure of the detention basin. As explained in Section 4.4, t_2 is a function of the opening time t_1 and the crest height H_c. In case the basin is never completely full, t_2 is defined as: $t_2 = \infty$.

In the optimization problems discussed in the current section and in Sections 5.3 and 5.6 it is assumed that the relevant part of the hydrograph of the flood wave, i.e. its discharge as function of time, is known.

5.2.1. 1D Analytical Model Applied to the HQ100 Scenario for Four Basins

For the HQ100 flood wave, Figure 5.3 shows the contour plot of the reduced peak discharge after the first of the four basins, as function of the opening time t_1 and crest height H_c. The peak discharge in the HQ100 hydrograph (i.e. without the detention basins) is 172.48 m^3/s and the corresponding maximum water height is $h = 73.96$ m +NHN. The optimal operational strategy gives a reduced peak discharge of 161.68 m^3/s and peak water height of 73.92 m, i.e. a reduction of only 4 cm.

The black dashed line in Figure 5.3 indicates the time $t_{\text{max}} = 200.75$ hours at which the maximum discharge of the HQ100 hydrograph reaches detention basin 1. The white curve 5.3 is the function $t_c(H_c)$ as defined in (5.1). For opening times and crest height combinations (t_1, H_c) which are to the right of the white curve in the contour plot, the basin is opened after the water height has reached the crest height, whereas if they are to the left of the white curve, the water flows into the basin only after time $t_c(H_c)$ Therefore, in Figure 5.3, the peak discharge is the same along all horizontal lines to the left of the white curve.

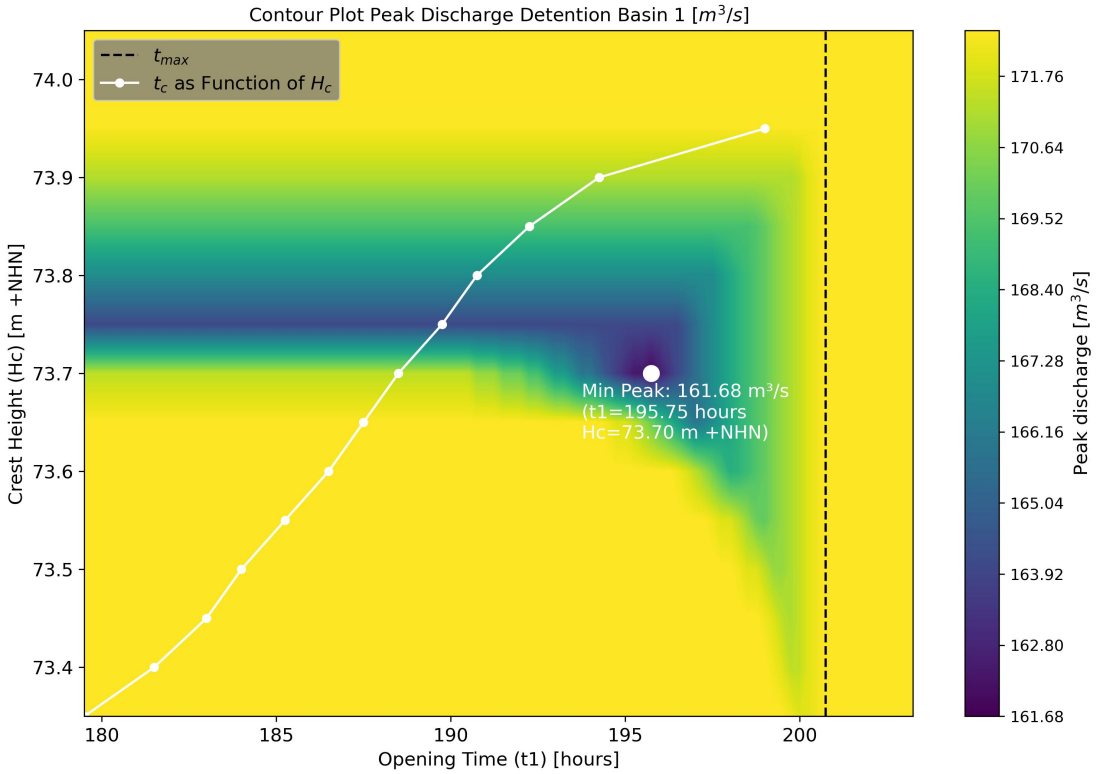

Figure 5.3: Contour plot of peak downstream discharge of detention basin 1 as function of opening time t_1 and crest height H_c for flood wave HQ100.

In the light green/yellow regions of the contour plot, the peak discharge is not reduced. The reason is that the opening time is too early and/or the crest height is too low, both resulting in the basin being full before the maximum discharge has arrived at the inlet, i.e. $t_2 < t_{\text{max}}$. Furthermore, also all opening times: $t_1 > t_{\text{max}}$ are ineffective, for the obvious reason that the flood peak has already passed at the time the basin is opened. Finally, for all opening times and for all crest heights above 73.96 m +NHN, no peak reduction occurs because then the water height at the inlet never exceeds the crest height.

Figure 5.4 shows a countour plot of the time t_2 that the basin is full as function of opening time t_1 and crest height H_c for flood wave HQ100. The dashed black line has the same meaning as in Figure 5.3. The white area corresponds to $t_2 = \infty$, which means that the basin is never filled. It is seen that when the crest height is too large or the opening time is too late, or both, the basin is never filled. t_2 is the same for all opening times t_1 to the left of the white curve because then the time form which water only flows in the basin is after time $t_c(H_c)$.

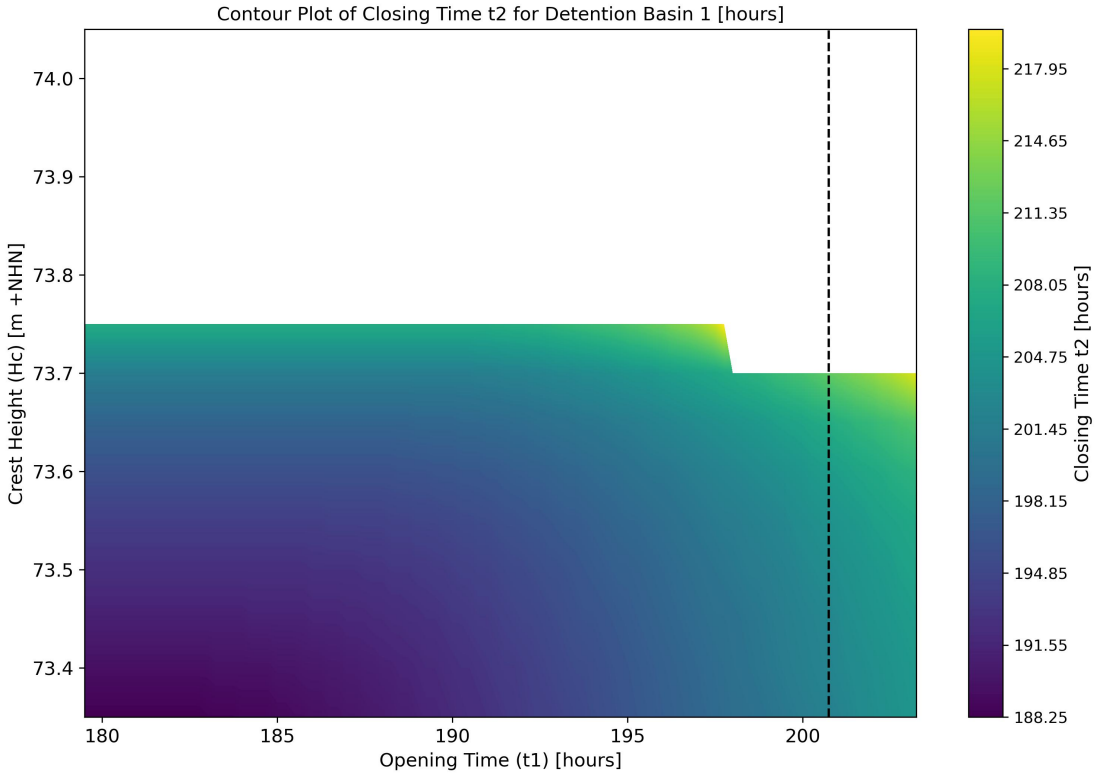

Figure 5.4: Contour plot of the time t_2 (hours) that basin 1 is full as function of opening time t_1 and crest height H_c for flood wave HQ100.

In Figure 5.5 the original discharge Q_0 of the given hydrograph is shown as function of time at the inlet of basin 1 (dashed curve) and is compared to the discharge just downstream of the inlet as function of time for the case of maximum downstream peak reduction (continuous curve). The maximum reduction occurs for opening time $t_1 = 195.75$ hours as marked by the red dashed line, and for optimum crest height of $H_c = 73.7$ m +NHN. The orange dashed line indicates the time t_c satisfying (5.1) and the green dashed line indicates the time t_2 at which the basin is full, which is 9 hours after the opening time t_1. It is seen that the optimum opening time is after time t_c and hence the discharge decreases discontinuously at time t_1. Furthermore, the opening time is 5.0 hours before the maximum discharge arrives at the weir.

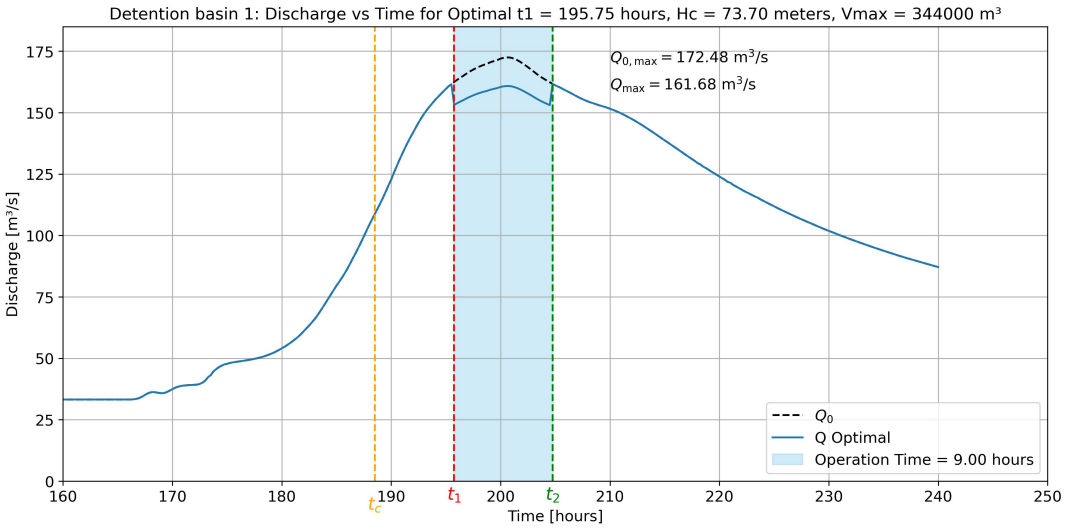

Figure 5.5: Original HQ100 hydrograph (dashed curve) and the reduced discharge as function of time (continuous curve) as obtained by optimizing the opening time and crest height of detention basin 1.

Figure 5.6 shows the water height $h(t)$ with respect to NHN as function of time for the original hydrograph (dashed curve) and downstream of the weir for the optimized opening time and crest height. The horizontal dashed orange and brown lines are the optimized crest height and the bed level of the floodplain adjacent to basin 1, respectively. The vertical red and green lines have the same meaning as in Figure 5.5. The maximum water height was reduced by 4 cm which amounts to a maximum water depth reduction of 10% on the floodplain next to the basin. This small reduction, along with the short period during which the basin is open, shows that the current detention basin 1 is too small to substantially reduce the water heights.

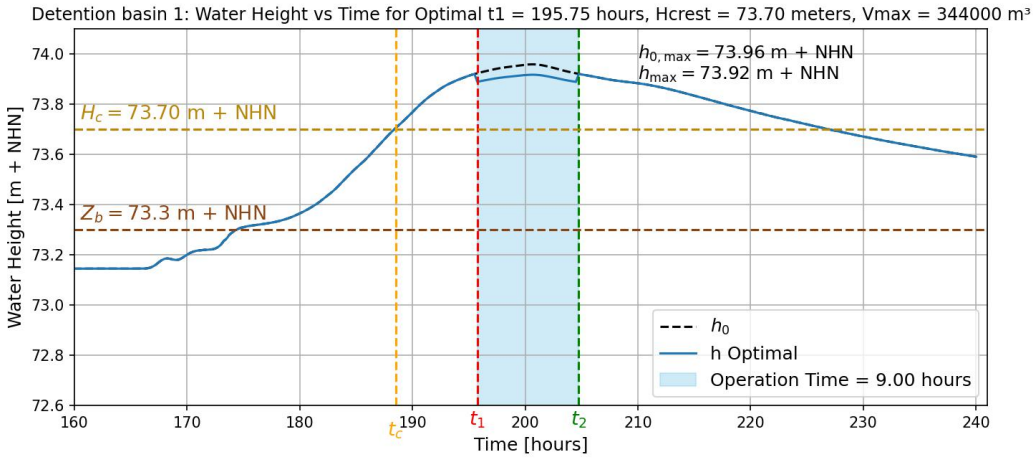

Figure 5.6: Water height of the original hydrograph of the HQ100 flood wave and the reduced water height as function of time, for the optimized opening time and crest height of detention basin 1.

As discussed previously in Chapters 3 and 4, the weir width was assumed to be 60 m for this investigation. A wider inlet permits more water to enter the basin, potentially causing it to fill too quickly. Conversely, a smaller inlet width could make the basin ineffective by capturing water too slowly. In Section 5.3 a much larger basin is considered and also different inlets are studied.

To see whether the predicted reduction in water height is significant the downstream error in water

height based on the difference between the upstream water heights in the 1d model and in HydroAs2D obtained for the case that the basins are all closed was estimated. From the red and blue dashed curves in Figure 5.1 the difference $\Delta h(t)$ in upstream water heights can be derived. The corresponding error $\widetilde{\Delta h}(t)$ downstream of the weir follows from (4.47) and is shown in Figure 5.7 as the dashed curve, together with the water height reduction as function of time t predicted by the 1D model (blue curve). It is seen that the error is everywhere negative, implying that the water height according to HydroAS2D is always larger than in the 1D model. Furthermore the absolute reduction in water height is smaller than the absolute error, hence the peak reduction of 4 cm is not significant.

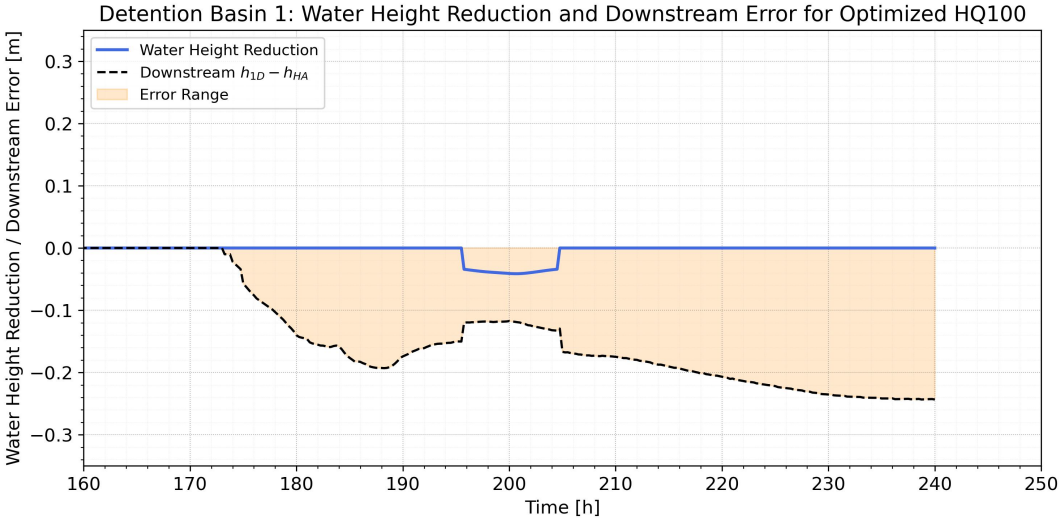

Figure 5.7: Water height reduction achieved optimized operation of detention basin 1 with the 1D model (blue curve), compared to the estimated downstream error of the model (black dashed curve).

After optimizing the operation of the weir in the first detention basin, the optimized downstream discharge was propagated to the fourth detention basin, where the optimization procedure was repeated. Recall that the operation of basins 2 and 3 is not considered since the water depth on the floodplains there is too small for flood wave HQ100. When the flood wave propagates downstream to the fourth detention basin, multiple tributary streams confluence with the main river, and the additional discharges is added to the total discharge incident on the fourth detention basin.

The optimal opening time, t_1 for basin 4 was estimated at 214.25 hours and the optimal crest height was the lowest possible: 32.75 m +NHN. This optimization reduced the peak discharge from 210.56 m^3/s with a peak water height of 32.890 m +NHN to 207.07 m^3/s and 32.877 m +NHN, respectively. Hence, detention basin 4 achieves a peak water height reduction of only 1.4 cm, mainly due to the small storage volume of only 45,000 m^3 at the low crest height of 32.75 m above NHN (recall that the storage volume depends on the crest height because the basin is shallow). Furthermore, the floodplain at detention basin 4 is quite wide (100 m) and has a high bed elevation, which results in a relatively small water height at the detention basin inlet during the HQ100 flood event.

The discharge of the propagated optimized flood wave from detention basin 1, with the discharges from tributary streams added, is shown as the black dashed curve in Figure 5.8. The reduced discharge as function of time immediately after basin 4 obtained by maximizing the peak reduction is shown as the solid blue curve. The vertical orange, red and green dashed lines have the same meaning as in Figure 5.5.

Figure 5.9 shows the corresponding water heights as function of time. The reduction of the peak water height is only 1.4 cm. The bed level of the floodplain and the optimal crest height are indicated by the brown and orange dashed lines, respectively. The floodplain bed level is relatively high compared to the peak water height, which is an important reason for the small effect of detention basin 4 on peak reduction.

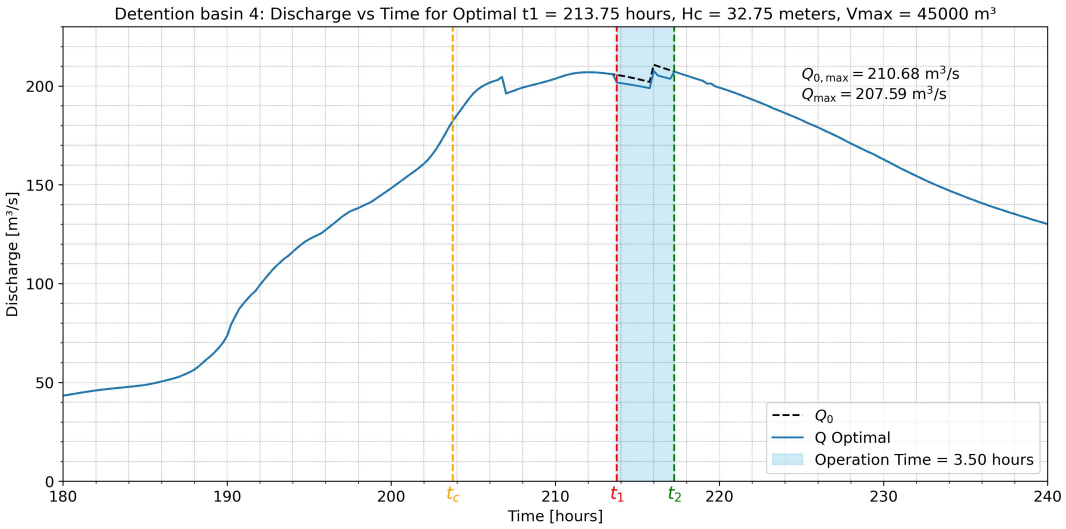

Figure 5.8: Discharge as function of time just before the inlet of detention basin 4 (dashed curve) and the reduced discharge (continuous curve) as function of time as obtained by optimizing the opening time and crest height of detention basin 4.

Simulations consistently confirmed that when the upstream hydrograph Q_0 has only one maximum and the maximum of the reduced hydrograph $Q(t)$ (i.e. downstream of the basin) is lower than the maximum of $Q_0(t_1)$ and $Q_0(t_2(t_1))$ for all t_1, then the optimum opening time t_1 is such that:

$$Q_0(t_1) = Q_0(t_2(t_1)). \tag{5.2}$$

Here $t_2(t_1)$ is the time the basin is full when it is opened at t_1 (assuming that the basin is filled in finite time). An example is Figure 5.5. Note that when $t_1 = t_c$, i.e. when the time that the water height reached crest height is optimum, (5.2) also holds, but then the weir can obviously be opened earlier than t_c, however (5.2) holds then only for t_c. However, when the hydrograph upstream of the weir has several local maximum as in the case of basin 4, the optimum opening time does in general not have this property (see Figure 5.8, where the vertical red and green dashed lines do not intersect the black dashed curve for the same discharge).

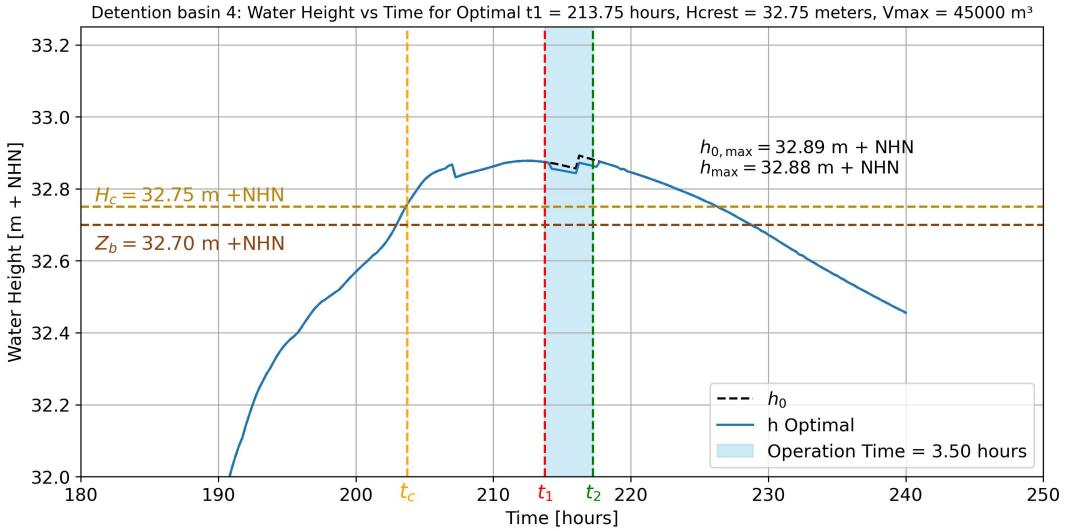

Figure 5.9: Water height as function of time just before the inlet of detention basin 4 and reduced water height as function of time for the optimized opening time and crest height of detention basin 4.

Finally, in Figure 5.10, the total reduction of the discharge achieved by the combined optimized operated detention basins 1 and 4 is shown downstream of basin 4 (continuous curve). It is compared

to the flood hydrograph at the same downstream position in the absence of detention basins but with added discharge due to tributaries (dashed curve). The total peak discharge reduction achieved just downstream of detention basin 4 amounts to 11.48 m^3/s, corresponding to a peak reduction of only 6.3% relative to base flow conditions.

These findings indicate that the proposed four detention basins along the Lower Rur river as analyzed in this section, achieve only limited peak reduction. This is primarily due to too small storage capacities and high floodplain bed elevation of most basin locations. Excavation of the basins could enhance the storage volumes and thereby the peak reduction.

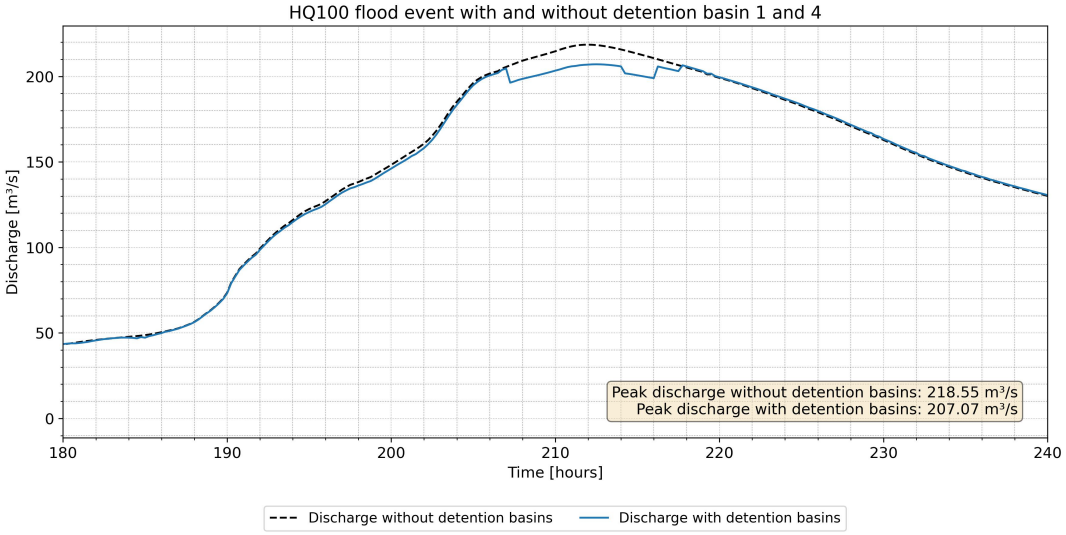

Figure 5.10: Discharge as function of time just after the inlet of detention basin 4 in the case of no detention basins (dashed curve) and the reduced discharge as function of time just after detention basin 4 as function of time (continuous curve) as obtained by combined optimization of the opening times and crest heights of detention basin 1 and 4.

5.2.2. Validation against HydroAs2D

As discussed in Section 5.1.1, the water heights on the flooplains in the 1D model and HydroAS2D did not align, with the 1D model underestimating water heights compared to HydroAS2D. It was mentioned in Section 4.6.2 that the weir can not be opened directly at time t_1 but only indirectly by monitoring the water height on the floodplain in front of the inlet. Since the water height on the floodplain in HydroAS2D was higher than in the 1D model, the weir was opened in HydroAS2D too early, i.e. earlier than the time t_1 determined with the 1D model.

Figure 5.11 shows the reduced water heights in the point on the floodplain in front of the weir of basin 1 in HydroAS2D when operated using the optimal strategy derived with the 1D model (red solid curve), along with the optimized reduced water height from the 1D model itself (blue solid curve). The horizontal orange dashed line marks the threshold height at which the weir is opened in HydroAS2D, indicating that this threshold is reached earlier than t_1. As a result, the basin is already filled in HydroAS2D, before the peak of the flood has arrived (indicated by the vertical black dashed line). The mean absolute error (4.49) between the reduced water heights on the floodplain of the 1D model and HydroAs2D starting from time 170 hours is: $L1 = 0.17$ m

In Figure 5.11, both the 1D model and HydroAS2D show a drop in water height at the moment the weir opens and is set to the optimal crest height of 73.70 m +NHN. Furthermore, it appears that the detention basin fills more quickly in HydroAS2D than in the 1D model. This discrepancy comes most likely from the different methods used to estimate inflow: the 1D model applies a weir equation, while in HydroAS2D the 2D shallow water equations are solved over a dike breach.

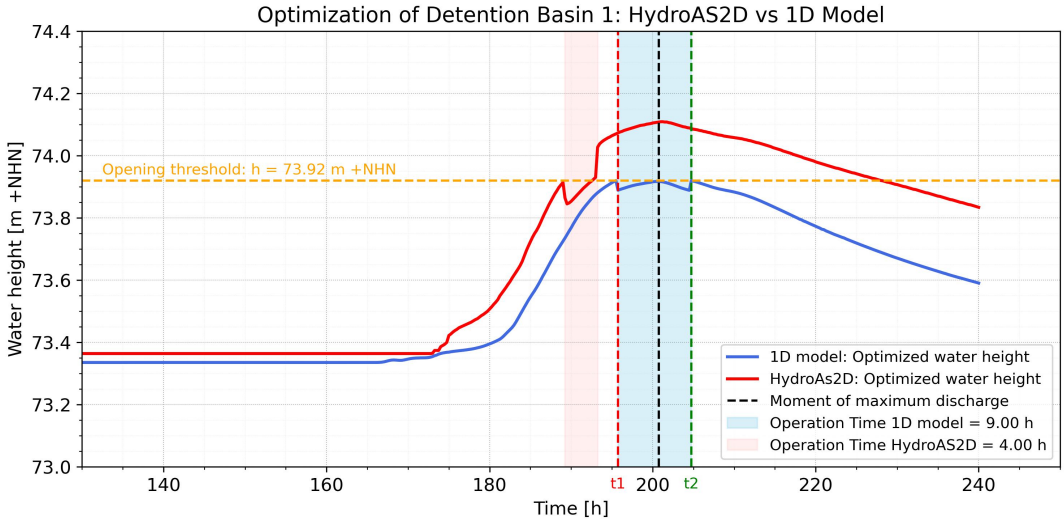

Figure 5.11: Water height at a point on the floodplain in front of the weir of basin 1 as computed with HydroAS2D and as computed with the 1D model for the optimized operated weir of flood wave HQ100.

Figure 5.12 shows the difference in inflow. The discharge into the basin as calculated by HydroAS2D begins earlier and reaches a higher magnitude than in the 1D model, where the inflow discharge is lower for each given timestep. In Section 5.4 the differences caused by using the dike breach model in HydroAS2D instead of the weir equation is further considered.

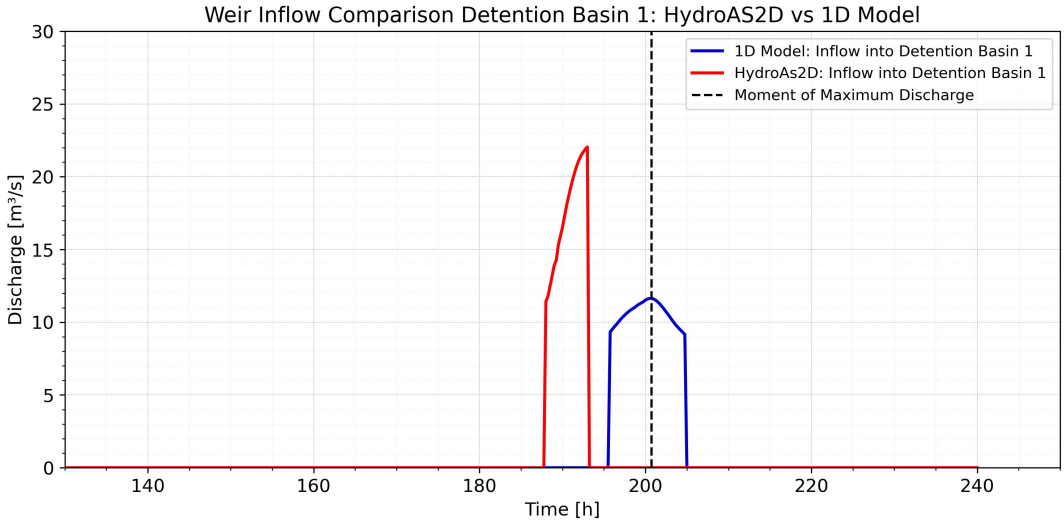

Figure 5.12: Inflow in basin 1 as predicted by HydroAS2D (red curve) and the 1D model (blue curve).

With HydroAS2D it was found that Detention Basin 1 fills to 97% of its estimated total capacity of 344,000 m^3, as previously calculated using the DEM. This slight discrepancy with the 1D model where the basin completely fills, arises from the method used in HydroAS2D to model basin closure. The closing time, t_2, in HydroAS2D is similarly to the opening time t_1, based on a water height threshold, namely at gauge 2 in Figure 4.12.

Although this gauge is positioned towards the back of the basin, the threshold can still be met even if the water height in some areas within the basin have not yet reached this height. Figure 5.13 clearly shows that substantial areas within the basin are not inundated due to higher terrain that lies above the crest height. This demonstrates that it is important to determine the relationship between crest height and maximum storage capacity of the basins, as was done in Section 4.3.4 and presented in Figure 4.7.

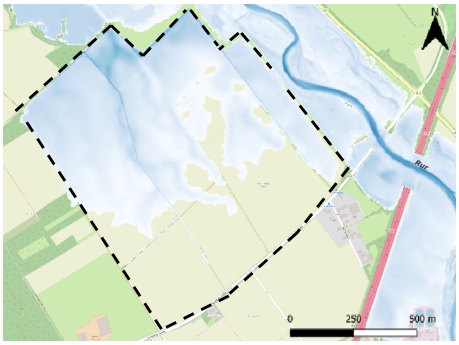

Figure 5.13: Water captured according to HydroAS2D inside detention basin 1.

Regarding detention basin 2, the results from HydroAS2D confirmed the findings of the 1D model, showing that detention basin 2 has no effect on peak reduction, as the water height on the floodplain remains too low for the basin to fill during a HQ100 flood event. Similarly, the negligible impact of detention basin 3, as indicated by the 1D model, was also confirmed.

In Section 5.2.1, the 1D model showed that only a minimal peak reduction of 1.4 cm could be achieved at detention basin 4, relative to the peak reduction already achieved by detention basin 1. Since due to water height based operation in HydroAS2D, detention basin 1 gave no significant peak reduction, the hydrograph at the inlet of detention basin 4 remained essentially the same as when basin 1, 2 and 3 are closed. In Figure 5.14 the solid red curve is the optimized water height at the inlet of detention basin 4 as simulated with HydroAS2D, and the blue curve shows the water height estimated with the 1D model. The orange dashed line indicates the opening threshold of $h = 32.88$ m + NHN, while the red and green dashed lines mark the opening and closure moments of detention basin 4 in the 1D model. the absolute difference (4.49) between the reduced water heights on the floodplain as computed by HydroAS2D and the 1D model, starting at 198 hours is $L1 = 0.18$ m

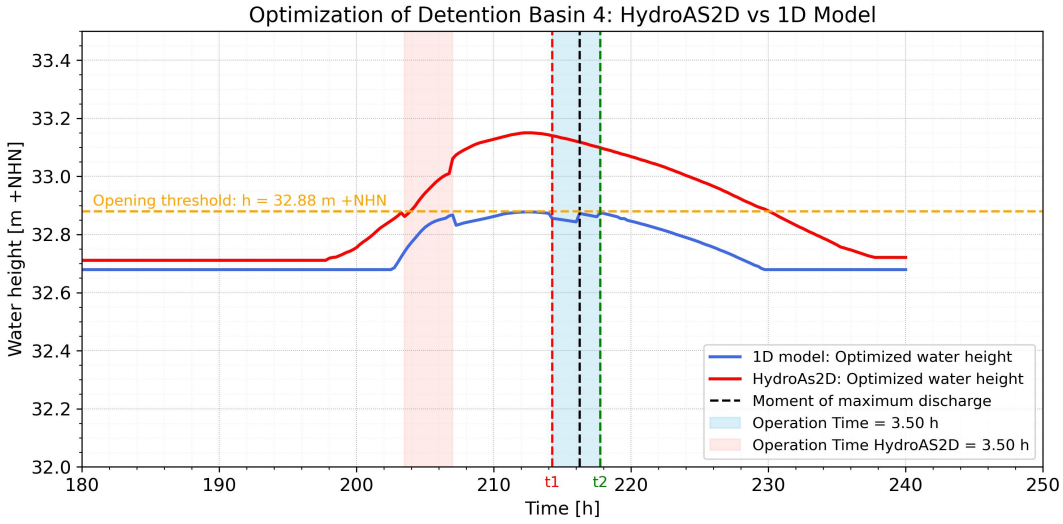

Figure 5.14: Water height at a point on the floodplain in front of the inlet of basin 4 as computed with HydroAS2D (red curve) and with the 1D model (blue curve) for the optimized operated weir of flood wave HQ100 at detention basin 4.

Similar to detention basin 1, basin 4 is opened too early in HydroAS2D, again due to higher water levels on the floodplain than in the 1D model. The early opening in HydroAS2D is evident from the dip in the red solid red curve, where the basin opens as this curve intersects with the orange dashed threshold line. The fact that both detention basins were opened too early is also evident in Figure 5.15, where it can be observed that the discharge is only slightly lower before the peak is reached.

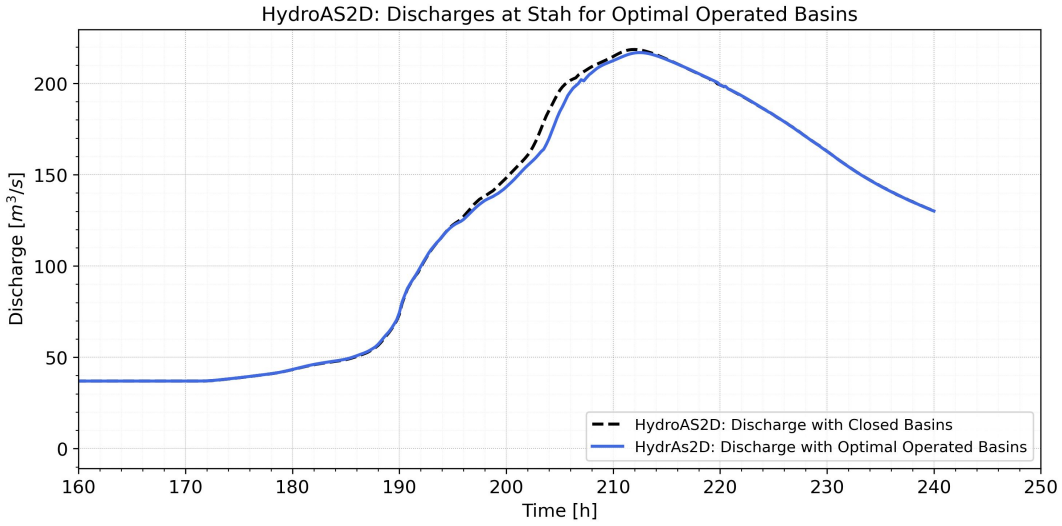

Figure 5.15: Hydrographs at the gauging station Stah, located just downstream of detention basin 4. The dashed curve is the discharge of the HQ100 flood wave at Stah when all four detention basins are closed and the continuous curve is the discharge of the HQ flood wave at Stah when the basins are operated optimally.

Even if detention basin 4 would be opened at the right time, the storage capacity of basin 4 would have been insufficient to achieve a considerable peak reduction. This is clear from Figure 5.16, which shows the inflow into detention basin 4 over time. It can be seen that the detention basin would only be open for approximately 3.5 hours before it would reach is maximum capacity of only 45000 m^3 at the crest height of 32.75 m +NHN.

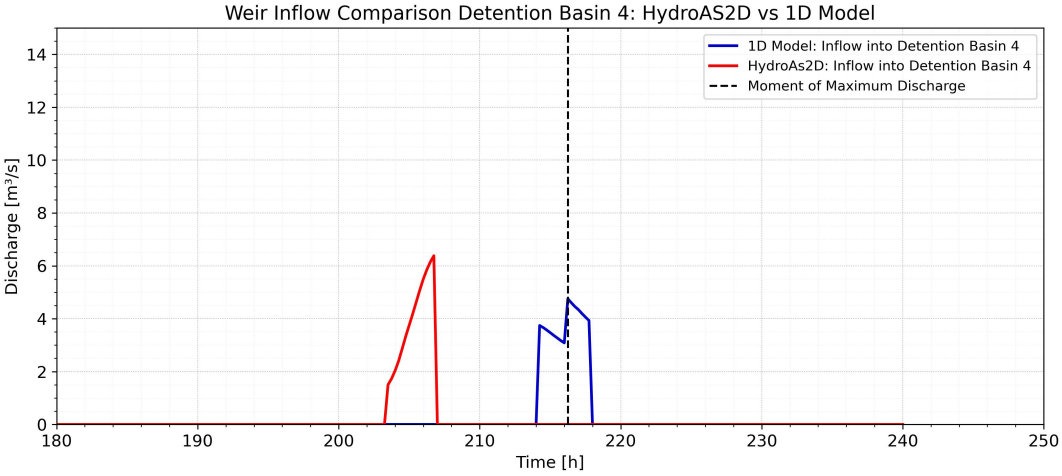

Figure 5.16: Inflow into basin 4 according to HydroAS2D model (red curve) and the 1D model (blue curve).

In HydroAS2D, the detention basin capacity reached 99%, with the slight discrepancy due to the chosen location of the gauging station within the basin.

Needless to say, the predicted 1.4 cm decrease in peak water height is smaller than the error in the water height propagated using (4.47) and hence not only very small but also insignificant.

Figure 5.17 shows the water that was captured by detention basin 4. A significant area remained not inundated, which can be attributed to the internal terrain. The eastern side of the detention basin has higher ground, exceeding the crest height of the weir, while the western side is lower. The relationship between crest height and basin volume is shown in Figure 4.7. Northeast of the detention basin, an inundated area can be observed. During an HQ100 flood event, it appears that a small lake, known as "Ophovener Baggersee" (indicated as "Ophoven lake" in Figure 5.17), captures some floodwater without exceeding its capacity.

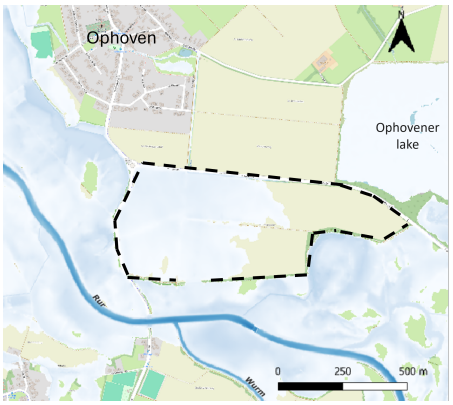

Figure 5.17: Water captured according to HydroAS2D inside detention basin 4.

5.2.3. 1D Analytical Model Applied to the 2021 Flood Event

A preliminary study has been conducted into the effect of the four detention basins along the Lower Rur during the 2021 flood event. The data for the flood hydrographs at the locations of Jülich and Stah were provided by S. Hartgring, who investigated numerical models for hindcasting the 2021 flood event in his recent thesis research (Hartgring, 2023). The hydrograph at Stah is shown in Figure 3.5.

As expected, the results obtained from the optimization for the 2021 flood event indicated similar to the HQ100 flood event that the detention basins had a negligible effect on peak reduction. In contrast to the HQ100 event, detention basin 3 captures some floodwater during the 2021 flood. However, since this basin has the smallest capacity, it did not lead to a relevant peak reduction.

One key difference between the HQ100 flood event and the 2021 flood event was the contribution of the Wurm tributary to the severity of the flood. For the HQ100 event HydroAS2D predicted a peak discharge in the Wurm of approximately 20 m^3/s , whereas during the 2021 flood event, the Wurm contributed much more, with a peak discharge of up to 80 m^3/s (Hartgring, 2023). Furthermore, in the 2021 flood event the peak discharge from the Wurm did not coincide with the peak discharge from the Rur river itself, resulting in a very different elongated shape for the downstream flood hydrograph compared to the hydrograph further upstream at Jülich. For the village Ophoven, located just downstream of the Wurm tributary, the contribution of the Wurm tributary should therefore not be underestimated. It is advised to further explore the effect of one or more (operated) detention basin(s) along the Wurm to capture floodwaters before converging with the Rur.

It should be remarked that the small peak discharge of 20 m^3/s in the Wurm river obtained from HydroaS2D for the HQ100 flood seems rather small compared to the overall magnitude of the HQ100 flood event.

5.3. Optimization of the Operation of the Large Basin "Indesee"

From the previous sections on the optimization of the detention basin operation along the Lower Rur river, it was concluded that the total volumes of the four basins, given their current terrain, are generally too small to have a significant impact on peak reduction. To investigate whether a substantially larger basin could yield better results, the rather extreme volume of the Indesee was used.

5.3.1. 1D Analytical Model Applied to the HQ100 Scenario for "Indesee"

In this analysis, it was assumed that the Indesee would maintain a water height buffer of 1 meter. Given the huge area of Indesee, this implies a total available storage volume of 11.6 million m^3. The basin is sufficient deep for the storage volume to be considered independent of the crest height. This means that, contrary to the four basins studied in Section 5.2, in the optimization problem described in Section 4.4, V_{max} in the right-hand side of (4.30) is constant.

The volume of 11.6 million m^3 is roughly 30 times larger than the total volume of the first and fourth

basins used in the HQ100 flood wave studied in Section 5.2 Although the Indesee is located slightly further upstream from detention basin 1 and the geographical conditions at this site differ somewhat from those at detention basin 1, the cross-sectional geometry of detention basin 1 was used to provide an estimate of the potential order of magnitude for peak reduction which such a large basin could give. The inlet structure was initially defined to have the same dimensions as that of detention basin 1, i.e. with the inlet width is 60 m.

In optimizing the operation of the weir for the HQ100 flood wave, the opening time t_1 and crest height H_c were again optimized, with crest heights varying between 73.35 to 74 m +NHN in steps of 5 cm. The results are shown in Figure 5.18. The peak discharge is reduced from 172.48 m^3/s to 130.42 m^3/s and the peak water height is reduced from 73.96 to m +NHN to 73.80 m +NHN, i.e. a reduction of 16 cm. The optimum crest height was the lowest possible crest height and the optimum opening time was the earliest time that the water height was above that crest height ($t_1 = t_c(H_c)$ for optimum $H_c = 73.35$ m +NHN). The basin is so large that the maximum storage capacity of 11,6 million m^3 is never reached (meaning that $t_2 = \infty$). The dashed curve is the percentage of the storage volume which is filled as function of time. The maximum volume is approximately 5.25 million m^3, which is only about half the storage capacity.

Because $t_1 = t_c(H_c)$ and the optimum crest height is the lowest allowed, a peak of 130.42 m^3/s actually is the lowest achievable discharge for the HQ100 flood wave for the chosen parameters. But by enlarging the inlet, more water can enter the basin and the peak discharge can be reduced further.

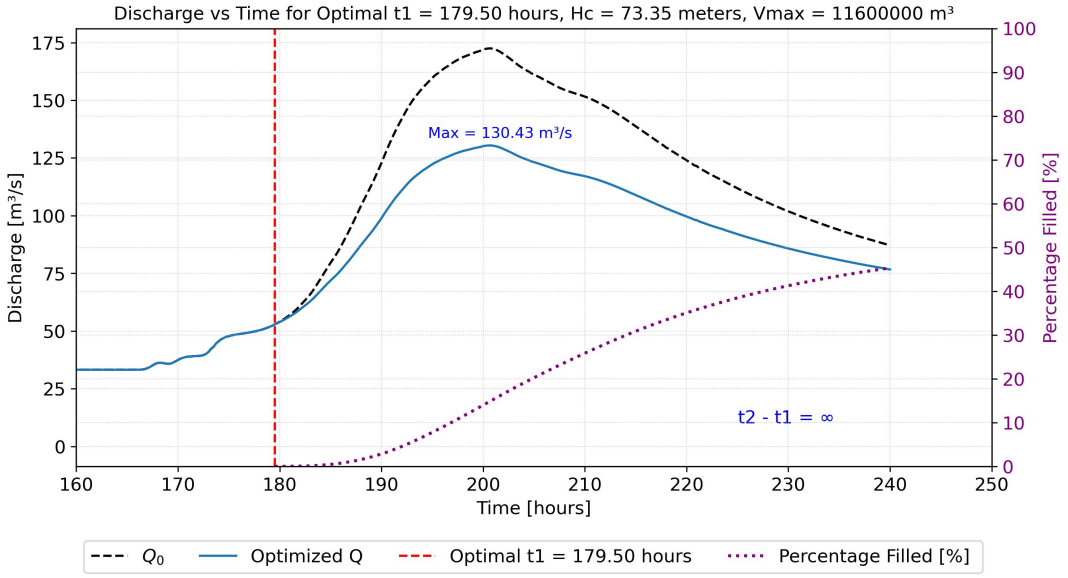

Figure 5.18: HQ100 hydrograph (dashed curve) and reduced discharge as function of time (continuous curve) by optimization of the opening time and crest height of the basin "Indesee" with large volume of 11.6 million m^3 and width of the inlet equal to 60 m. The dotted curve is the percentage of the storage volume that is captured as function of time.

Figure 5.19 shows the peak reduction achieved for the HQ100 flood with the large basin and with inlet width of 120 m. Now the peak discharge is reduced to 88.39 m^3/s which is 51% from the original peak discharge. The peak water height is now 73.59 meter +NHN which is a reduction of 37 cm. As before, the optimum crest height was found to be the lowest allowed (73.35 m +NHN) and the optimum opening time was the earliest time that the water height was above this crest height.

In spite of the larger inlet, the basin's maximum capacity was still not reached so that still $t_2 = \infty$. However, this time the basin captured approximately 10.5 million m^3 of water, approaching its maximum volume of 11.6 million m^3. The fact that $t_1 = t_c(H_c)$ implies that for the HQ100 (and similar flood waves), the basin can be permanently open, i.e. operation is not required in such case.

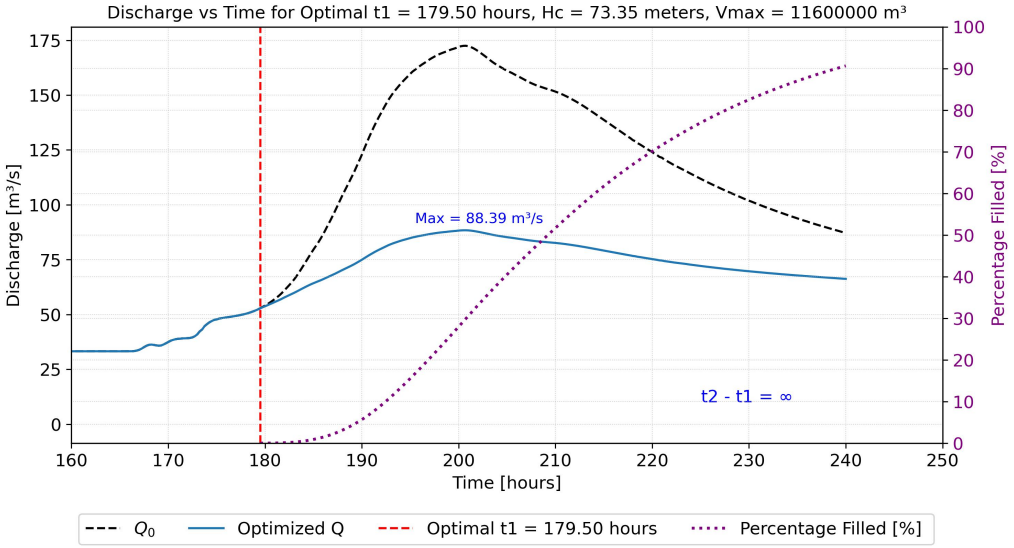

Figure 5.19: Same as Figure 5.18 except that the width of the inlet of the large basin is 120 m.

This analysis shows that merely increasing the detention basin volume is insufficient to achieve maximum possible peak reduction. When the optimum crest height is low and the basin is so large that no closing time exists, i.e. $t_2 = \infty$, this indicates that further reduction of the peak discharge can be realized by enlarging the inlet. For much smaller detention basins, however, the opening time t_1 and closing time t_2 are very important to capture the flood wave peak, with t_1 occurring before the peak and t_2 after.

To determine whether the decrease of the peak water height as predicted by the 1D model is significant, the error $\widetilde{\Delta h}(t)$ downstream of the large basin from the difference in water height $\Delta h(t)$ on the floodplain in front of the basin as predicted by the 1D model and HydroAS2D with all basins closed is estimated. The downstream error $\widehat{\Delta h}(t)$ is obtained from Figure 5.1 and shown in Figure 5.20 as the dashed curve together with the decrease of water height as predicted by the 1D model (blue curve). It can be concluded that in particular at times that the reduction is large, the downstream error is much smaller than the reduction, hence the reduction can be considered significant.

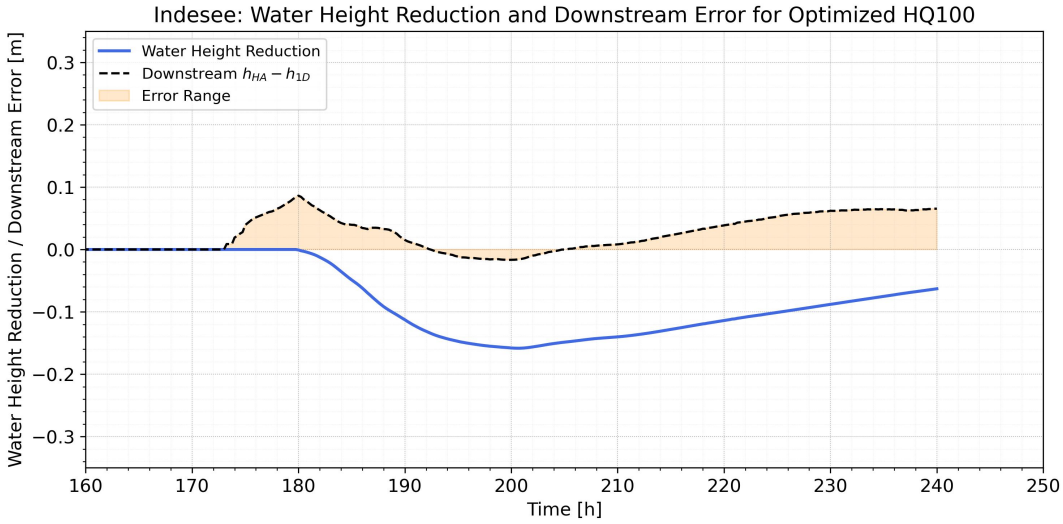

Figure 5.20: Water height reduction achieved by optimized operation of detention the Indesee for floodwave HQ100 with the 1D model (blue curve), compared to the estimated downstream error of the water height (black dashed curve).

5.3.2. Validation against HydroAS2D

The first investigated scenario, with an inlet width of 60 meters, was also analyzed using HydroAS2D. The optimal operation strategies for the HQ100 flood wave, as determined in the 1D model, were implemented in HydroAS2D through a Lua script based on the water height as threshold for opening the weir. The crest height was set to 73.35 m +NHN, which is the lowest possible for this location. The weir was operated such that it opens at the first moment the water height on the floodplain exceeded the crest height.

The effect of the Indesee a few kilometers downstream as computed with HydroAS2D (red curve) are compared to the effect estimated with the 1D model (blue curve) for the discharge and the water heights in Figure 5.21 and Figure 5.22, respectively. The dashed curve in Figure 5.21 is the original HQ100 hydrograph. The results of the 1D model and HydroAS2D align quite well. The achieved peak discharge reduction in the 1D model was 42.05 m^3/s, while in HydroAS2D it was 37.80 m^3/s. The mean absolute error (4.49) in the discharge (Figure 5.21) starting from t=180 hours is $L_1 = 2.31$ m^3/s and the relative absolute error (4.50) in the discharge is only $RL_1 = 2.3\%$. The mean absolute error in water height on the floodplain starting from 170 hours is: $L_1 = 0.047$ m.

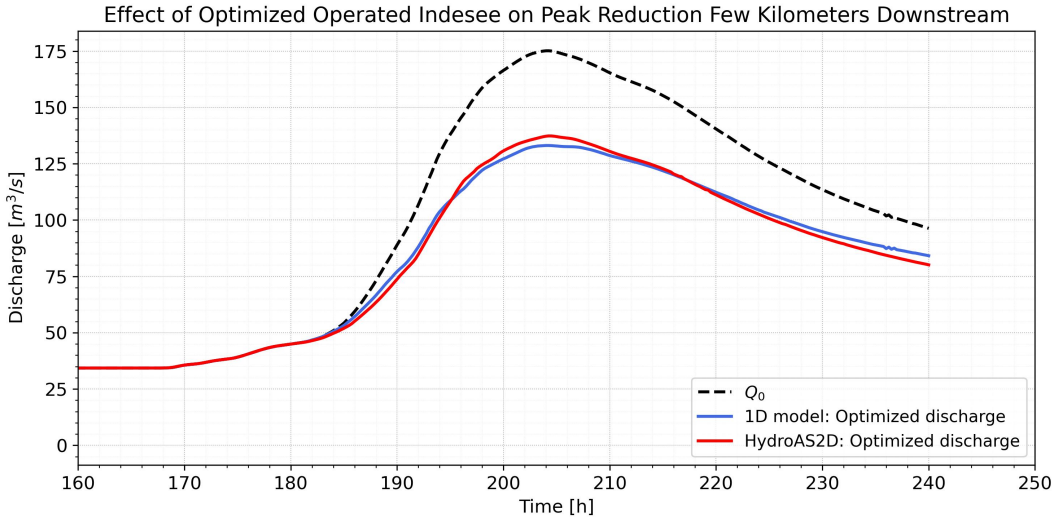

Figure 5.21: Effect of operated optimized Indesee for the HQ100 flood wave on discharge a few kilometers downstream of Indesee.

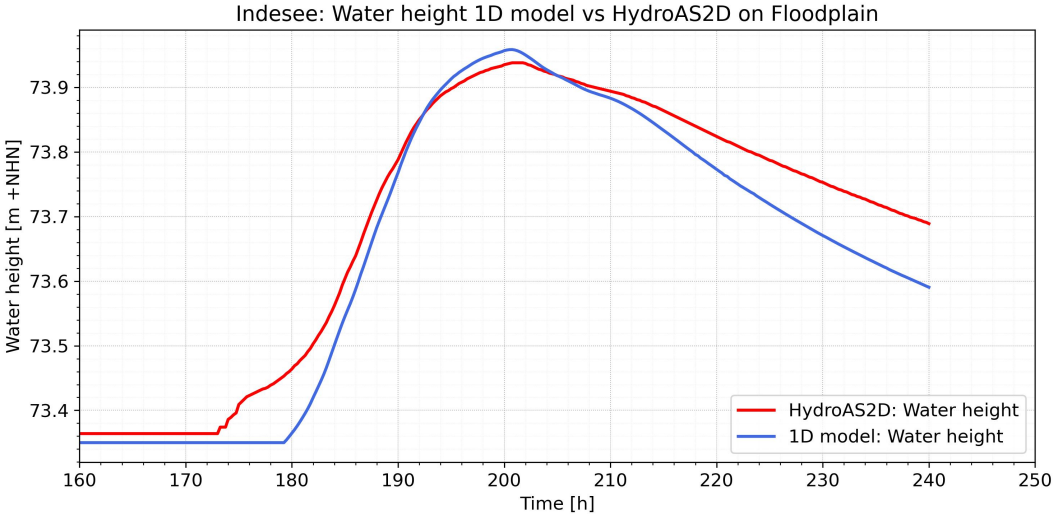

Figure 5.22: Water height difference of the 1D model and HydroAS2D for the optimized Indesee for the HQ100 flood wave a few kilometers downstream of Indesee.

The discharges as computed by the two models further downstream at gauging station Stah near Ophoven are shown in Figure 5.23, with the blue and red curves representing the 1D model and HydroAS2D results, respectively, and the black dashed line representing again the discharge without reduction. To the unreduced discharge and the reduced discharge as computed by the 1D model the discharges of tributaries between the Indesee and Stah as estimated by HydroAS2D have been added. The mean absolute error (4.49) in the discharges at Stah computed from $t = 190$ hours is L_1= 4.78 m^3/s and the relative error is RL1= 3.3%. The peak discharge in HydroAS2D is somewhat higher, but the predictions still align quite well. Since the 1D model assumes a kinematic wave, the shape of the discharge curve is preserved. In contrast, in HydroAS2D the flood wave changes shape somewhat as it propagates the approximately 30 km downstream from the Indesee to the Stah gauging station. The peak reduction estimated with the 1D model remains 42.05 m^3/s due to the kinematic wave assumption, while in HydroAS2D the peak reduction decreases from 37.80 m^3/s to 30.29 m^3/s. This indicates that the Indesee remains 80% effective further downstream.

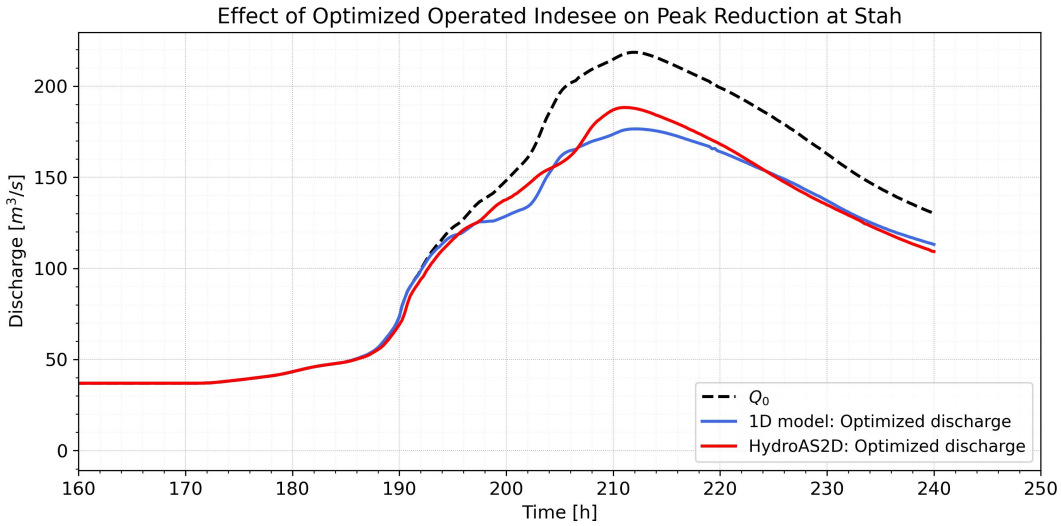

Figure 5.23: Effect of optimally operated basin Indesee for floodwave HQ100 on the discharge at Stah.

The inflow as function of time into the Indesee for both the 1D model (blue curve) and HydroAS2D (red curve) are shown in Figure 5.24. The 1D model slightly overestimates the peak inflow into the basin but underestimated it after the peak.

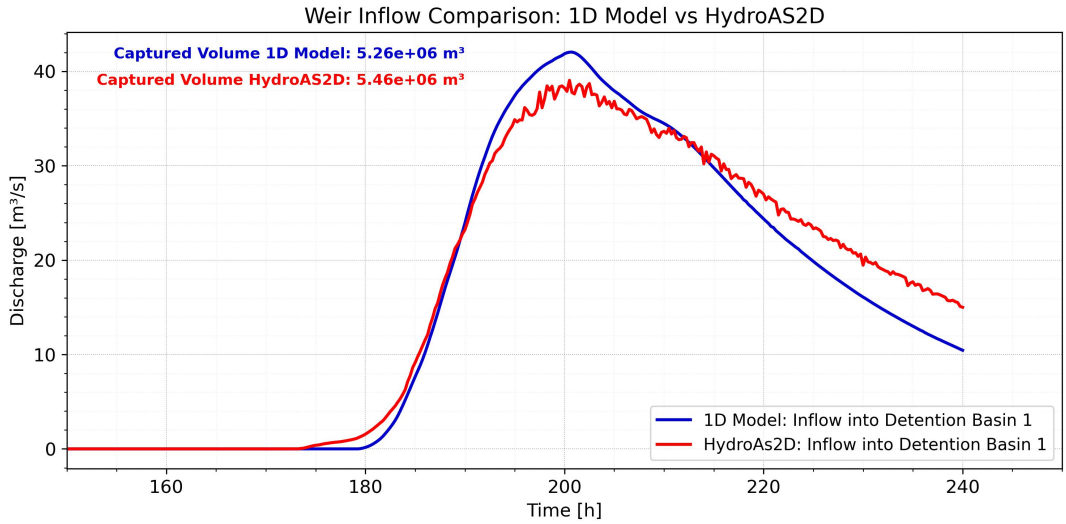

Figure 5.24: Inflow into the Indesee: HydroAS2D vs 1D model for optimized operation for the HQ100 flood wave.

One reason for the better alignment for the large basin than for the small basin considered previously is that the inflow into the larger basin is much more gradual compared to the abrupt opening of a smaller basins, which can lead to pronounced 2D effects that the 1D model cannot capture. The sensitivity of the model to the opening time is significantly reduced in the case of larger detention basins. Furthermore, the representation of the Indesee in HydroAS2D as a very deep basin, likely reduced the water level at the gauging station that operates the weir. This reduction in water height might have caused the water levels on the floodplain in the 1D model and HydroAS2D to align more closely.

The total volume captured in the 1D model was 5.26 million m^3, while in HydroAS2D it was 5.46 million m^3, resulting in a difference of 4%.

5.4. Comparison of the Dike Breach Model and the Weir Equation

In the 1D model the weir equation (4.37) is used to model the flow in a basin, whereas in the HydroAS2D simulations a dike breach was applied as described in Section 4.6.2. To investigate the impact of this difference, the water height $h_{\text{HA}}(t)$ as computed by HydroAS2D at gauging station 1 in Figure 4.12 in front of the inlet, is substituted in the weir equation used in the 1D model:

$$Q_{\text{weir}}(t) = \frac{2}{3} \cdot \mu \cdot b \cdot \sqrt{2g} \cdot [h_{\text{HA}}(t) - H_c]_+^{3/2} . \tag{5.3}$$

The resulting discharge is compared to the discharge $Q_{weir}^{HA}(t)$ over the weir into the basin as computed by HydroAS2D. Both discharges as functions of time are shown in Figure 5.25 for the optimized operated weir of width 60 m of basin 1 and for flood wave HQ100. The average difference between the two discharges relative to the average discharge of HydroAS2D is 30%.

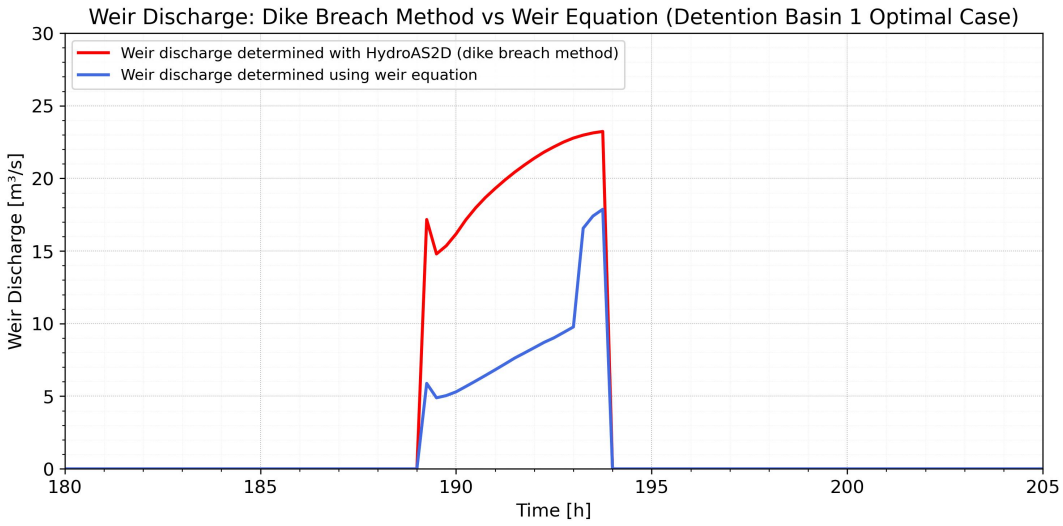

Figure 5.25: Dike breach vs weir equation for optimized operation of the 60 m wide weir of basin 1. The crest height is 73.70 m.

The comparison was also done for the large basin Indesee, again for the weir with width 60 m and optimized operation for flood wave HQ100. The two discharges into the large basin are shown in Figure 5.26. The curves now have no discontinuities because in contrast to the case of the small basin, the weir is opened at (or before) the time the water level reaches the crest height and the basin is never completely full. The mean relative error is 8.6% in this case. The Figure is very similar to Figure 5.24. The red curves in both figures are actually identical but the blue curves differ slightly because in Figure 5.24 the water height as computed in the 1D model is used whereas in Figure 5.26 the water height of HydroAS2D was used in the weir equation. The mean relative error is 8.6% in this case.

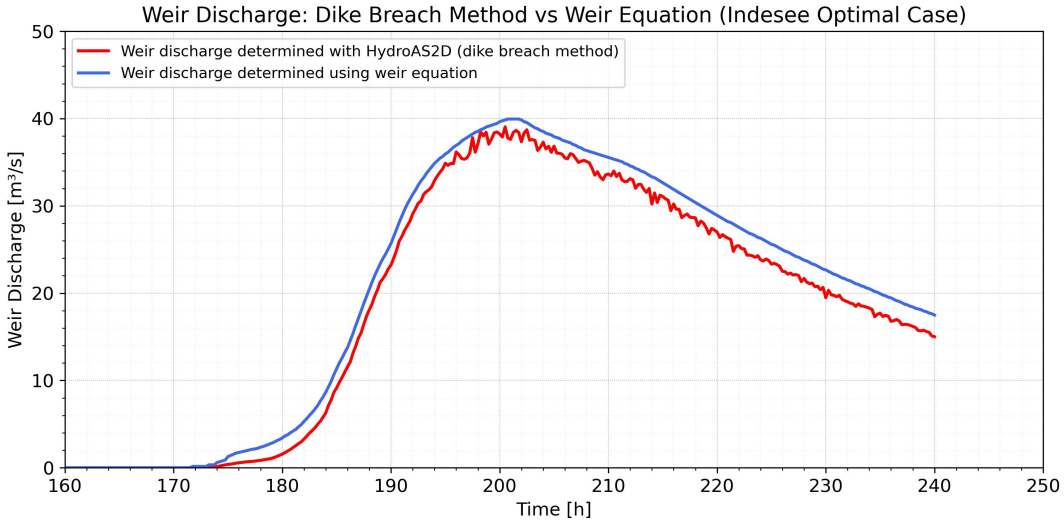

Figure 5.26: Dike breach vs weir equation for optimized operation of the 60 m wide weir of basin Indesee. The crest height is 73.35 m.

In summary, the different models for the flow over the weir seem to have a rather large impact on the difference between the results obtained with HydroAs2D and the 1D model for small basins. The differences seem to be larger when the crest height is higher and also when the weir is opened after the water height has exceeded the crest height ($t_1 > t_c$) as is the case in Figure 5.25. It could be that the sudden decrease of the crest is difficult to simulate with a 2D hydrodynamic model.

For a larger basin such as the Indesee, where the opening process is more gradual and the water inflow aligns with the flood wave shape, the dike breach method and the weir equation agree well.

5.5. Determination of the Storage Volume for a Desired Peak Reduction

It was concluded in Section 5.2 that the storage capacity of the four detention basins along the Lower Rur river is insufficient to achieve a substantial reduction of the water height at Ophoven. This raises the question: what level of peak discharge reduction is required to achieve a certain desired reduction in water height near Ophoven, and what would be the required storage volume of a basin to achieve that?

According to the results of the reference run of HydroAS2D shown in Figure 3.6, Ophoven remains almost completely dry during the HQ100 flood event, except for some outskirt areas and agricultural land. The maximum water depth there was observed to be approximately 35 cm (inundation depth). The aim is now to achieve 35 cm water height reduction to ensure that also the outskirts and direct neighborhood of Ophoven remain dry.

The maximum peak water height without basins at the inundated area of Ophoven is according to HydroAS2D 32.79 m +NHN. Subtracting the desired 35 cm reduction yields a new peak water height of 32.44 m +NHN. To understand what peak discharge reduction corresponds to this peak height, an H-Q plot based on (4.16) was generated for the location near Ophoven (Figure 5.27). From the plot, it follows that the target peak water height corresponds to a discharge of 142.96 m^3/s.

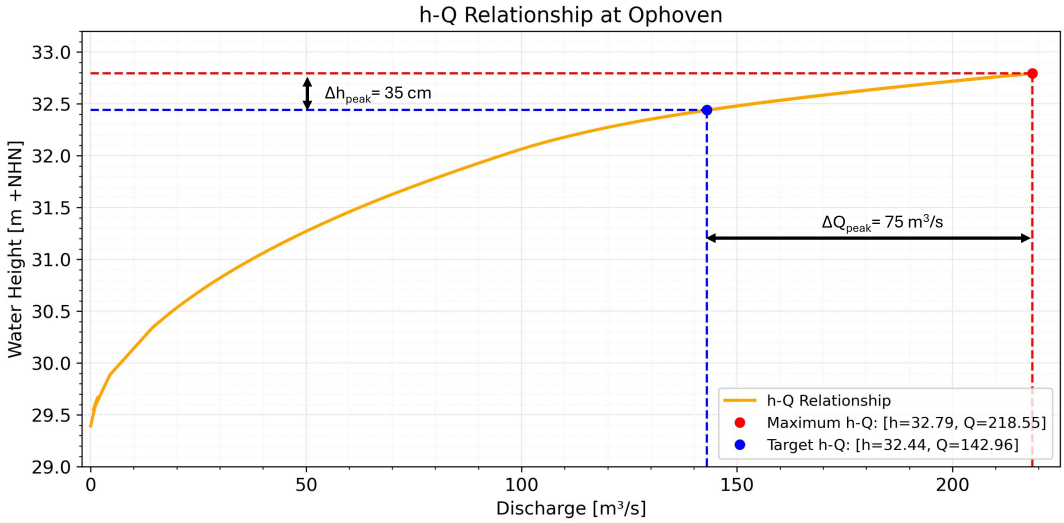

Figure 5.27: Water height-discharge relation at Ophoven.

5.5.1. Application to Flood Scenarios

The required storage volumes for the maximum allowable peak discharge and water height at Ophoven have been estimated for the HQ100, HQ1000, and the 2021 flood events. For the HQ100 flood event, the estimated storage volume was verified by assuming that detention basin 1 would provide this capacity and assessing whether the desired peak reduction could be achieved.

HQ100 flood event

The peak discharge of the HQ100 flood wave at Ophoven is 218.55 m^3/s. To achieve a desired peak discharge of 143.81 m^3/s, a reduction of 75 m^3/s is required. The necessary storage capacity at Detention Basin 1, located near J"ulich as shown in Figure 3.2, can be estimated by subtracting this reduction from the hydrograph at the location of the basin.

This reduces the original peak discharge of 172.48 m^3/s at Basin 1 to 97.48 m^3/s. By integrating the yellow-shaded region in Figure 5.28, the volume of water that must be stored was estimated to be 6.56 million m^3. This further demonstrates that the storage capacities of the basins considered in Section 5.2 are much too small.

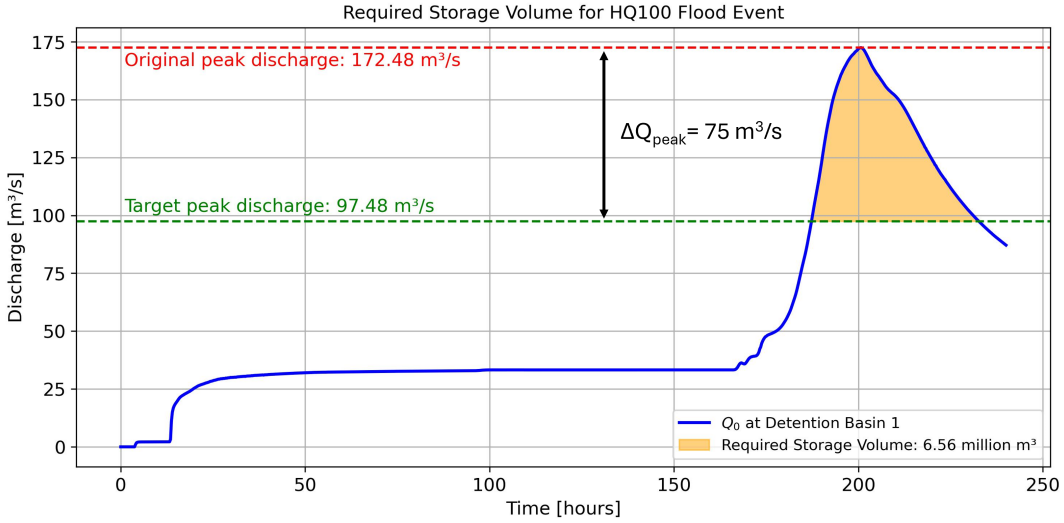

Figure 5.28: Required storage volume to reduce the peak discharge by the amount ΔQ_{peak}.

As in Section 5.3, it is assumed here that the detention basin is sufficiently deep, so that the volume does not depend on the crest height, i.e. V_{max} in (4.30) is independent of H_c. Provided that the width of the inlet of the weir was chosen to be 240 m (four times the initial value), it was found by optimizing the crest height and the opening time of the weir that the required peak discharge reduction can indeed be achieved with a basin storage volume of 6.56 million m^3. The optimal crest height is $H_c = 73.60$ m above NHN, which is 30 cm above the bed level of the floodplain.

Figure 5.29 illustrates that the basin reaches full capacity because t_2 is finite (specifically, $t_2 = 232$ hours). The optimal opening time, t_1, occurs when the water level reaches the crest height ($t_1 = t_c =$ 187 hours) or earlier. In this case, $t_1 = 180$ hours corresponds to the moment water begins to flow onto the floodplain. The reduced discharge exhibits a top hat shape. If the inlet width is only 120 m, the discharge over the weir is too small, resulting in smaller reduction of the downstream discharge. This shows that the inlet width is a critical parameter for effective peak reduction.

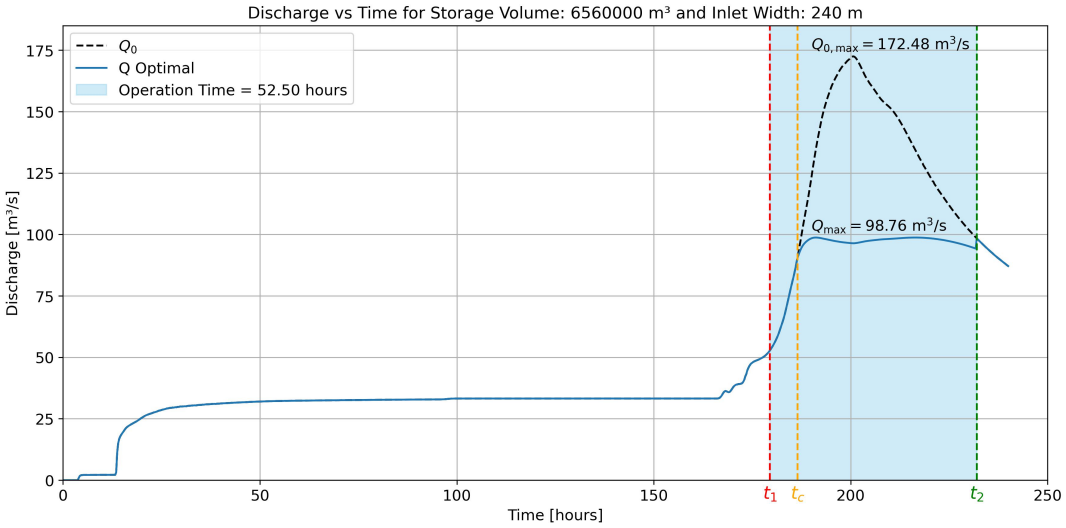

Figure 5.29: Original HQ100 hydrograph as a function of time (dashed curve) and the reduced discharge as a function of time (continuous curve), corresponding to the optimized opening time and crest height. The basin has a storage volume of 6.56 million m^3 and an inlet width of 240 m. The storage volume is assumed to be independent of the crest height.

This analysis suggests that the required storage volume for detention basins to achieve a specified peak reduction can be estimated by integrating under the hydrograph. This approach was proposed in e.g. Homagk and Bremicker (2006). While this investigation involved only a single detention basin, it is possible that the total estimated required volume could be distributed over several basins. However, the effectiveness of such a distributed approach has not been examined here. It is expected that the results may differ from one large basin with the same storage, as inflow into detention basins depends on several factors, including inlet dimensions, bed elevation adjacent to the inlet, and the crest height of the weir.

HQ1000 Flood event

The required storage volume for a detention basin has also been estimated for the HQ1000 flood event. As can be seen in Figure 3.5, the flood peak for the HQ1000 event is not significantly higher than that of the HQ100 flood but it is considerably broader. To achieve the same peak reduction of 143.81 m^3/s to prevent flooding in Ophoven, the volume beneath the flood peak was once again integrated to estimate the required storage volume for this flood event. The HQ1000 flood hydrograph near Ophoven and the integrated area are shown in Figure 5.30. The volume estimated to be necessary to attenuate the flood peak is 18.7 million m^3. This volume is 1.6 times larger than the volume of the Indesee, which was investigated in 5.3. However, the volume of the Indesee was estimated assuming a buffer of only 1 meter of water height, and by making it 1.6 meter deep the required volume is obtained.

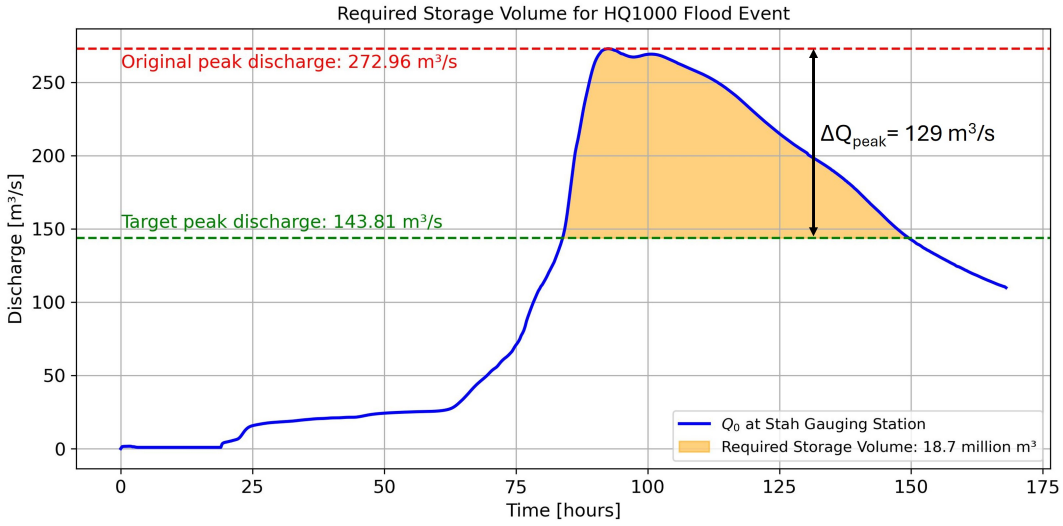

Figure 5.30: Required storage volume to reduce peak discharge of the HQ1000 flood event by ΔQ_{peak}.

2021 Flood event

The 2021 flood event, which caused flooding in Ophoven, has also been analyzed in terms of the required storage volume that would be needed to reduce the peak to a desired level. The 2021 flood hydrograph closely resembles the HQ1000 flood event. Figure 3.5 shows a comparison of the flood hydrographs at the Stah Gauging Station, located near Ophoven. Some data is missing at the trailing edge of the 2021 flood event, as the flood hydrograph terminates while the discharge is still relatively high.

To reduce the flood peak of the 2021 event from 270.76 m^3/s to 148.81 m^3/s, a storage volume of approximately 14.9 million m^3 would be needed, which could be obtained by making Indesee 1.3 m deep. Some more storage will be needed to accommodate the missing tail of the hydrograph.

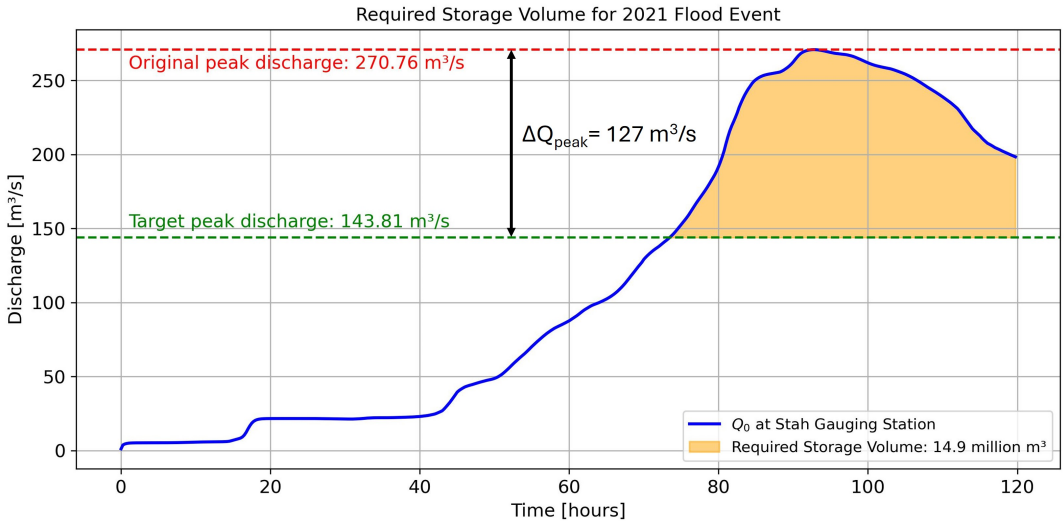

Figure 5.31: Required storage volume to reduce peak discharge of the 2021 flood event.

5.6. Optimization of the Compound Weir

A compound weir consists of multiple fixed crest heights distributed evenly across the inlet. The advantage of a compound weir over an operated weir is that it has a fixed structure and that therefore its effectiveness does not depend on human operation or mechanical movements. But the disadvantage of the fixed design is that it can not be adapted to the flood wave.

The optimization problems for the operated weir and the compound differ in two aspects:

1. The operated weir is opened at an optimum time.
2. If the water height in the basin reaches the crest height in the case of the operated weir the basin is full and is then closed. If the water level in the basin reaches the level of the lowest crest in the case of the compound weir, the water level rises and drops together with the water on the floodplain.

The following connection can now be made between the optimization problems for the operated weir and for the compound weir exists when the same flood wave is considered and the storage volume and width of the inlet are the same in both problems. As remarked before, if the optimum opening time of the operated weir is found to be identical to the time that the water height reaches the optimum crest height ($t_1 = t_c$), and the basin is so large that it is never completely filled ($t_2 = \infty$), then the weir can just as well always be left open. The compound weir is of course always open, so in this case the optimum compound weir gives a reduction of discharge which is at least as large as the optimized operated weir because by choosing the crest heights all equal to the optimum crest height of the operated weir, the same reduction is achieved as for the optimized operated weir. It is possible that due to the fact that the crest heights of the components of the compound weir can be different, an even better solution is obtained in the case of the compound weir.

5.6.1. Detention Basin Site 1 along the Lower Rur River

A compound weir was investigated for the first of the four detention basins in Figure 3.1. The modeling approach for the compound weir is discussed in Section 4.5. The compound weir considered consists of four components. In the optimization, in total 2380 crest height combinations have been simulated. This number of combinations is the result of 15 possible crest heights for each of the 4 components, while respecting the ordering as defined in (4.33).

Figure 5.32 shows the discharge of the compound weir which was optimized for the HQ100 flood wave (blue curve) and the optimized operated weir (orange dashed curve) for the same flood wave. The inlet has width 60 m, hence each of the four components has width 15 m.

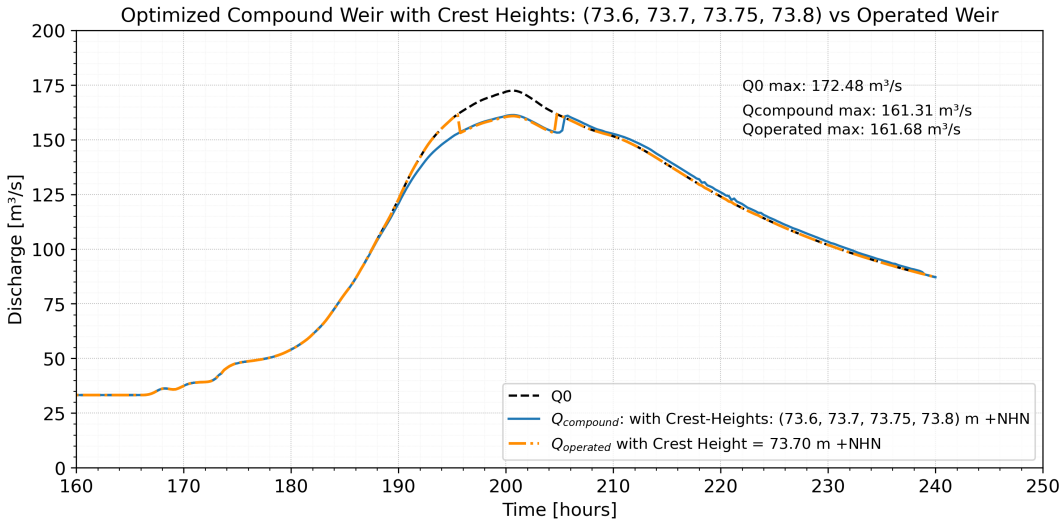

Figure 5.32: Peak discharge reduction for optimum compound weir (blue curve) and optimum operated weir (dashed-dotted orange curve) of basin 1. The discharge of the HQ100 hydrograph is also shown (black dashed curve). The results are for basin 1 in Figure 3.1 and the width of the inlet is 60 m.

The discharge of the original hydrograph of the HQ100 flood wave is also shown (dashed blue curve). It is seen that a similar peak reduction of a flood wave is achieved with the compound weir as with the operated weir when both are optimized for that flood wave HQ100. This true in spite of the fact that the optimum opening time of the weir is later than t_c and the basin is filled ($t_2 < \infty$). The optimal crest height configuration was found to be [$Hc1 = 73.60$ m , $Hc2 = 73.70$ m, $Hc3 = 73.75$ m, $Hc4 = 73.8$ m].

Other crest height combinations similar to the optimum configuration resulted in comparable peak reduction. This is illustrated by Figure 5.33, where the downstream discharges as a function of time are shown for the ten best crest height combinations (in blue) and the ten worst combinations (in red). The optimal crest height combination gives the green curve. The green curve almost overlaps with the blue curves.

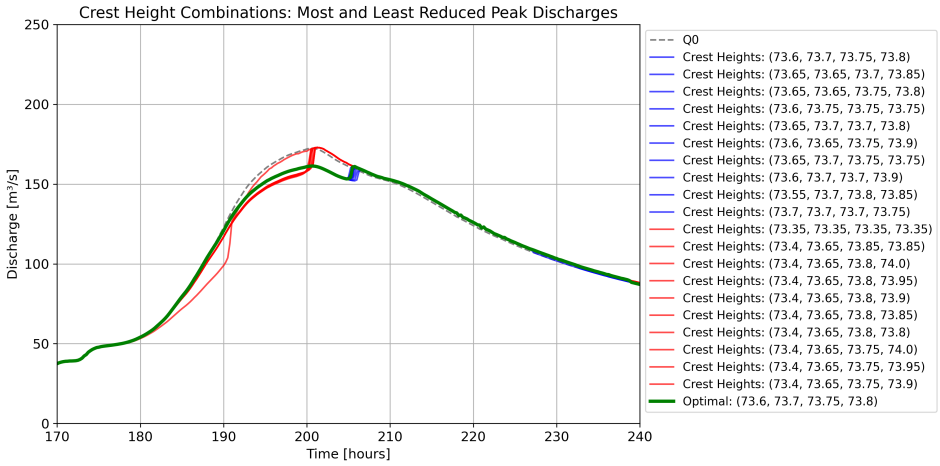

Figure 5.33: Comparison of different crest height combinations and their effect on peak reduction. The results are for flood wave HQ100 and for basin 1 with inlet width of 60 m. Blue curves correspond to the ten best crest height combinations which are close to optimum; the red curves correspond to the ten worst crest height combinations giving no peak reduction.

Figure 5.34 shows the percentage of crest height combinations for 12 values of the peak reduction for the simulated 2380 crest height combinations. Many crest combinations (more than 60%) give very little or even small negative peak reduction. A peak increase can occur due to back flow from the basin to the floodplain. Less than 1% of the crest height combinations give peak discharge reduction between 11 and 12 m^3/s.

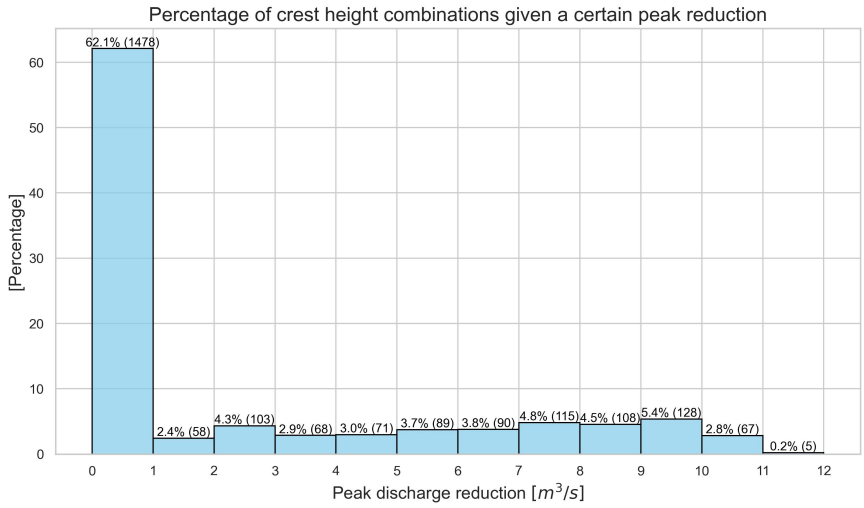

Figure 5.34: Percentages of peak discharge reductions for all 2380 simulated combinations of crest heights. The results correspond to flood wave HQ100 and basin 1 with inlet width 60 m.

Since the compound weir is fixed, the question rises whether a crest height combination which is optimized for the HQ100 flood wave is also sufficiently effective for another flood wave. To investigate this, the extreme scenario of a 1000-year return period flood (HQ1000) was tested using the crest height combination optimized for the HQ100 scenario. Additionally, the HQ1000 scenario was also tested with an operated weir, optimized for the HQ1000 flood wave to compare its effectiveness with the fixed compound weir. The width of the inlet of basin 1 is again 60 m. The black dashed curve in Figure 5.35 shows the original hydrograph for the HQ1000 event. It has peak discharge of 210.16 m^3/s. The discharge of the compound weir which was optimized for the HQ100 flood wave (blue curve) and the discharge of the operated weir which was operated for the HQ1000 flood wave (orange dashed curve) are also shown as functions of time. It can be seen that the compound weir does not reduce the peak of the HQ1000 flood event. However, this outcome is not solely due to the compound weir design. As previously noted for the operated weir, the lack of impact is primarily due to the limited volume of the basin relative to the scale of the design flood events. Figure 5.35 also shows that, while the operated weir achieves a peak reduction, the reduction is very small namely 7.72 m^3/s due to the small volume of the basin. Therefore, the compound weir could still be a viable alternative to the operated weir if the detention basin volume is larger.

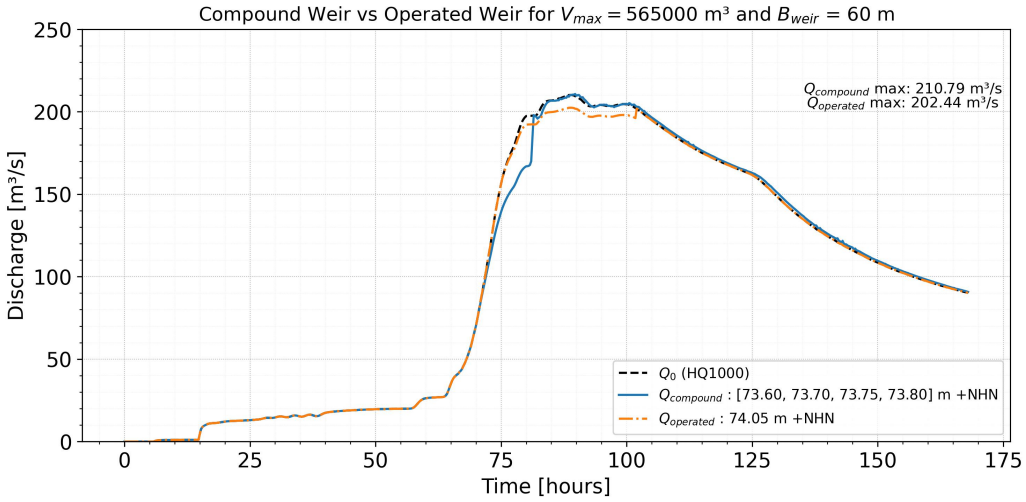

Figure 5.35: Effect of the compound weir, which was optimized for the HQ100 event, for the case of the HQ1000 flood event (blue curve). The discharge of the operated weir optimized for the HQ100 event (orange curve) and the original hydrograph (black dashed curve) are also shown. The results are for basin 1 with inlet width of 60 m.

5.7. Practical Aspects of Operated and Multi-Compound Weirs

Operating a weir allows for achieving the same water height reduction with a smaller storage volume compared to scenarios without operation. For very large basins, the weir can be opened as soon as the discharge Q_0 of the hydrograph reaches a level where downstream flooding is expected. However, for smaller basins, there is a risk that the basin will reach its capacity before the maximum peak discharge arrives, having no mitigating effects. This risk is even greater when the weir remains permanently open, as is the case for an un-operated weir. In addition to storage volume, the width of the inlet is a crucial parameter. If the inlet width is too narrow, the storage volume may not be fully used, leading to a less peak reduction than otherwise could have been achieved.

Once a suitable storage volume and inlet width have been found for a set of relevant flood waves, determining the optimal opening time t_1 and crest height to minimize downstream discharge requires knowledge of the upstream hydrograph $Q_0(t)$. As Q_0 is measured at an upstream gauging station, the flood wave continues to propagate toward the basin. Therefore, it is important for the gauging station to be positioned sufficiently far upstream of the basin to allow enough time for optimizing the operation parameters and the actual operation of the weir.

For the Indesee basin, the upstream gauging station located farthest upstream is at the Obermaubach Dam, approximately 30 km away. According to the HydroAS2D simulation, the HQ100 flood wave

propagates at a high wave speed of approximately 1.85 m/s, resulting in a travel time of only 4.5 hours from the dam to the basin. Alternatively, the wave speed of a flood wave can be measured in real time using methods such as satellite imaging or drones.

The wave speed of 1.85 m/s limits the optimization process to a 4.5-hour segment of the hydrograph, which must encompass the period of maximum discharge. Once the maximum discharge is detected, measurements must continue for an additional 2.25 hours. The relevant portion of the hydrograph for optimization is then the segment spanning 2.25 hours before and after the maximum discharge. Consequently, the discharge reduction achievable is constrained by the maximum discharge values within this 4.5-hour window.

Alternatively, it may be assumed that the hydrograph is symmetric about its maximum. In this case, once the maximum discharge is identified, a longer time interval from 4.5 hours before to 4.5 hours after the maximum can be used for optimization. This approach allows for a greater reduction in peak discharge.

So the circumstances at the Rur river for applying optimized operation of a weir at the Indesee basin are not favorable. In general, applying optimizing of the operation of a weir in real time requires a larger time between the measurement and the arrival of the flood wave at the basin.

It should also be noted that when optimizing the operation, a safety margin should be applied to the predicted peak reduction to account for potential inaccuracies inherent in the 1D model. This safety margin can be determined by comparing the results from the 1D model with those obtained from a more accurate model, such as HydroAS2D, or by comparing the predictions against observed measurements.

For an operated weir, the Obermaubach dam is too close, resulting in a very short operation interval that makes real-time optimization not feasible. This is why the application of a compound weir is more promising, as it eliminates the need for real-time control and can be designed to effectively manage various flood scenarios. First an appropriate storage volume and inlet size must be estimated. Once these parameters are determined, the crest heights should be optimized to achieve satisfactory peak reduction for a representative set of flood waves, rather than focusing solely on maximizing peak reduction for a single flood event. Additionally, a safety margin should be incorporated into the optimization process to account for potential inaccuracies in the 1D model. The optimization of the multi-compound weir, following this approach, is recommended as a focus for future research.

5.8. Summary of Results

This section summarizes the main results of the chapter. Table 5.1 contains all configurations and results obtained by optimizing the operated weir for the HQ100 flood wave and for both the 1D model and HydroAS2D. First the results of the 1D model for the HQ100 scenario with optimized operated weirs of the four proposed detention basins are listed. The predicted discharge and water height reduction at Ophoven are listen in yellow and bold. Next in the table the results obtained with HydroAS2D are listed for the same basins and the HQ100 scenario with optimized operation of the weirs. Then the results of optimizing the operation of the big basin Indesee for the HQ100 scenario is given for two inlet widths. The corresponding effect for Ophoven are again highlighted in yellow and bold.

It should be noted that detention basins 1 to 4 are used with their current terrain, which implies that the basins are relatively shallow. Consequently, the storage volume of these basins is highly sensitive to the crest height of the weir ($V_{max}(H_c)$). In contrast, the Indesee is assumed to be sufficiently deep such that its storage volume may be considered independent of the crest height of the weir. It followed from the analysis in Section 5.3.2, that the small reductions in water height downstream of detention basins 1 and 4 are negligible compared to the discrepancies between the 1D model and HydroAS2D. In contrast, for the Indesee the reduction in water height downstream of the weir was shown to be significant.

The lack of peak reduction observed for detention basins 1 to 4 in the HydroAS2D simulations can be attributed to both the water height on the floodplain next to basin being higher in HydroAS2D than in the 1D model and the fact that in HydroAS2D the weir can not be opened at a specific time but instead has to be opened by monitoring the water height (which shows discrepancies with the 1D model). This

has led to premature inflow into the basins. Additionally, differences in the modeling of the weir, which in HydroAs2D is treated as a dike breach while in the 1D model a weir equation is used, has led to differences in the inflow in the basin. Specifically, the dike breach model in HydroAS2D produced higher inflow discharges, particularly for detention basin 1, causing the basin to fill faster than predicted by the 1D model. As a result, the basin reached full capacity before the arrival of the peak of the discharge.

In contrast, the results for the Indesee were very promising. A significant reduction in peak discharge was achieved, particularly when the inlet width was increased, showing the critical role of inlet width as a design parameter. Moreover, the 1D model and HydroAS2D showed good agreement.

Table 5.1: Overview of the results of the cases and scenario's for the optimization of operated weirs.

Case/Scenario	Model	Weir Type	Inlet Width (m)	Storage Volume (m^3)	Local Peak Discharge Reduction (m^3/s)	Local Water Level Reduction (cm)
Detention Basin 1 HQ100	1D model	Operated	60 m	344,000 m^3	10.8 m^3/s	4 cm
Detention Basin 2 and 3 HQ100	1D model	Operated	60 m	N.A.	0 m^3/s	0 cm
Detention Basin 4 HQ100	1D model	Operated	60 m	45,000 m^3	3.09 m^3/s	1 cm
Total 4 Basins HQ100 at Ophoven	**1D model**	**Operated**	**60 m**	**389,000 m^3**	**11.48 m^3/s**	**4 cm**
Detention Basin 1 HQ100	HydroAS2D	Operated	60 m	344,000 m^3	0 m^3/s	0 cm
Detention Basin 2 and 3 HQ100	HydroAS2D	Operated	60 m	N.A.	0 m^3/s	0 cm
Detention Basin 4 HQ100	HydroAS2D	Operated	60 m	45,000 m^3	0 m^3/s	0 cm
Total 4 Basins HQ100 at Ophoven	**HydroAS2D**	**Operated**	**60 m**	**389,000 m^3**	**0 m^3/s**	**0 cm**
Indesee HQ100	1D model	Operated	60 m	11.6 million m^3	42.06 m^3/s	16 cm
Indesee HQ100	1D model	Operated	120 m	11.6 million m^3	84.09 m^3/s	37 cm
Total Indesee HQ100 at Ophoven	**1D model**	**Operated**	**60 m**	**11.6 million m^3**	**42.06 m^3/s**	**18 cm**
Indesee HQ100	HydroAS2D	Operated	60 m	11.6 million m^3	37.80 m^3/s	N.A.
Total Indesee HQ100 at Ophoven	HydroAS2D	Operated	60 m	11.6 million m^3	30.29 m^3/s	N.A.

Because the four detention basins along the Rur river were found to be not effective for the HQ100 flood event, an investigation was conducted to determine the storage volume required to ensure that the peak discharges of the HQ100, HQ1000, and 2021 flood events do not exceed at target discharge. The target discharge corresponds to a desired reduction of 35 cm of the water height on the floodplain at Ophoven. The results of this investigation are listed in Table 5.2.

The results show that the HQ100 flood event, being the least extreme, requires the smallest storage volume to achieve the desired water height reduction. The HQ1000 and 2021 flood events have similar peak discharges. However, the HQ1000 flood event needs a greater storage volume due to its longer duration of high peak discharges than the flood wave associated to the 2021 flood event (see Figure 3.5).

Table 5.2: Overview of the required storage volume for desired peak reduction at Ophoven.

Scenario	Target Peak Discharge	Target Peak Reduction	Required Storage Volume
HQ100	142.96 m^3/s	75 m^3/s	6.56 million m^3
HQ1000	142.96 m^3/s	129 m^3/s	18.70 million m^3
2021 Flood Event	142.96 m^3/s	127 m^3/s	14.90 million m^3

The results of the optimization of the compound weir optimization are shown in Table 5.3. Only the 1D model was used, i.e. no verification with HydroAS2D has been done. The findings that when optimizing the crest heights for a specific scenario, in this case, the HQ100 flood event, it can achieve peak reductions comparable to that of an operated weir. However, when applying the optimized compound weir crest height configuration from the HQ100 flood event to the HQ1000 flood event for detention basin 1, it was observed that the basin fills too quickly under this crest height configurations. This outcome is primarily due to the limited storage capacity of the detention basins.

These results suggest that the compound weir must be optimized taking account of multiple flood scenarios, rather than solely for the HQ100 flood event, to achieve good effect across various flood events. Additionally, the total inlet width and storage volume are critical parameters that significantly influence the effectiveness of the detention basins.

Table 5.3: Overview of the results of the cases and scenarios for the optimization and verification of the compound weirs.

Case/Scenario	Weir Type	Inlet Width (m)	Crest Heights (m + NHN)	Storage Volume (m^3)	Local Peak Discharge Reduction (m^3/s)	Local Water Level Reduction (cm)
Detention Basin 1 HQ100	Compound	4 x 15 m	[73.60, 73.70, 73.75, 73.80]	344,000 m^3	11.17 m^3/s	4 cm
Detention Basin 1 HQ1000	Compound	4 x 15 m	[73.60, 73.70, 73.75, 73.80]	344,000 m^3	0 m^3/s	0 cm

6

Discussion

6.1. Summary of Main Results

In the first phase of the project the general and versatile tool RCT-Tools was used. This tool has been and still is being developed by Deltares to implement techniques from operational research to design operational strategies for time-dependent steering in hydraulic engineering. While RTC-Tools was initially considered, its general setup and the necessity for a more complex library required for the applications studied in this thesis, led to the decision to develop an own tool to optimize the operation of detention basins along the Rur river.

The main objective was to determine operational strategies of weirs of detention basins along the Lower Rur river for a prior-known flood event (HQ100) in order to minimize the flood peak. In this study a 1D kinematic wave model which incorporates floodplains was developed to determine the optimal opening time and crest height of the inlet weirs. The advantage of this model was short computation times, which made it suitable for optimization. Furthermore, because of its fast computation time it can be be used in real time applications, which depend on measured hydrograph sufficiently far upstream. The 1D model was also applied to determine the crest heights of a compound weir consisting of four components. The compound weir can be designed off-line and can not be adapted to different flood waves.

In the optimization the flood wave HQ100 was of prime interest. The four basin locations proposed in a previous study in the river reach between Jülich and Ophoven were initially adopted without modifying the terrain. The weirs of the four basins were optimized sequentially, with the optimized reduced discharge of one weir used as hydrograph for the next weir. It turned out that the combined volume of 398000 m^3 of these basins was too small to achieve a significant peak reduction at Ophoven for the HQ100 wave.

A single large detention basin at the site of the Indesee of 11.6 million m^3 was investigated. For an inlet width of 60 m the local water height reduction was 16 cm, while for a 120 m inlet the reduction was 37 cm.

A method was proposed to estimate a suitable volume for a detention basin to achieve a given water height reduction downstream. For a water height reduction of 35 cm at Ophoven for floodwave HQ100, a basin at Indesee should have storage volume of 6.56 million m^3, while for the extreme case of a HQ1000 flood wave the required volume was estimated at 18 million m^3.

Although only a limited number of cases were studied, the optimization of the crest heights for the compound weir showed results comparable to those of the optimized operated weir for the specific flood wave it was optimized for. The effectiveness of the compound weir for other flood waves, however, depends on the degree of variability between the flood waves. If the flood waves are significantly different from the one for which the compound weir was optimized, it may be less effective or ineffective.

The results of the optimized operated weirs for the HQ100 flood wave were compared with simulations

from HydroAS2D, which is based on the 2D Saint-Venant equations and is therefore expected to be more accurate than the 1D model. For large basins, the agreement between the two models is quite good. However, for smaller basins, such as the four basins mentioned, the results are highly dependent on the timing of the weir opening. In HydroAS2D, the weir can only be opened indirectly by monitoring the water depth, which leads to discrepancies. Additionally, the fact that HydroAS2D models the weir as a dike breach, while the 1D model uses a weir equation, causes differences, particularly for smaller basins.

6.2. Interpretations

Optimizing the opening time and crest height provides a flexible method to reduce peak discharge, depending on the flood waves. In the optimization, the basin is considered full when the water height reaches the crest height, after which the weir is closed. The weir should always be opened before the maximum peak discharge arrives, but not so early that the basin reaches its full capacity before the peak occurs.

It was found that, for an upstream hydrograph with a single maximum and for which the maximum of the reduced hydrograph downstream of the weir is lower than the maximum of the upstream discharge at times t_1 and $t_2(t_1)$ for all t_1, then the optimal opening time occurs when the upstream discharge is equal to the upstream discharge at the time when the basin reaches its full capacity. For very large basins, the optimal opening time tends to be earlier, either occurring before or at the moment the water height reaches the crest height. In contrast, for smaller basins, it is advantageous to open the weir later, allowing the basin to capture the higher discharges. In general, an operated weir enables the use of a smaller storage volume for the basin.

If the terrain of the basin is not modified, as in the case of the four detention basins initially studied, the volume of water in the basin becomes a complex, non-linear function of crest height elevation. This complicates the optimization process, as lowering the crest height has two opposing effects: it allows more water to flow into the basin, but it also causes the basin to fill more quickly, while a low crest height yields smaller volume. For a sufficiently deep basin, such as the Indesee, the storage volume can be considered independent of the crest height.

In contrast to the operated weir, a compound weir can experience backflow from the basin to the floodplain when the water heights in both the basin and floodplain are the same and above the lowest crest. This leads to an increase in the discharge downstream of the weir during these times. Additionally, for the compound weir, the proper choice of inlet width is important. It plays a key role in determining the flow dynamics and overall efficiency of the system.

A more severe flood event than the HQ100, such as the HQ1000 flood event, is associated with higher discharges and consequently higher water levels on the floodplain in front of the weir. Opening the weir early and setting the crest to a low level would cause the basin to fill too quickly, potentially reaching full capacity before the flood peak arrives and thereby having no effect. Conversely, setting the crest higher and delaying the opening of the weir would result in only a small peak reduction, with the reduction occurring only shortly before and after the peak. Thus, in the optimization, the trade-off between opening time and crest height is crucial.

While choosing appropriate opening time and crest height of the weir reduces the peak discharge by a certain amount, the flood wave often maintains its original shape. However, for very large inlet width, allowing large volumes of water to enter the basin during a specific time, the shape of the flood wave can be drastically changed, even to the extend that the entire peak is cut-off. The inlet width, however, is not an adjustable parameter during operation and must be designed in advance to accommodate various flood scenarios. The inlet width of 60 m, used in the majority of runs in this study, resulted in only 50$\%$ of the volume being used of the Indesee for the HQ100 wave. This caused the Indesee to be much less effective than for twice the inlet width, where a greater volume of floodwater can be captured, leading to more peak reduction.

6.3. Implications

Detention basins present a promising solution to mitigate future flood damage in villages and properties near the Rur river. In particular, using (part of) the Indesee as a detention basin could significantly reduce water heights at Ophoven. For the HQ100 flood wave, the storage volume required to achieve a water height reduction of 35 cm at Ophoven with the optimized operated weir is less than 11.6 million m^3, provided that the inlet width is 240 m. The crest height is set to a medium level, and the weir should be opened before the water height reaches the crest. This approach could also be implemented using a compound weir, which is simpler, but may not always be effective for other flood waves.

To achieve the required storage volume with one (or all) of the proposed four basins, these basins would need to be excavated to considerable depths, as there is only a limited amount of area available.

In contrast, because of the large area of the Indesee, the basin would only need a depth of 1 m to realize the required volume of 11.6 million m^3. Alternatively, only part of the area could be used, provided the basin is made deeper. Currently, the location of the Indesee contains a operational lignite mine, which is scheduled for closure in 2030. The plan is to repurpose this area into a lake, which seems to align well with its potential function as a detention basin.

In a simulation of the 2021 flood wave the peak discharge in the Wurm river tributary was found to be very high. While the simulations should be verified, if the results are accurate, it may be beneficial to consider developing a separate detention basin for the Wurm tributary.

6.4. Limitations

To optimize the operation of a weir in real time, it is essential to have knowledge of a relevant segment of the hydrograph around the peak discharge. The time interval around the moment of maximum discharge that can be used is determined by the time it takes for the flood wave to propagate from the gauging station to the basin. Consequently, the gauging station must be located sufficiently upstream from the basin. This presents a challenge for the Indesee basin on the Rur, as the Obermaubach dam, situated only 30 km upstream, results in the flood wave reaching the Indesee basin in approximately 4.5 hours, given the estimated wave speed for the HQ100 flood wave. This implies that the maximum time window for considering the hydrograph centered on the peak discharge is limited to 4.5 hours, thus constraining the reduction to discharges close to the peak.

In contrast, the compound weir is not subject to this limitation since it is pre-designed. Although the compound weir performs well for the flood wave it was optimized for, it is generally less effective for other flood waves.

The validation of the 1D model was complicated by the fact that the weir in HydroAs2D was modeled as a dike breach instead of the weir equation as in the 1D model. This discrepancy led to significant differences in inflow estimates for smaller basins, even for the same water height.

The 1D model includes many parameters that must be determined, such as the Manning coefficients for both the main river and floodplains, as well as the bed slope. These parameters need to be either calibrated or taken from databases. The Manning coefficients for floodplains are expected to be influenced by vegetation, which can vary seasonally. At present, only the configuration of the river and floodplains near the basin inlet is relatively accurately approximated through the Vertical Interface procedure. In this model, selected cross-sections are subdivided into segments, at least three: two for the floodplains and one for the main river, and bed levels are averaged to ensure the water volumes in these segments align with actual values. However, in cases where the river near an inlet is curved, or where backwater effects occur due to hydraulic structures or river confluences, water height variations may arise which the 1D model cannot simulate. These variations can lead to errors, which in some cases leads to insignificant results obtained of the 1D model.

6.5. Recommendations

1. Further study investigating the application of the Indesee as a detention basin, potentially incorporating a compound weir.
2. The large discharge observed in the Wurm during the 2021 flood event should be verified. If

it is confirmed that the Wurm significantly contributed to the flooding of Ophoven in 2021, the feasibility of implementing a detention basin at the Wurm should be investigated.

3. The option of using the weir equation in HydroAS2D should be further explored. To better study the operation of a weir, it would be beneficial if HydroAS2D allowed for the weir to be opened at any desired time.
4. When using the 1D model to optimize the operation of a weir or the crest heights of a compound weir, a safety margin should be added to the required water height reduction to account for potential modeling inaccuracies.
5. The compound weir should not be optimized for a single flood wave but rather for a set of relevant flood waves. While this approach may not result in an optimal design for each individual flood wave, it will ensure peak reduction across the entire set of flood waves.
6. To improve the accuracy of the optimization, HydroAS2D could be used to simulate water heights on the floodplain with closed basins. These simulated water heights could then be incorporated into the weir equation during the optimization of the crest heights of the compound weir. This approach could improve the accuracy of the optimization results while maintaining reasonable computation times, as HydroAS2D would only need to be run once. However, this method would not be applicable for real-time optimization of the operated weir.
7. Finally a proposal for a rather theoretical but interesting research topic is made, which is motivated by the observation that not only the opening time and the crest height but also the width of the inlet of the basin is an important parameter. It is suggested to investigate an operated compound weir, of which the opening time of the weir as a whole and the heights of crests are optimized depending on the flood wave. By choosing the crest heights appropriately, the width of the inlet of the basin can effectively be changed and this can be done depending on the flood wave. By choosing sufficiently many components a large range of inlet widths can be realized.

7

Conclusion

The main research question was:

How can operational strategies for potential detention basins along the Lower Rur river in Germany be optimized, to achieve maximum peak reduction at Ophoven?

Operational strategies for potential detention basis along the lower Rur river were based on optimizing the opening time and the crest height of the weir of a basin depending on the flood wave. Connected to this were the sub-questions:

1. **What model can be developed to optimize operational strategies for detention basins?**
   A 1D kinematic flow model was developed that incorporated the floodplains and used a weir equation to model the discharge into the detention basin. This model was fast and therefore well-suited for optimization purposes.
2. **What are the optimum operational strategies for the detention basins, and how much do they attenuate the flood peak?**
   It was found that, for a hydrograph such as the HQ100 flood wave, which has only a single maximum, and for which the maximum of the reduced downstream discharge is smaller than the maximum of the upstream discharge at opening time t_1 and corresponding closure time t_2, then the optimal opening time is at the moment that the upstream discharge equals the upstream discharge at the corresponding time t_2. The optimum crest height of the weir depends on the water height on the floodplain, where a lower crest height allows more peak reduction, but fills the basin faster, making it reach its capacity sooner. Conversely, a higher crest height restricts the inflow over the weir, resulting in a smaller effect on peak reduction. The inlet width is also of great importance, as it determines the magnitude of the inflow. A wider inlet, similar to a lower crest height, results in more peak reduction but causes the basin to fill more quickly.
3. **How do the prediction of the new 1D model compare to the results obtained with HydroAS2D?**
   For large basins, the 1D model and the 2D model HydroAS2D gave similar predictions, even though in HydroAS2D the weir is modeled as a dike breach and it cannot be opened directly at a desired time. However, for smaller basins, the differences in how the weir is modeled led to discrepancies between the two models.
4. **Can a compound weir with fixed crests be an alternative to operated weirs?**
   The four crest heights of a compound weir were optimized for the HQ100 flood wave, resulting in similar peak discharge reductions as those achieved with the optimized operated weir. However, unlike the operated weir, which can be optimized for any flood wave, the compound weir is optimized for a specific flood wave and thus may be less effective or even ineffective for other flood events.

First, the operation of four basins along the stretch of the Rur river between Jülich and Ophoven, for which the locations were proposed in previous research, was investigated. It was found that, without

modifications to the terrain, the volume of these basins is too small to enable a significant reduction in the peak discharge of the HQ100 flood wave. This conclusion also holds for the compound weir.

Close to Jülich, there is currently an active lignite mine, which is scheduled for closure in 2030 and will then be transformed into a lake, the ”Indesee.” This new lake could potentially be used as a detention basin. If a buffer depth of just one meter were made available, the resulting storage volume would be approximately 11.6 million m^3.

A method was developed to estimate the required volume of a basin to achieve a given reduction in water height at Ophoven. The results indicated that a volume on the order of 6.56 million m^3 would be required to reduce the water height by 35 cm at Ophoven. To achieve such a volume with the four proposed basins would need to be deepened due to the limited available area at the proposed locations, which makes the Indesee an attractive alternative.

For the optimized operated weir for a volume of 6.56 million m^3 the target water height reduction at Ophoven of 35 cm was achieved for the HQ100 flood wave, provided the width of the inlet was 240 m. It was found that for such large basins, the apart from the crest height, also the size of the inlet is an important parameter to enable sufficient water to flow into the detention basin.

The optimization of the opening time and crest height requires knowledge of the hydrograph over a significant interval of time centered around the time of the peak discharge. The maximum interval of time is equal to the time it takes for the flood wave to propagate from the upstream gauging station to the basin. Unfortunately, the gauging station which is farthest upstream from the basin at Indesee is at the Obermaubach dam which is so close that the said time interval is limited to 4-5 hours. Therefore it seems more promising to use the compound weir at Indesee. However a compound weir which is optimized for a certain flood wave does not always give satisfactory peak reduction for another possible flood wave. To improve the effectiveness of the compound weir for many relevant flood waves, it is therefore recommended to design the crest height such that for a representative set of flood waves the peak discharge reduction is satisfactory.

In the preliminary investigation of the 2021 flood event it was found that the Wurm tributary had a very high peak discharge. This should be verified and if it is confirmed, it is recommended to also consider one or several detention basin(s) for the Wurm.

By optimizing both the opening time and the crest heights of the components of a compound weir, it would be possible not only to control the crest height but also the width of the inlet. This can be achieved provided the compound weir consists of a sufficiently large number of components. While this type of weir may not be suitable for the Indesee basin during real-time control due to the reasons discussed earlier, it could hold significant potential for sites where the hydrograph can be measured at considerable distances upstream of the basin.

References

Asenkerschbaumer, M., Skublics, D., & Rutschmann, P. (2012). *Verzögerung und abschätzung von hochwasserwellen entlang der bayerischen donau* (Abschlussbericht). München.

Asselman, N., De Jong, J. S., Kroekenstoel, D., & Folkertsma, S. (2022). The importance of peak attenuation for flood risk management, exemplified on the Meuse River, the Netherlands. *Water Security*, *15*, 100114. https://doi.org/10.1016/j.wasec.2022.100114

Asselman, N., van Heeringen, K.-J., de Jong, J., & Geertsema, T. (2022). *Juli 2021 overstroming en wateroverlast in zuid-limburg: Eerste bevindingen voor valkenburg, geulmonding, roermonding en eygelshoven* (Deltares report, published on April 26, 2022). Deltares. https://www.waterschaplimburg.nl/publish/pages/7013/juli_2021_overstroming_en_wateroverlast_in_zuid-limburg.pdf

Avakyan, A. B., & Polyushkin, A. A. (1989). Flood control experience in the USA. *Hydrotechnical Construction*, *23*(1), 53–58. https://doi.org/10.1007/BF01433192

Avakyan, A., Saltantin, V., & Pianese, D. (1986). The effect of fluid-mitigation reseroir configuration on peak-discharge reduction during preliminary design. *VJ. of Hydrology.*, (52).

Battjes, J. A., & Labeur, R. J. (2017, February). *Unsteady Flow in Open Channels* (1st ed.). Cambridge University Press. https://doi.org/10.1017/9781316576878

Becker, B. P. J., Jagtenberg, C. J., Horváth, K., Mitchell, A., & Rodríguez□Sarasty, J. A. (2024). Optimization methods in water system operation. *WIREs Water*, e1756. https://doi.org/10.1002/wat2.1756

Cao, Z. (2006). Flow resistance and momentum flux in compound open channels. *J. Hyd. Engg. ASCE*, *132*(12), 1272–1282.

Chow, V., Maidment, D., & Mays, L. (1988). *Applied hydrology*. McGraw Hill.

Deltares. (2024). *Rtc-tools - control and optimisation*. Retrieved October 28, 2024, from https://www.deltares.nl/en/software-and-data/products/rtc-tools-control-and-optimisation

Demny, G., & Lohr, H. (2014). Hochwassermerkmalsimulation zur quantifizierung des klimawandels. *Simulationsverfahren und Modelle für Wasserbau und Wasserwirtschaf*.

Dickson, D. (2018, October). Dry Detention ponds (2004) | CT Stormwater Quality Manual. Retrieved June 25, 2024, from https://ctstormwatermanual.nemo.uconn.edu/11-design-guidance/dry-detention-ponds-2004/

DKKV. (2022). *Die flutkatastrophe im juli 2021 in deutschland*. Deutsches Komitee Katastrophenvorsorge e.V. (DKKV). https://dkkv.org/wp-content/uploads/2023/02/DKKV__Schriftenreihe_Juli_2022__Webversion__-_2te_Version_August3.pdf

Eingrüber, N., & Korres, W. (2022). Climate change simulation and trend analysis of extreme precipitation and floods in the mesoscale Rur catchment in western Germany until 2099 using Statistical Downscaling Model (SDSM) and the Soil & Water Assessment Tool (SWAT model). *Science of The Total Environment*, *838*, 155775. https://doi.org/10.1016/j.scitotenv.2022.155775

flosm. (2024). *Stromnetzen mit umspannwerken und detaillierter infrastruktur*. Retrieved November 2, 2024, from https://www.flosm.org/de/Stromnetz.html?lat=51.08520562&lon=6.14418502&r=2274.8615&st=1&sw=cabledistributioncabinet,powerbay,powerbusbar,powercable,powercompensator,powerconverter,powerline,powerline110k,powerline115k,powerline20k,powerline220k,powerline220v,powerline225k,powerline30k,powerline380k,powerline3k,powerline400k,powerline420k,powerline500v,powerline50k,powerline6k,powerline750k,powerline765k,powerlinedchigh,powerlinedclow,powerminordistribution,powerplantarea,powerpole,powersubstation,powerswitch,powertower,separationzone,transformer

Gerner, A., & Blaurock, M. (2018). *Handbuch hydraulische modellierung*. Bayerisches Landesamt für Umwelt (LfU). Augsburg.

Giehl, S. (2019). Optimierung der wirkung gesteuerter flutpolder am bayerischen inn mithilfe zd-hn-modellierung. *21. Treffen der JuWi*, 69–74.

Glinowiecka-Cox, M. (2022). *Analytical solution of the 1d-diffusion-convection equation with varying boundary conditions* (Definitief rapport). Portland State University.

Gourbesville, P., & Caignaert, G. (Eds.). (2022a). *Advances in Hydroinformatics: Models for Complex and Global Water Issues—Practices and Expectations*. Springer Nature Singapore. https://doi.org/10.1007/978-981-19-1600-7

Gourbesville, P., & Caignaert, G. (Eds.). (2022b). *Advances in Hydroinformatics: Models for Complex and Global Water Issues—Practices and Expectations*. Springer Nature Singapore. https://doi.org/10.1007/978-981-19-1600-7

Hager, W. H. (1987). Lateral Outflow Over Side Weirs. *Journal of Hydraulic Engineering*, *113*(4), 491–504. https://doi.org/10.1061/(ASCE)0733-9429(1987)113:4(491)

Hartgring, S. (2023). *On forcasting the rur river*. Delft University of Technology.

Homagk, D.-I. P., & Bremicker, D. M. (2006). Steuerungsstrategien für die rückhaltemaßnahmen am oberrhein. *Proceedings zum Kongress Wasser Berlin*.

Horn, G., & Hurkmans, R. (2022, December). *Analyse & maatregelen wateroverlast roer: Definitief rapport* (Definitief rapport). HKV.

Horritt, M. S., & Bates, P. D. (2001). Predicting floodplain inundation: Raster-based modelling versus the finite-element approach [_eprint: https://onlinelibrary.wiley.com/doi/pdf/10.1002/hyp.188]. *Hydrological Processes*, *15*(5), 825–842. https://doi.org/10.1002/hyp.188

Hydrotec Ingenieurgesellschaft für Wasser und Umwelt mbH. (2023, May). *HydroAS Reference Manual: 2D-flow model for water management applications* (Version 6.0.0) [All rights reserved. Any form of reproduction – even extracts – is only allowed with permission.]. Version 6.0.0. Aachen, Germany. https://www.hydrotec.de

Jaffe, D. A., & Sanders, B. F. (2001). Engineered Levee Breaches for Flood Mitigation. *Journal of Hydraulic Engineering*, *127*(6), 471–479. https://doi.org/10.1061/(ASCE)0733-9429(2001)127:6(471)

JCAR ATRACE. (2024). *About us*. Retrieved November 8, 2024, from https://www.jcar-atrace.eu/en/about-us

Junghänel, T., Bissolli, P., Daßler, J., Fleckenstein, R., Imbery, F., Janssen, W., Lengfeld, K., Leppelt, T., Rauthe, M., Rauthe-Schöch, A., Rocek, M., Walawender, E., & Weigl, E. (2021). *Hydroklimatologische Einordnung der Stark- und Dauerniederschläge in Teilen Deutschlands im Zusammenhang mit dem Tiefdruckgebiet „Bernd“ vom 12. bis 19. Juli 202*.

Keßels, J., Wolf, S., Römer, W., Dörwald, L., Schulte, P., & Lehmkuhl, F. (2024). Enormous headward and gully erosion in a floodplain area reclaimed for open-cast lignite mining during the July 2021 flood in the Inde River valley (Western Germany). *Environmental Sciences Europe*, *36*(1), 182. https://doi.org/10.1186/s12302-024-00997-4

Köln, B. (2024). Umsetzung der eg-hochwasserrichtlinie [Accessed: 2024-10-01]. https://www.bezreg-koeln.nrw.de/themen/umwelt-und-natur/wasserwirtschaft/hochwasserschutz/umsetzung-der-eg

LandesverbandNRW. (2023). Tagebaurestsee inden: Mehr platz für die natur [Accessed: 2024-10-27]. https://www.bund-nrw.de/meldungen/detail/news/tagebaurestsee-inden-mehr-platz-fuer-die-natur/

LANUV. (2024). *Hochwasserportal*. Retrieved November 30, 2024, from https://hochwasserportal.nrw/lanuv/webpublic/#/overview/Wasserstand?filter=%7B%22WTO_OBJECT%22%3A%22Rur%22%7D&period=P7D

Liu, Q., Qin, Y., Zhang, Y., & Li, Z. (2015). A coupled 1D–2D hydrodynamic model for flood simulation in flood detention basin. *Natural Hazards*, *75*(2), 1303–1325. https://doi.org/10.1007/s11069-014-1373-3

Manandhar, B., Cui, S., Wang, L., & Shrestha, S. (2023). Post-Flood Resilience Assessment of July 2021 Flood in Western Germany and Henan, China. *Land*, *12*(3), 625. https://doi.org/10.3390/land12030625

Mertins, S. (2021). Flutgebiet Ophoven: «Mit einem neuen Damm wären wir hier nicht abgesoffen», sagt der Ortsvorsteher. *NZZ*. https://www.nzz.ch/international/unwetter-in-deutschland-ophoven-kaempft-gegen-das-wasser-ld.1787829

Miller, J. E. (1984). *Basic concepts of kinematic-wave models* (Professional Paper). U. S. GEOLOGICAL SURVEY PROFESSIONAL PAPER 1302.

Milly, P., Betancourt, J., Falkenmark, M., Hirshc, R., Kundzewicz, Z., Lettenmaier, D., & Stouffer, R. (2008). Stationarity is dead: Whither water management? *Science*, *319*(5863), 573–574.

Ministerium für Umwelt, Naturschutz und Verkehr. (2024). *Hochwasser*. Retrieved April 4, 2024, from https://www.umwelt.nrw.de/themen/umwelt/umwelt-und-wasser/gewaesser/hochwasser

Morales-Hernandez, M., Petaccia, G., Bufrau, P., & Garcia-Navarro, P. (2009). Conservative 1d-2d coupled numerical strategies applied to river flooding: The tiber (rome). *International J. Heat and Mass Transfer*, *52*, 3297–3304.

Nakamura, F. (Ed.). (2022). *Green Infrastructure and Climate Change Adaptation: Function, Implementation and Governance*. Springer Nature Singapore. https://doi.org/10.1007/978-981-16-6791-6

Perez-Guerrero, J., Pimentel, L., Skaggs, T., & Van Genuchten, M. (2016). Analytic solution of the advection-diffusion transport equation using a change-of-variable and integral transform technique. *Applied Mathematical Modelling*, *40*, 2087–2105.

Pirone, D., Cimorelli, L., & Yakovleva, V. (2024). Reservoirs of the usa. *Vodno Resur.*, *52*, 101676.

Sanders, B. F., Pau, J. C., & Jaffe, D. A. (2006). Passive and active control of diversions to an offline reservoir for flood stage reduction. *Advances in Water Resources*, *29*(6), 861–871. https://doi.org/10.1016/j.advwatres.2005.07.015

Schweim, L. (2024). *Deich-potenzialstudie und ableitung von ansätzen zur flutpolderbewirtschaftung am beispiel der unteren rur*. RWTH Aachen.

Shishegar, S., Duchesne, S., Pelletier, G., & Ghorbani, R. (2021). A smart predictive framework for system-level stormwater management optimization. *Journal of Environmental Management*, *278*, 111505. https://doi.org/10.1016/j.jenvman.2020.111505

StadtJülich. (2012). Rahmenplan indesee. https://www.juelich.de/lw_resource/datapool/_items/item_2374/indeland_juelich_2012-02-09.pdf

Sturm, T. (2001). *Open channel hydraulics*. McGraw Hill.

Subramanya, K. (2009). *Flow in open channels* (3th ed.). Tata McGraw Hill.

Sun, X., Shiono, K., Rameshwaran, P., & Chandler, J. H. (2010). Modelling vegetation effects in irregular meandering river. *Journal of Hydraulic Research*, *48*(6), 775–783. https://doi.org/10.1080/00221686.2010.531101

Wang, K., Wang, Z., Liu, K., Cheng, L., Bai, Y., & Jin, G. (2021). Optimizing flood diversion siting and its control strategy of detention basins: A case study of the Yangtze River, China. *Journal of Hydrology*, *597*, 126201. https://doi.org/10.1016/j.jhydrol.2021.126201

Woolderink, H., Cohen, K., Kasse, C., Kleinhans, M., & Van Balen, R. (2021). Patterns in river channel sinuosity of the Meuse, Roer and Rhine rivers in the Lower Rhine Embayment rift-system, are they tectonically forced? *Geomorphology*, *375*, 107550. https://doi.org/10.1016/j.geomorph.2020.107550

WVER. (2024a). *Die rur*. Retrieved May 3, 2024, from https://wver.de/fluss/die-rur/

WVER. (2024b). Faktencheck zum hochwasser [Accessed: 2024-10-17]. https://wver.de/faktencheck-zum-hochwasser/

WVER. (2024c). *Hochwasserschutz*. Retrieved May 3, 2024, from https://wver.de/hochwasserschutz/

WVER. (2024d). *Unsere talsperren*. Retrieved May 7, 2024, from https://wver.de/unsere-talsperren/

Zidan, A. (2015). Review of frinction formulae in open channel flow. *IWTJ*, *5*(1), 101676.

A

Optimization of detention basins with RTC-Tools

This appendix discusses the application of RTC-Tools in developing a model aimed at optimizing the operation of detention basins along the Lower Rur River.

RTC-tools is an open source-tool developed by Deltares to support decision-making processes for the control and optimization of hydraulic assets and water systems. It comes in the shape of a Python package, making it compatible with other software such as Modelica, which is used for modeling water systems with an user-interface (Deltares, 2024). RTC-Tools can be used for (multi-)objective optimization, which makes it a promising model to optimize detention basin operation for the Lower Rur.

However, currently RTC tools has limitations regarding the incorporation of the effect of floodplains. This required a shift to a more complex library, which incorporates a numerical solver for the De Saint Venant equations. This library has only been developed recently. The alternative approach based on solving De Saint Venant equations was more time-consuming than the 1D analytical model and is therefore more cumbersome to use in the optimization of the operation of detention basins. There turned out to be a small bug within the library, which caused some delay. Therefore it was decided to discontinue using RTC tools and instead make a more specialized model for in particular the lower Rur where broad floodplains are common.

In this appendix the progress and results obtained with the initial model implemented in RTC-Tools are discussed, and an outline is given of how the model could have been set up using the more complex library.

A.1. Basic model

The basic model in RTC-Tools is describes the basic relationship between the volume of water in a reservoir (or detention basin) V and the inflow Q_{in} and outflow Q_{out} (Becker et al., 2024):

$$\frac{\partial V}{\partial t} = Q_{in} - Q_{out} \tag{A.1}$$

The inflow into the detention basin as a function of time, $Q_{in}(t)$, and the outflow as a function of time, $Q_{out}(t)$, were defined as the optimization variables. Furthermore, an inequality constraint was imposed on the detention basin volumes to ensure the capacity of the basin will not be exceeded.

Initially, a single detention basin was modeled using RTC-Tools library ”Simple Routing”, focusing on the basin near Ophoven, which has a maximum storage capacity of 100,000 m^3. This setup was visualized using Modelica and is shown in Figure A.1. The model configuration includes an inflow boundary condition, represented by a hydrograph with a return period of 1-in-100 years (indicated by the pink star). A subsequent node (red-yellow dot) was introduced to divert flow either into the detention

basin (red square) or further downstream along the Rur River. The basin is linked to this diversion node and the outflow from the basin connects to a second node, which discharges water from the detention basin back to the Rur river. The outflow boundary is indicated with a pink rectangle. It is important to note that this model set-up water flows from the river directly into the detention basin, without accounting for floodplain storage area in between the basin and the river.

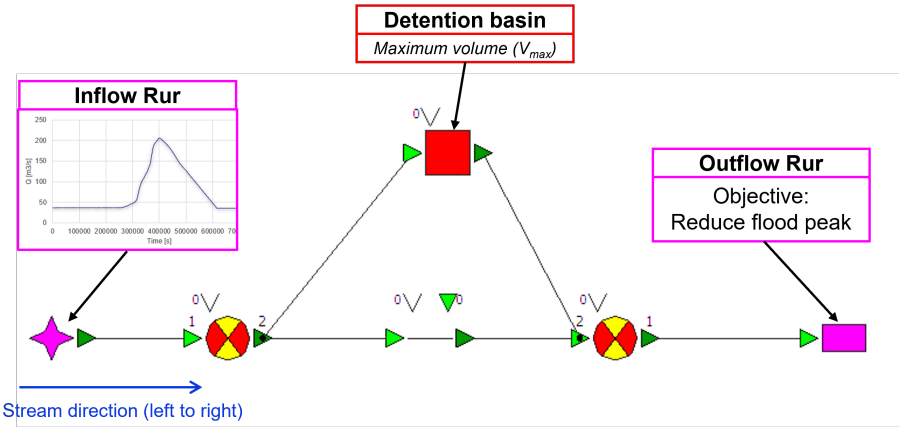

Figure A.1: One detention basin modeled in RTC-Tools.

The objective of the optimization was to minimize the peak discharge at the outflow boundary. The optimal operational strategy to achieve the optimum reduction as obtained with RTC-Tools, showed that only a minimal peak reduction could be achieved. This agrees with the predictions of the 1D analytical model and is primarily caused by the limited storage volume of 100,000 m^3. Figure A.2 illustrates these results, with the optimized flood hydrograph shown in blue (barely distinguishable due to the basin's minimal impact). The original flood hydrograph, Q_0, is given by the orange curve. The results further indicate that the basin operates by allowing inflow just prior to the peak, capturing as much flow as possible during the flood's peak phase.

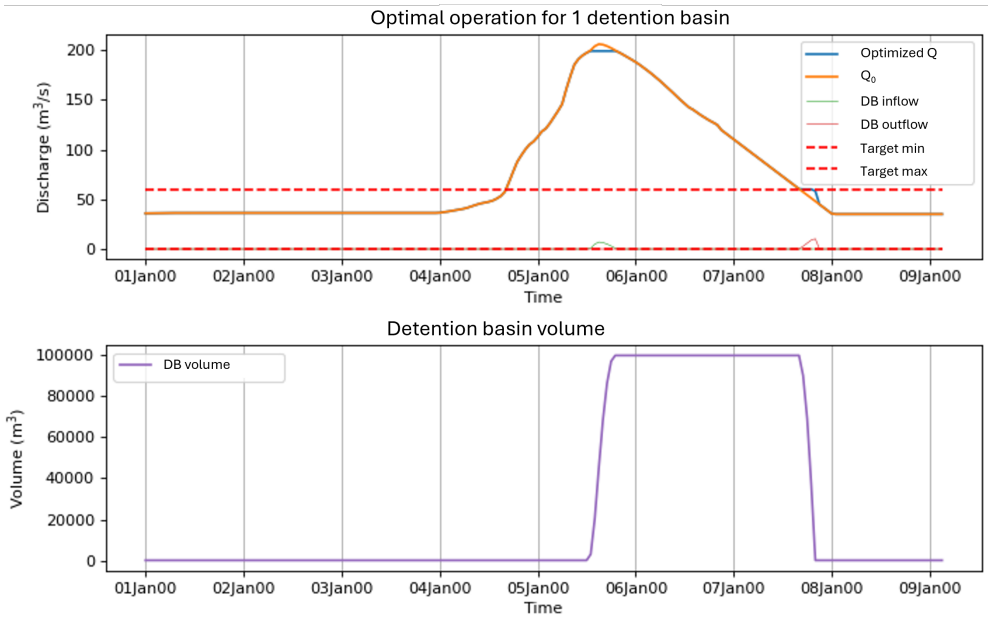

Figure A.2: Result of one operated detention basin in RTC-Tools.

Given the limited effect of a single detention basin, the RTC-Tools model was expanded to include four detention basins, each with a storage capacity of 100,000 m^3, as well as one large basin with a capacity

of 11.6 million m^3, referred to as the Restsee or Indesee. The Restsee represents a potential future project, involving the filling of a decommissioned lignite mine with water. Examining the impact of such a large basin is of interest to determine the extent of peak reduction achievable. More details on the Restsee are provided in Section 5.3.

The model setup is shown in Figure A.3. The river now includes a network of detention basins, each connected by a ”delay-branch” to ensure the flood wave arrives at each basin at the appropriate time. Additionally, the Wurm tributary has been incorporated into this expanded model. Positioned near detention basin 4, it is assumed in this setup that flow from the Wurm can be directed into detention basin 4.

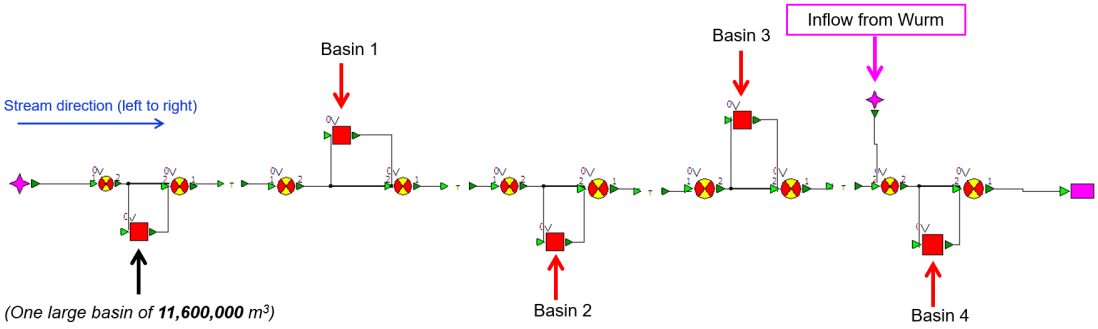

Figure A.3: Four small detention basins of 100,000 m^3 and one large basin of 11.6 million m^3 modeled with RTC-Tools.

First the peak reduction achieved through the optimized operation of four small detention basins, each with a capacity of 100,000 m^3, is provided in Figure A.4. As shown, the peak discharge has been reduced more effectively than in the configuration with only one detention basin, although this reduction remains quite small. Additionally, a time shift in the optimized hydrograph can be observed. This shift can be attributed to the fact that the inflow hydrograph (represented by the orange curve) is imposed approximately 30 kilometers upstream of the outflow boundary.

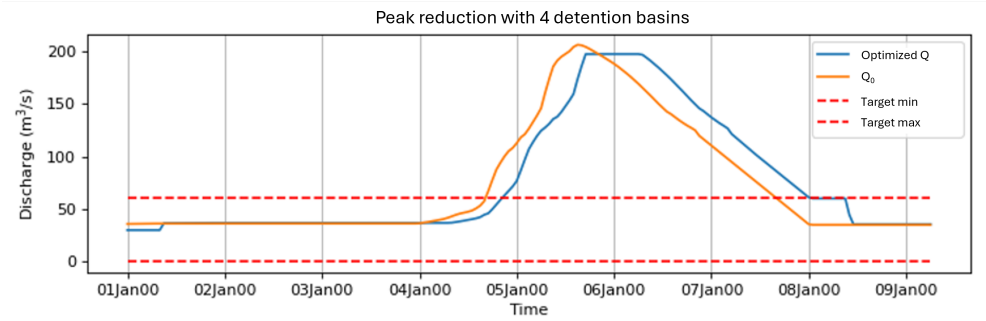

Figure A.4: Peak reduction with 4 small detention basins of 100,000 m^3.

Given the limited effectiveness of the four small detention basins, the very large detention basin with a capacity of 11.6 million m^3 was added to the network, which is positioned furthest upstream. This large basin demonstrates substantial impact on peak reduction, as illustrated in Figure A.5. The peak discharge was reduced by 100 m^3/s, showing great influence of the large basin compared to only the four smaller basins. However, these results are based on an idealized scenario in which flow is directed

into the basins in an optimal manner to maximize peak reduction. Further investigation is required to determine if this operation is physically feasible, necessitating additional constraints that account for realistic physical limitations.

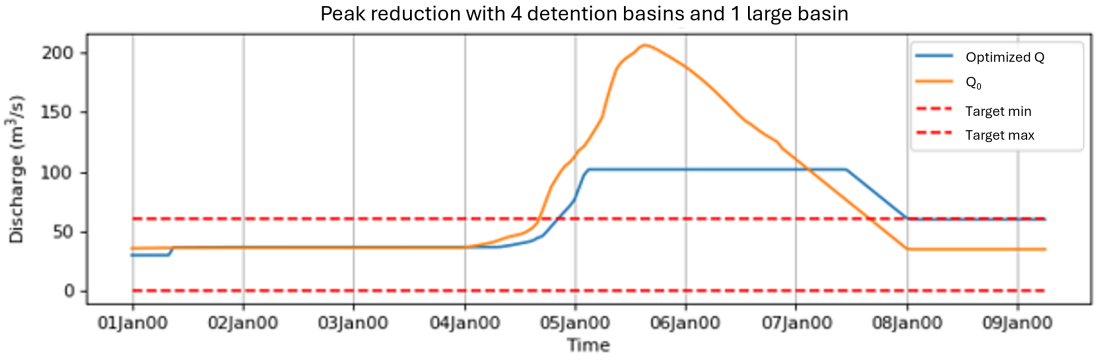

Figure A.5: Peak reduction with 4 small detention basins of 100,000 m^3 and 1 large basin of 11.6 million m^3.

A.2. Incorporation of floodplains

As mentioned in the introduction to this Appendix, incorporating the effects of floodplains required an alternative modeling approach beyond the basic model. To achieve this, the RTC-Tools Hydraulic library was used, which includes a river routing element suitable for representing floodplains. The river was divided into sections, similar with the segmentation approach discussed in Section 4.2.

To accurately model the inflow boundary condition (hydrograph), the flow was distributed over three branches, ensuring that the sum of their discharges at each timestep is equal to the discharge of the hydrograph. Each branch was assigned specific parameters, including friction coefficient, river slope, and bed elevation. By segmenting the river cross-section into three parts, consisting of the main channel and two adjacent floodplains, this approach enabled a more realistic estimation of floodplain discharge near the detention basin, yielding a more physically accurate representation of potential inflows into the basin compared to the basic model.

The setup incorporating floodplains is shown in Figure A.6 in Modelica, with flow direction from left to right. Here, the hydrograph is applied at the inflow boundary (pink triangle), with discharges at each time step divided among three branches, marked by blue rectangles. In this configuration, flow from the leftmost branch is directed into the detention basin indicated by the red square. The the outflow from the basin re-enters the river again. Of course, water also continues to flow over the floodplain without entering the detention basin. Downstream of the basin, the three branches recombine again and flow toward the downstream boundary, defined by a water level. Since this water level boundary condition is based on empirical data and requires calibration, it introduces some uncertainty into the model.

This model setup has potential for further extension, but was discontinued in this MSc thesis due to a small bug in the library, which caused some delays. Additionally, the Hydraulic library within RTC-Tools is still under development and not yet widely implemented, which made it challenging to use in this study, particularly for an application like detention basin inflow, which it had not been tested for.

That said, the model shown in Figure A.6 could have been extended to include multiple detention basins, and it would have been possible to integrate a weir equation to provide more realistic estimates of detention basin inflow. Further investigation would be needed into the optimization algorithm and the definition of goals/objective functions to effectively achieve peak reduction at the downstream boundary. Additionally, the 30-kilometer river reach, which has varying floodplain widths and changing bed elevations, would need to be modeled in the network to obtain accurate routing results.

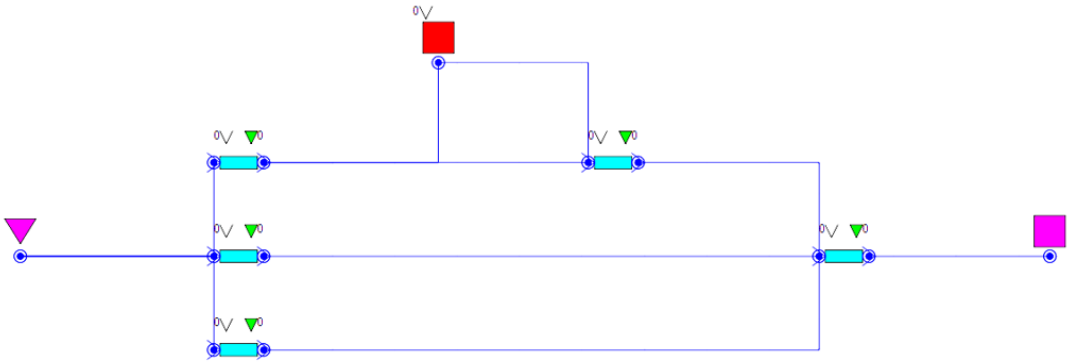

Figure A.6: RTC-Tools model with floodplains.

B

Inundation depths reference case

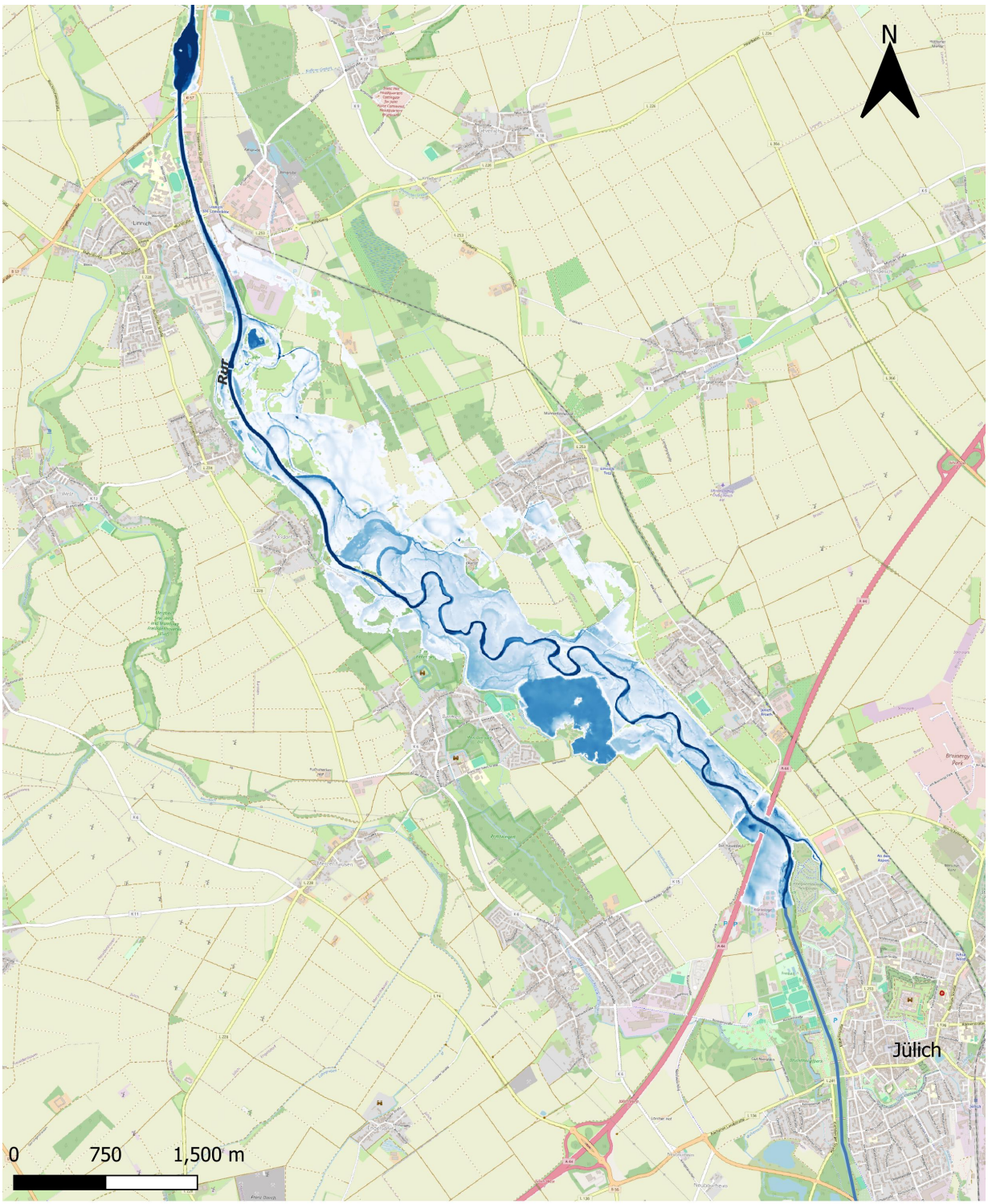

Figure B.1: Inundation depth reference case HQ100 near Jülich

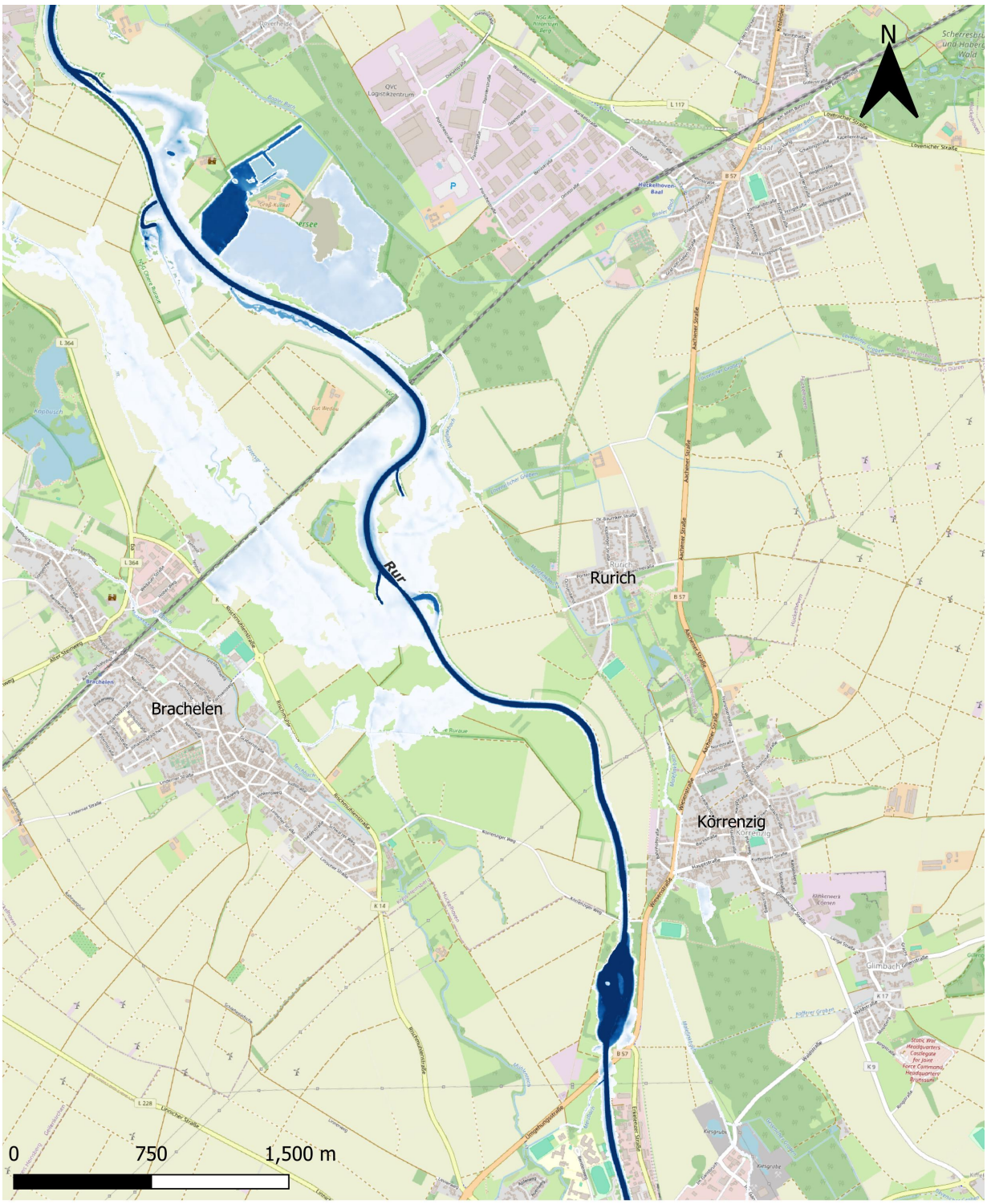

Figure B.2: Inundation depth reference case HQ100 near Brachelen

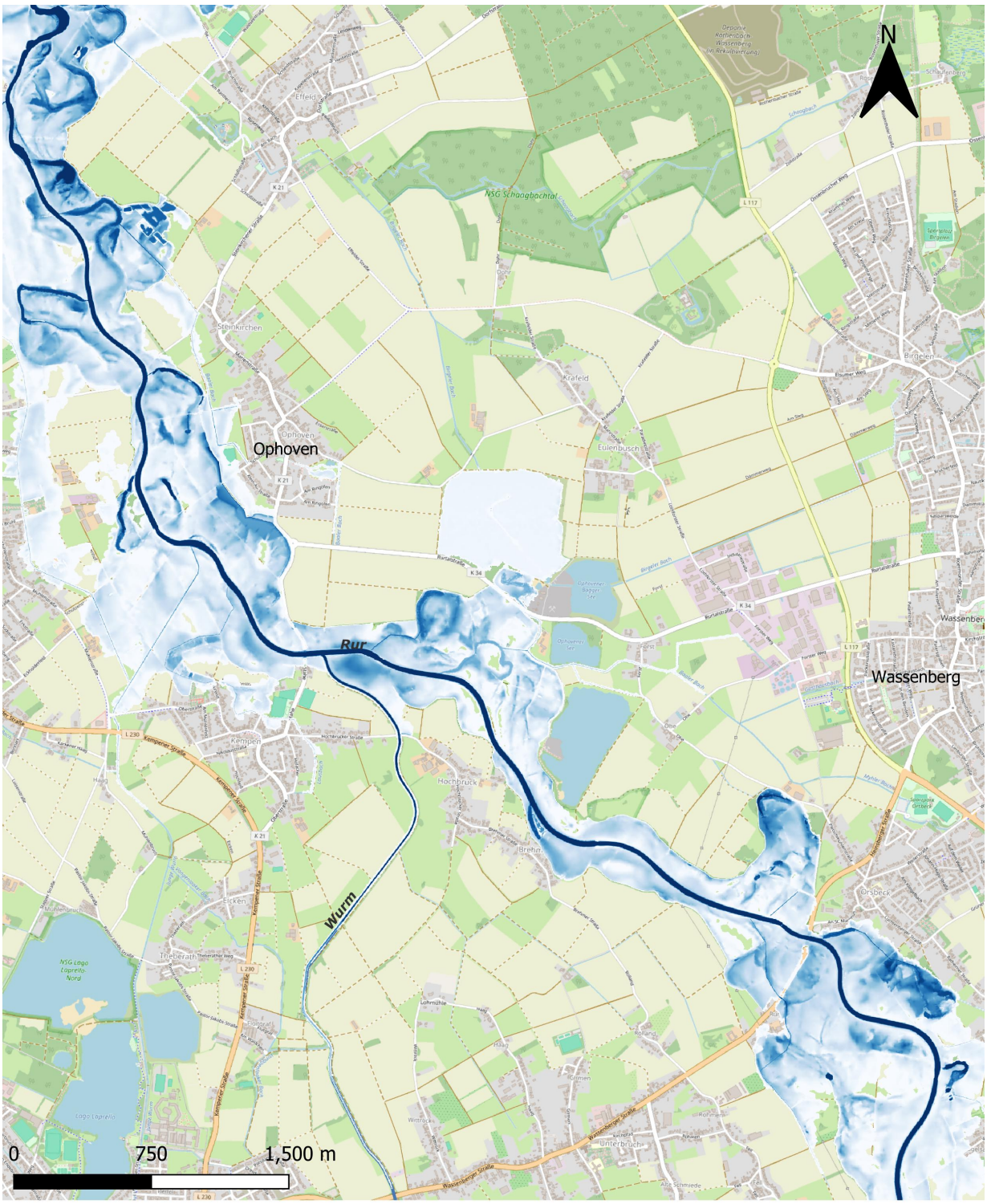

Figure B.3: Inundation depth reference case HQ100 near Ophoven

C

Quasi-Steady Approach

In the one-dimensional analytical model, it is assumed that temporal derivatives in the momentum equation (4.2) can be neglected while keeping them in the mass-balance equation (4.1). This is known as the quasi-steady approximation, according to Battjes and Labeur, 2017. This appendix examines the justification for this assumption by analyzing the relative magnitude of the inertial terms compared to the gravity and resistance forces. The goal is to assess whether neglecting the inertial terms is a reasonable assumption for the Rur river.

First the momentum-equation has been rewritten using differential approximation as shown in C.1. Subsequently, the relative importance of local inertia compared to resistance forces, as well as advective inertia compared to gravity forces, can be estimated using Equations C.2 and C.3, respectively.

$$\frac{U}{T} + \frac{U^2}{L} + g\frac{H}{L}c_f\frac{U^2}{D} = 0 \tag{C.1}$$

$$\frac{\textit{resistance}}{\textit{local inertia}} = \left(\frac{c_f U U}{D}\right) / \left(\frac{U}{T}\right) = \frac{c_f U T}{D} \tag{C.2}$$

$$\frac{\textit{gravity forcing}}{\textit{advective inertia}} = \left(\frac{gH}{L}\right) / \left(\frac{U^2}{L}\right) = \frac{gH}{U^2} \tag{C.3}$$

The analysis is conducted at two locations: near Jülich (upstream) and near Wassenberg (downstream). The HQ-100 flood hydrograph, representing a flood with a 100-year return period, is used for this analysis. The flood wave has a duration of 3 days with peak heights of 1.0 meters at Jülich and 2.0 meters at Wassenberg. The data has been retrieved from the 2D hydrodynamic model HydroAs2D.

At Jülich, the uniform water depth d_u is 2 meters, while at Wassenberg, it is 1.5 meters. The bed slope i_b is 0.0016 at Jülich and 0.001 at Wassenberg. The Manning friction coefficient n is 0.030 $m^{-\frac{1}{3}}s$ for both locations. The friction coefficients c_f have been calculated using: $c_f = \frac{gn^2}{d^{1/3}}$, resulting in a value of 0.007.

The velocity is approximated using the uniform flow equation:

$$U_e = \sqrt{\frac{g d_u i_b}{c_f}} = \sqrt{\frac{d_u^{4/3} i_b}{n^2}} \tag{C.4}$$

Substituting the values into Equations C.2 yields approximately 1900 for Jülich and 1700 for Wassenberg. Similarly, using Equation C.3, the ratio of gravity forcing to advective inertia is 2.5 at Jülich and 18 at Wassenberg. These results demonstrate that the resistance and gravity forces are significantly greater than the local and advective inertia terms, justifying their neglect in the analysis.

D

Cross-section Approximations at Detention basin Inlet Locations

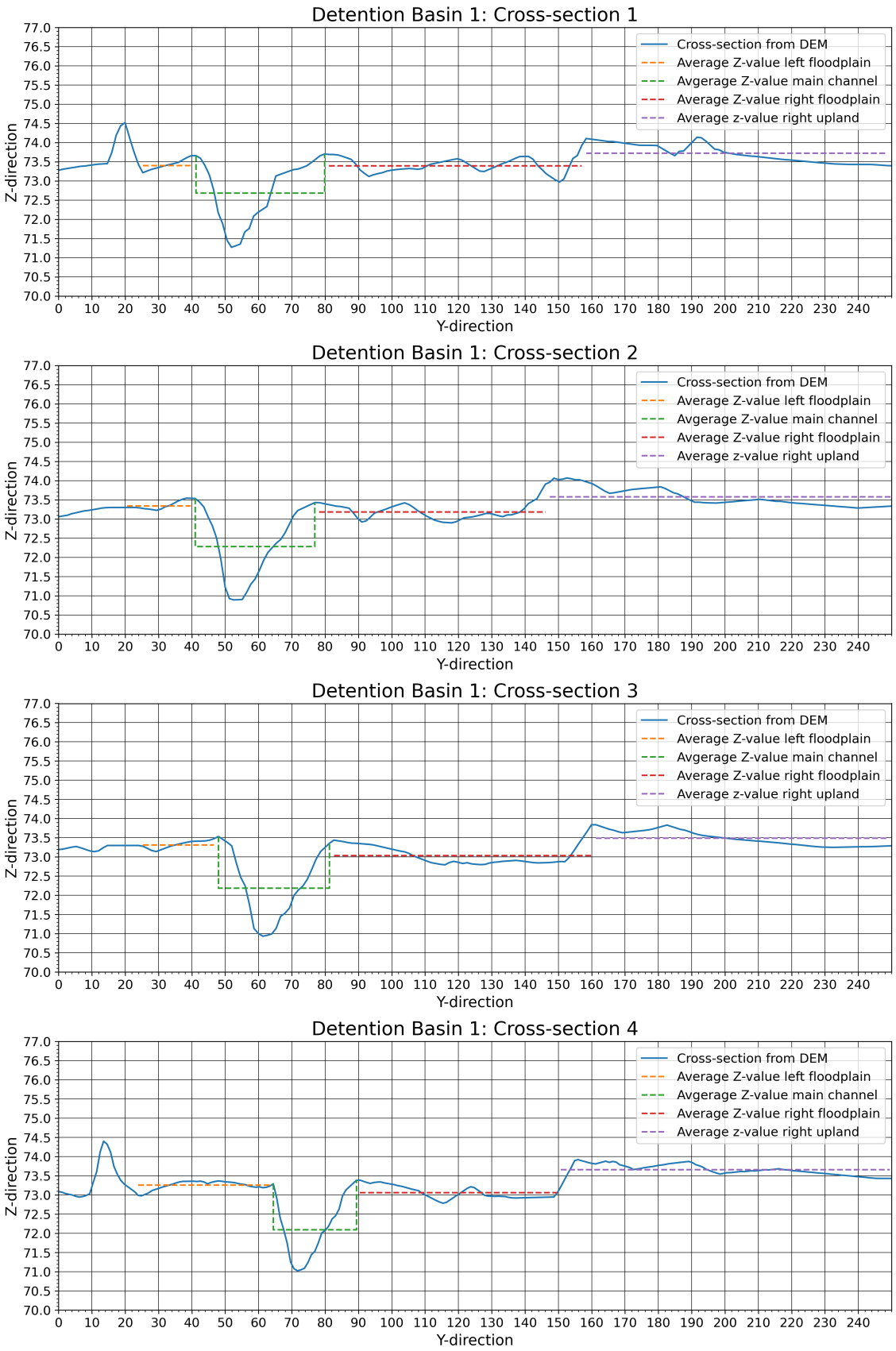

Figure D.1: Cross-sections at the inlet of detention basin 1. The bain is at the left.

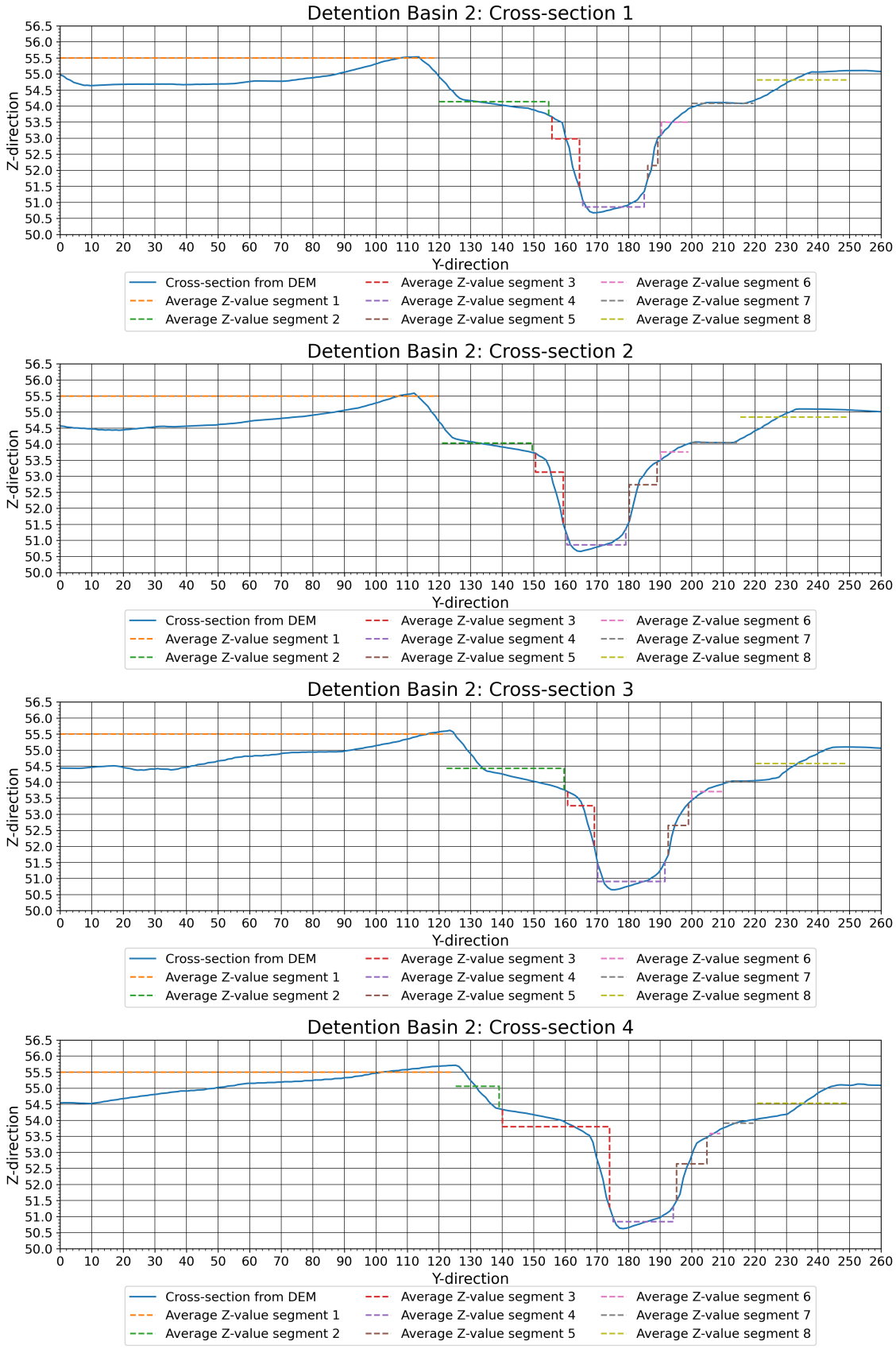

Figure D.2: Cross-sections at the inlet of detention basin 2. The basin is at the right.

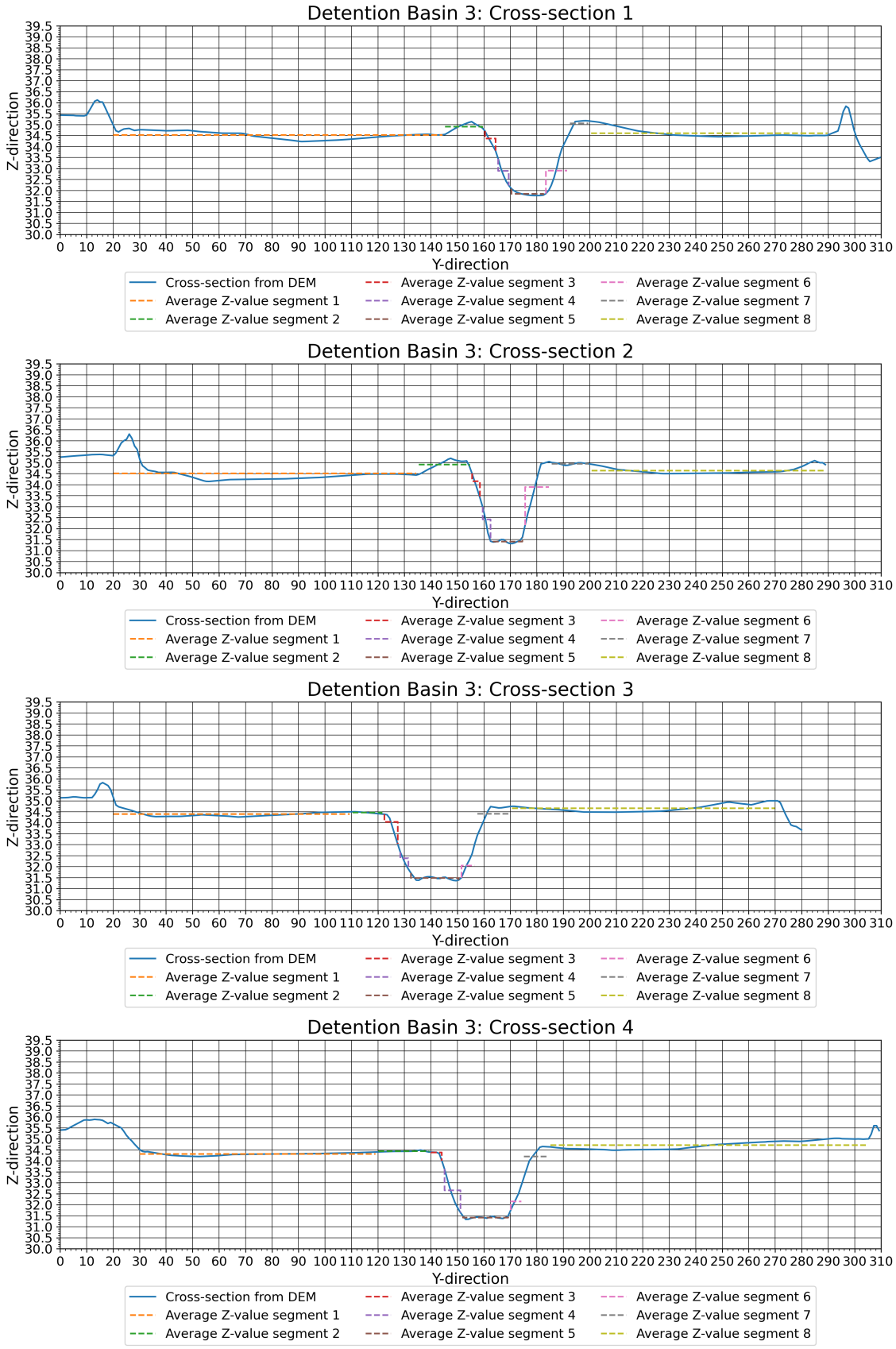

Figure D.3: Cross-sections at the inlet of detention basin 3. The basin is at the right.

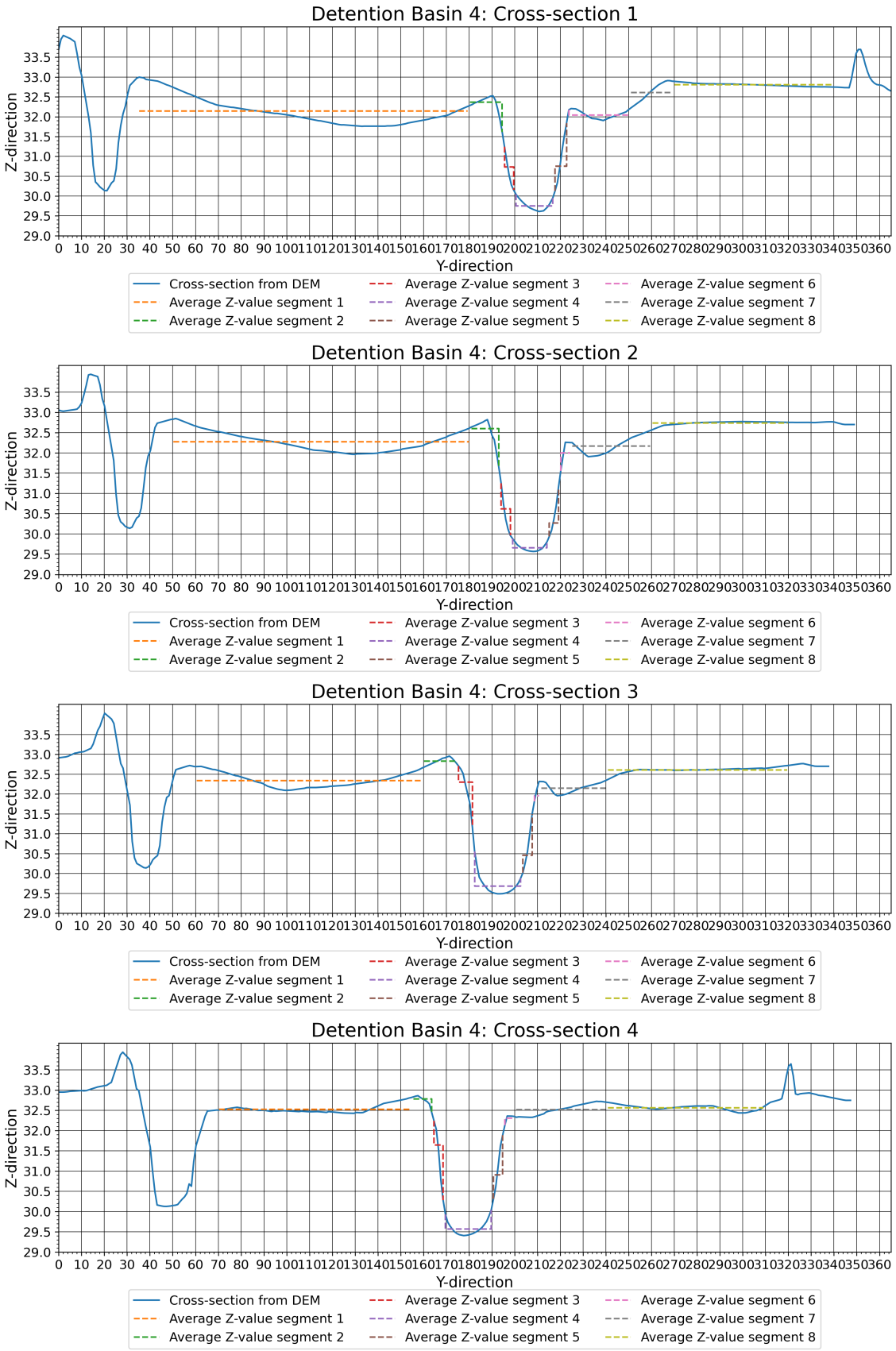

Figure D.4: Cross-sections at the inlet of detention basin 4. The basin is at the left.

E

LUA-Script Detention Basin 1 and 2

```
-- Establish access to HydroAS-Modell
local hydroas = require("hydroas")

-- Function to create a DurationCurve object
local function DurationCurve(nodeName)
    local durations = {}
    local maxIndex = 0
    local node = hydroas.Node.new(nodeName)  -- Create Node using new

    return {
        step = function()
            local index = math.floor(node:h() * 100)
            durations[index] = (durations[index] or 0) + hydroas.Global.
                timestepLength()
            maxIndex = math.max(maxIndex, index)
        end,
        writeToFile = function()
            local file = io.open(nodeName .. ".dc", "w")
            file:write("h[m] duration[sec]\n")
            local sumDuration = 0
            for index = maxIndex, 0, -1 do
                sumDuration = sumDuration + (durations[index] or 0)
                file:write(string.format("%10.2f %10.0f\n", index / 100,
                    sumDuration))
            end
            file:close()
        end
    }
end

-- Function to ensure the output directory exists
local function ensureDirectoryExists(dir)
    local success, err = os.rename(dir, dir)  -- Try to rename the directory to
        itself
    if not success then
        os.execute("mkdir " .. dir)  -- Create the directory if it does not exist
    end
end

-- Ensure the output directory exists
local outputDir = "Script_output"
ensureDirectoryExists(outputDir)
```

```
40
41 -- Function to check if NodeSet was created
42 local function checkNodeSet(nodeSet, label)
43     if not nodeSet then
44         print("Error: Failed to create NodeSet with label:", label)
45     else
46         print("Successfully created NodeSet with label:", label)
47     end
48 end
49
50 -- Function to initialize NodeSet z-values directly if supported
51 local function initializeNodeSet(nodeSet, defaultZ)
52     local success = pcall(function()
53         nodeSet:setZ(defaultZ)
54     end)
55
56     if success then
57         print("Initialized NodeSet z-value to", defaultZ)
58     else
59         print("Failed to initialize NodeSet z-value")
60     end
61 end
62
63 -- POLDER 1
64 local weir1 = hydroas.NodeSet.newByNodeString("PolderWeir1")
65 checkNodeSet(weir1, "PolderWeir1")
66 local weirStatus1 = 0
67 local gauge1 = hydroas.Node.new("Gauge1")
68 local gaugePolder1 = hydroas.Node.new("GaugePolder1")
69
70 -- POLDER 2
71 local weir2 = hydroas.NodeSet.newByNodeString("PolderWeir2")
72 checkNodeSet(weir2, "PolderWeir2")
73 local weirStatus2 = 0
74 local gauge2 = hydroas.Node.new("Gauge2")
75 local gaugePolder2 = hydroas.Node.new("GaugePolder2")
76
77 -- Instantiate two DurationCurves
78 local d1 = DurationCurve("Gauge1")
79 local d2 = DurationCurve("Gauge2")
80
81 -- Initialization Flag
82 local initialized = false
83
84 -- Initialize flags to track whether the weirs have been opened or closed
85 local weir1Opened = false
86 local weir1Closed = false
87 local weir2Opened = false
88 local weir2Closed = false
89
90 -- Return to HydroAS the functions which shall be called by HydroAS
91 return {
92     step = function()
93         -- Update both duration-curves
94         d1.step()
95         d2.step()
96
97         -- Initialize weir z-values if not already done
98         if not initialized then
99             print("Initializing Weir1 to 100 meters")
100             initializeNodeSet(weir1, 100)
```

```
            print("Initializing Weir2 to 100 meters")
            initializeNodeSet(weir2, 100)
            initialized = true
        end

        -- Control for PolderWeir1
        if not weir1Opened and gauge1:w() > 73.92 then
            print("Opening Weir1")
            weir1:setZ(73.7)
            weirStatus1 = 1  -- Change status to Open
            weir1Opened = true  -- Set flag to indicate Weir1 is opened
        elseif not weir1Closed and weirStatus1 == 1 and gaugePolder1:w() > 73.7
            then
            print("Closing Weir1")
            weir1:setZ(100)
            weirStatus1 = 0  -- Change status to Closed
            weir1Closed = true  -- Set flag to indicate Weir1 is closed
        end

        -- Control for PolderWeir2
        if not weir2Opened and gauge2:w() > 55 then
            print("Opening Weir2")
            weir2:setZ(55.05)
            weirStatus2 = 1  -- Change status to Open
            weir2Opened = true  -- Set flag to indicate Weir2 is opened
        elseif not weir2Closed and weirStatus2 == 1 and gaugePolder2:w() > 55.05
            then
            print("Closing Weir2")
            weir2:setZ(100)
            weirStatus2 = 0  -- Change status to Closed
            weir2Closed = true  -- Set flag to indicate Weir2 is closed
        end
    end,

    writeResult = function()
        -- Open or create a file to write weir statuses in the Script_output
            directory
        local filePath = outputDir .. "/weir_statuses.log"
        local file = io.open(filePath, "a")
        file:write("Time: ", hydroas.Global.timestepStart(), " s, ")
        file:write("Weir1 Status: ", weir1Opened and "Open" or (weir1Closed and "
            Closed" or "Not Changed"), ", ")
        file:write("Weir2 Status: ", weir2Opened and "Open" or (weir2Closed and "
            Closed" or "Not Changed"), "\n")
        file:close()
    end,

    close = function()
        -- Output the duration-curves
        d1.writeToFile()
        d2.writeToFile()
    end

}
```